UNIVERSITY OF NIŠ
FACULTY OF OCCUPATIONAL SAFETY
UNIVERZITET U NIŠU
FAKULTET ZAŠTITE NA RADU U NIŠU

Scientific Journal

Safety Engineering

Naučni časopis
Inženjerstvo zaštite

Safety of Technical Systems
Bezbednost tehničkih sistema

Vol. 11
Nº 2 (2021)

Journal for Scientists and Engineers

SAFETY ENGINEERING

Naučno stručni časopis

INŽENJERSTVO ZAŠTITE

Vol.11, No.2 (2021)

From Editor's desk

Pred visokoškolskim ustanovama u vreme pandemije se postavljaju novi zadaci - kako održati nivo nastave i naučno-istraživačkog rada. Između ovih zadataka, istraživači su našli vremena da svoju energiju usmere i na istraživanje načina kako da unaprede svoj rad i pomognu društvu u prevazilaženju negativnih posledica Covid pandemije.

Novi broj časopisa *Safety Engineering* ostaje fokusiran na teme inženjerstva zaštite, zaštite na radu, zaštite od požara sa posebnom osvrtom na zaštitu šuma od požara, kao i bezbednost sistema sa teorijskog aspekta i u praksi: u rafinerijama nafte, prilikom razvoja novih instrumenata za merenje magnetnih polja, energetskog potencijala u tretmanu otpada, kancerogenosti hemikalija u životnoj sredini, stresa na radnom mestu, standardizacije elektromagnentih zračenja i bezbednosti u elektroenergetici. Delatnost Fakulteta zaštite na radu iskazana je i kroz tehničko rešenje beskontaktnog merenja temperature, naučne i međunarodne projekte koji su realizovani u prošloj godine i izdavačku delatnost, o čemu detaljnije možete pročitati u ovom broju.

During the pandemic, new tasks have been set before higher education institutions - how to maintain the quality of education and scientific research. In between these tasks, the researchers found time to focus their energy on exploring ways to improve their work and help society overcome the negative impacts of the COVID-19 pandemic.

The new issue of Safety Engineering remains focused on safety engineering, occupational safety, fire protection, more exactly forest fire protection, systems safety both in theory and practice: in oil refineries, during the development of magnetic field measurement instruments, the energy potential of waste treatment, the carcinogenicity of chemicals in the environment, workplace stress, standardization related to electromagnetic radiation and safety in the power industry. Over the previous year, the activities of the Faculty of Occupational Safety involved issuing technical solution for non-contact temperature measurement, implementation of research and international projects, and publishing activity, which you can read more about in this journal issue.

On behalf of the editors
Prof. Dr. Dejan Krstić

Contents

Reviews of publications, project and technical solutions

Instructions for Authors

Sadržaj

Prikazi publikacija, projekta i tehničkih rešenja

Uputstvo za autore

UGLJEŠA JOVANOVIĆ[1]
DEJAN KRSTIĆ[2]

[1,2]University of Niš,
Faculty of Occupational Safety in Niš

[1]ugljesa.jovanovic@znrfak.ni.ac.rs
[2]dekikrs@gmail.com

TESLAMETER FOR MAGNETIC FIELD MEASUREMENT IN HIGH VOLTAGE FACILITIES

Abstract: *This paper presents a low-cost three-axis teslameter capable of measuring magnetic field intensity in industrial environments and high voltage facilities. It is based on an MFS-3A three-axis magnetic field sensor, and it can measure magnetic flux density up to ±5 mT in all three axes, with accuracy better than ±0.5% and excellent temperature stability. The proposed teslameter was calibrated using a state-of-the-art reference instrument, Helmholtz coil and temperature chamber. The paper describes the development and the calibration of the proposed teslameter. The obtained results are presented as well.*

Key words: magnetic field, teslameter, MFS-3A, high voltage facilities, calibration.

INTRODUCTION

Humans' immune system successfully performs its function in the preservation of human health under the Earth's natural magnitude field intensity. However, the intensity of the environmental magnetic field is often considerably above Earth's natural magnitude field intensity. Professional workers in power plants and high voltage facilities are exposed to magnetic fields on a daily basis [1]. In order to collect data about exposition and improve health status, it is essential to carefully monitor the magnetic field exposure of each worker.

Society and science, according to the state of art in the field of bioelectromagnetic, set a few recommendations regarding the exposure limits for magnetic fields generated by 50/60Hz electric current. A couple of recommendations are given in Table 1.

Table 1. *Recommended exposure limits*

Recommendation	Limit
IRPA/ICNIRP recommendation for "private individuals" (daily, constant)	100 µT
IRPA/ICNIRP recommendation for occupational exposure (daily, constant)	500 µT
IRPA/ICNIRP exposure limit for "private individuals" (daily exposure for a few hours)	1 mT
IRPA/ICNIRP recommendation for occupational exposure (daily exposure for a few hours)	5 mT

An instrument called teslameter, comprised of a magnetic field probe and an electronic processing circuit, measures magnetic flux density. Hall effect sensors emerged as the preferred selection for magnetic field probes due to their growing accuracy and low prices [2]. Proper exposure to the magnetic field monitoring requires measuring its intensity in all three axes, meaning that a three-axis magnetic field probe is mandatory.

There are many commercially available three-axis teslameters capable of performing measurements in the range of ± 5 mT, but they are usually either expensive or bulky. On the other hand, there is a handful of available yet portable, accurate and battery-powered three-axis teslameters with the same measurement range and prices less than 100$. It should be noted that there are no commercially available magnetic field dosimeters i.e. devices device that measures dose uptake of external magnetic field. There are a couple of similar devices, which can record measurements, but they are not commercially available [3, 4].

A cost-effective yet accurate three-axis teslameter can be realized using inexpensive off-the-shelf components in a similar way as the teslameter presented in the research [5].

SYSTEM DESIGN

The proposed teslameter was built around an 8-bit PIC18F2550 microcontroller (MCU) due to its performance-size ratio.

The key design requirements the proposed teslameter must accomplish are:

- simple design,
- low cost of components,
- good temperature stability and accuracy,

Following these requirements, an analogue three-axis magnetic field sensor MFS-3A was selected to measure magnetic flux density in all three axes. The MFS-3A consists of three CSA-1V single-axis Hall effect sensors mounted in a way their sensitive areas are mutually perpendicular so that each CSA-1V measures one direction of a magnetic field [6]. The CSA-1Vs are soldered on two perpendicular PCBs as shown in Figure 1 with angular alignment better than ±3° and then, they are sealed in a plastic case.
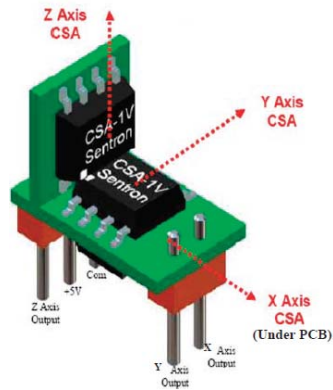
Figure 1. *Structure of the MFS-3A magnetic field sensor [6]*

The CSA-1V is a single-axis Hall effect magnetic field sensor fabricated using a conventional CMOS technology with an additional ferromagnetic layer placed above the sensitive area (see Figure 2), which amplifies the magnetic field by 10 times [7]. Output voltage can be either ratiometric or single ended. It also incorporates the spinning current technique to increase the output signal without increasing the inherent electrical noise [8, 9]. Moreover, the spinning current method can completely remove the 1/*f* noise.
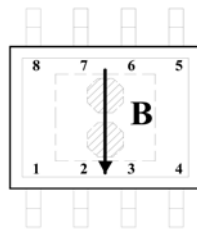
Figure 2. *Direction of sensitivity and location of sensing element [7]*

The high sensitivity of the CSA-1V and low-noise features make it suitable for accurate electric current measurement applications [10-13]. Key parameters of the CSA-1V are given in Table 2.

Table 2. *Key parameters of the CSA-1V Hall Effect sensor [7]*

Parameter	Value
Magnetic field measurement range	±7.3 mT
Sensitivity	280 mV/mT
Bandwidth	100 kHz
Accuracy on magnetic sensitivity trimming	±2%
Offset voltage	±20 mV
Nonlinearity	±0.2%
Magnetic sensitivity temperature drift	±0.02%/°C
Offset Temperature Drift	±0.2 mV/°C

Although the CSA-1V saturates around ±7.3 mT, it will not be damaged even if exposed to the magnetic field as high as ±1 T. Saturation recovery time is less than a few microseconds.

Figure 3 shows the block diagram of the proposed teslameter.
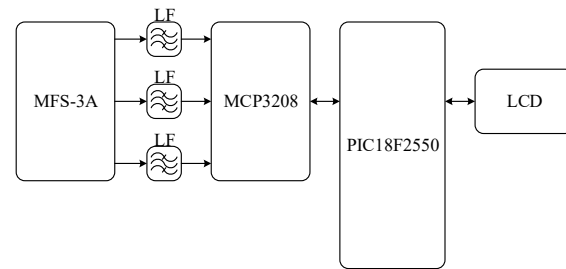
Figure 3. *Block diagram of the proposed dosimeter*

The output voltage of each CSA-1V is filtered with a low-pass Sallen-Key filter with a cut-off frequency of 500 Hz, unity gain and quality factor of 0.707, built around the AD822 rail-to-rail op-amp. The filtered voltages are then fed in the 12-bit MCP3208 analogue to a digital converter (ADC). Based on the output voltage of the corresponding CSA-1V, the MCU calculates magnetic field intensity of each axis per following expression:

$$B = \frac{V_{OUT} - V_{OFFSET} \pm V_{COMP}}{S} \qquad (1)$$

wherein V_{OUT} is the CSA-1V output voltage in [V], S is its sensitivity in [mV/mT], V_{OFFSET} is the sum of offset and quiescent voltages, i.e. output voltage of the CSA-1V when no magnetic field is applied and V_{COMP} is compensation voltage of ADC.

After the MCU calculates the magnetic flux density of each axis, it calculates total magnetic field intensity per the following expression:

$$B_{SUM} = \sqrt{B_X^2 + B_Y^2 + B_Z^2} \qquad (2)$$

MCP1541 voltage reference provides a 4.096 V reference voltage for the ADC, which means that the ADC quant is exactly 1 mV. In other words, the magnetic field resolution is equal to 3.5 µT. Based on the above mentioned, it can be concluded that the ADC resolution is perfectly acceptable since the resolution of the MFS-3A is equal to ±10 µT [6]. The absolute accuracy of the MCP3208 ADC is ±4 LSB, which equals ±14 µT.

In order to minimize the power consumption, the obtained results are displayed on a 2x16 LCD COG (Chip-On-Glass) display instead on classic LCD with background light. The proposed dosimeter is designed to be powered from a simple 5 V DC power bank used to charge tablets and cell phones via a micro USB port. This being said, the total power consumption of realized teslameter is less than 75 mA/h.

When the proposed dosimeter powers on, it begins measuring magnetic field intensity in all three axes after which the MCU calculates total magnetic field intensity, per Equation (2), and displays all four values on a LCD COG display. Sampling rate of measurements is 500 ms.

Photo of the proposed dosimeter is shown in Figure 4.
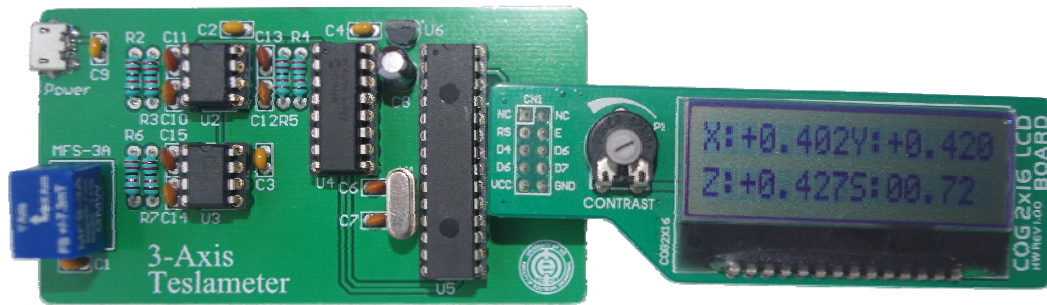
Figure 4. *Photo of the proposed dosimeter*

As can be seen from Figure 4, COG LCD is soldered on a separate PCB in order to minimize a size of enclosure as well as to provide greater selection of plastic boxes. In this case, connection between main board and LCD board can be realized using a 10-wire flat cable.

Although the proposed teslameter uses trough hole electronic components, thanks to its simplicity, the main PCB is only 85x45 mm in large. Greater minimization can be obtained with better track routing and by employing SMD components except for MFS-3A. Moreover, the proposed teslameter can be easily upgrade, with minimal costs, to record real-time measurements on a SD card, i.e. it can become a magnetic field dosimeter.

The total cost of realization of the proposed teslameter is well below 100 $ wherein the most expensive item is in fact a MFS-3A magnetic field sensor. Additional cost is a USB power bank whose price is determined by the user according to the desired power capacity.

CALIBRATION AND TEST RESULTS

Brand new CSA-1Vs have unequal specifications significantly different from the ones rated in [7]. For this reason, calibration of each CSA-1V is an essential procedure during their manufacturing process. Namely, the sensitivity of non-programmed CSA-1Vs is around 150 mV/mT, which is during calibration increased per the following expression:

$$S_{GAIN} = 1 + A \qquad (3)$$

wherein A represents the sum of one or more (or even none) following coefficients: 0.5, 0.25, 0.125, 0.0625, 0.03125 and 0.015625.

Due to a limited number of combinatons, it is almost impossible for each CSA-1V to have the exact sensitivity, which is why the sensitivity has a tolerance of ±5 mV/mT. This means that in order to obtain the most accurate measurements from the proposed teslameter, it is necessary to calibrate all three CSA-1Vs individually.

Calibration of all three CSA-1Vs is performed in the range between -5 mT and 5 mT by subjecting them to a homogeneous magnetic field generated by a Helmholtz coil. Reference measurements are obtained using a digital teslameter Senis 3MH3A [14], which has a resolution of 10 µT and accuracy better than ±0.05% in the range of -100 mT and 100 mT.

To accurately calibrate each CSA-1V and minimize angular errors, it was essential to precisely aligne the MFS-3A and the 3MH3A probe so they sit in parallel in the Helmholtz coil. During the calibration, the output voltage of each CSA-1V was measured by a highly accurate Agilent 34401A voltmeter. Figure 5 shows a photo of the Helmholtz coil used in the calibration procedure.
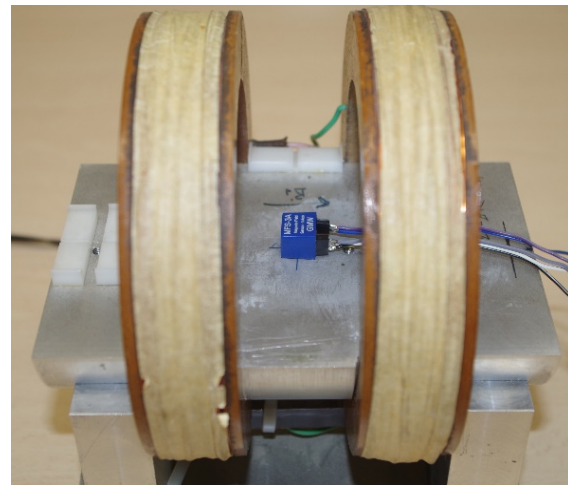
Figure 5. *Helmholtz coil used in the calibration procedure*

Calibration of each axis was performed by taking 12 measurements in the specified range. Additionally, zero flux measurements were recorded by inserting the MFS-3A in the zero gauss tube. Figure 6 shows the accuracy of all three axes relative to the Senis 3MH3A teslameter before calibration in the case when the sensitivity is assumed to be 280 mV/mT.
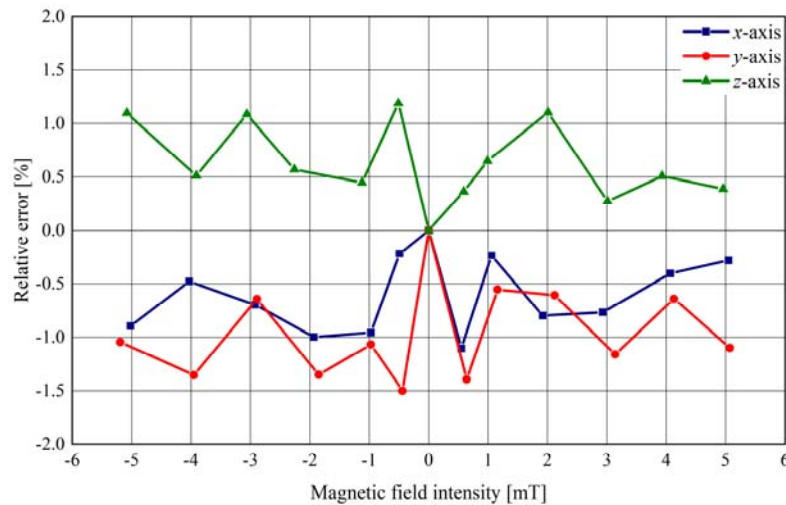
Figure 6. *Measurement results before calibration*

As can be seen from Figure 6, the relative error of obtained measurements is less than ±1.5%, when it is assumed that sensitivities of all three CSA-1Vs are exactly 280 mV/mT.

Exact sensitivities of each CSA-1V are calculated after based on comparative measurements taken by the Senis 3MH3A teslameter and they are 278.2 mV/mT for *x*-axis, 277.3 mV/mT for *y*-axis and 282.2 mV/mT for *z*-axis.

Figure 7 shows the accuracy of all three axes after proper sensitives are inserted in Equation 1, and it is apparent that the relative error is less than ±0.5%, which is quite good considering the fact that the proposed teslameter doesn't employ any linearization technique.
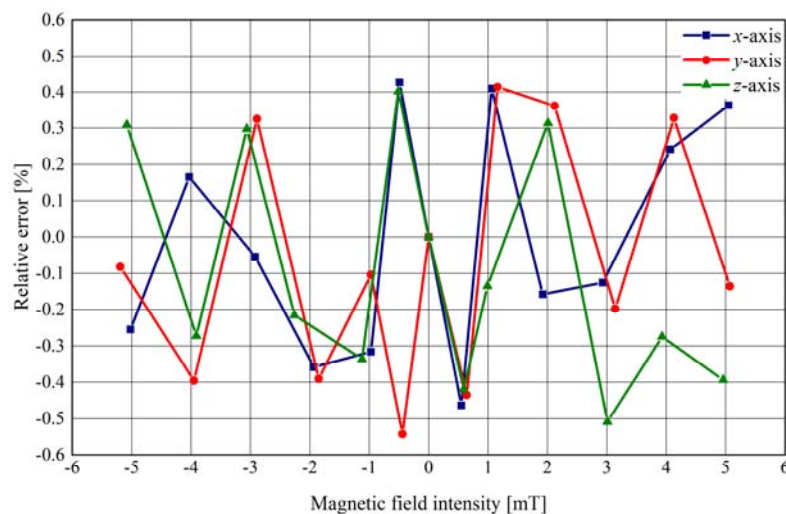
Figure 7. *Measurement results after calibration*

According to the specifications, the CSA-1V has good temperature stability. Magnetic sensitivity temperature drift is better than ±0.02%/°C while offset voltage temperature drift is better than ±0.2 mV/°C. However, magnetic sensitivity temperature drift can be adjusted during a calibration on a brand new CSA-1Vs, hence it is necessary to evaluate this parameter in order to determine whether a temperature compensation should be implemented.

In order to evaluate offset voltage temperature drift, the MFS-3A is inserted in the zero gauss tube and both of them are subjected to temperatures in the range between 25°C and 100°C in the temperature chamber TestEquity Model 115A. Figure 8 shows the results of this experiment for the *x*-axis.
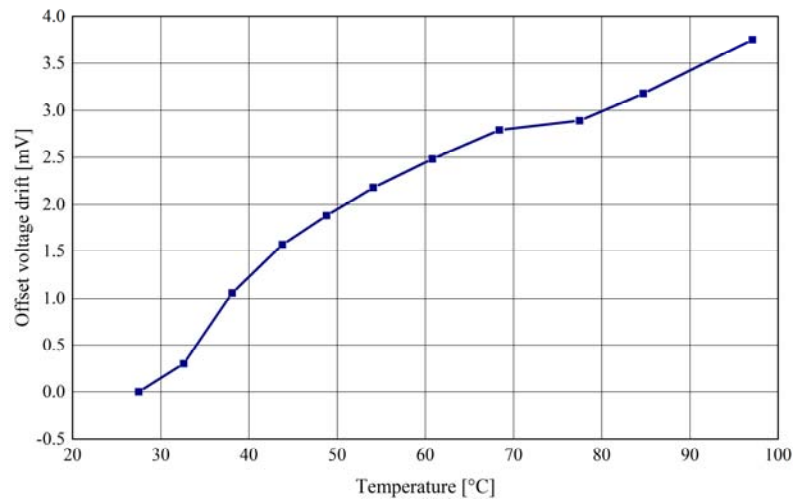
Figure 8. *Offset voltage temperature drift of x-axis*

As can be seen from Figure 8, maximal offset voltage drift is less than 4 mV or 0.06 mV/°C, which is far better than specified ±0.2 mV/°C.

To evaluate sensitivity temperature drift, the MFS-3A is inserted in the Helmholtz coil and both of them are placed in the temperature chamber TestEquity Model 115A where the temperature is gradually increased from 25°C to 100°C while the magnetic field generated by the Helmholtz coil is kept constant. Figure 9 shows the results of this experiment for the *x*-axis.
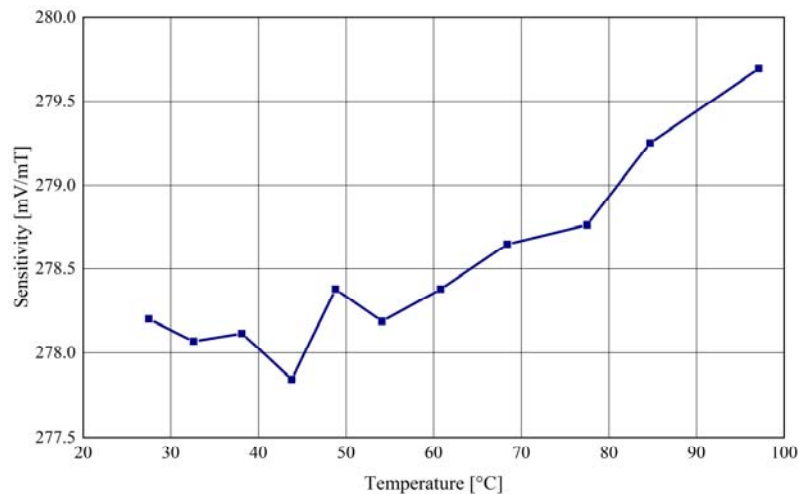
Figure 9. *Sensitivity temperature drift of x-axis*

Based on the results shown in Figure 9, the calculated sensitivity temperature drift is better than 0.01 %/°C, which is two times better than specified.

CONCLUSION

The low-cost teslameter based on the MFS-3A three-axis magnetic field sensor is realized. Measurement range of the proposed teslameter is ±5 mT.

The proposed dosimeter was calibrated using the Helmholtz coil and the state of the art Senis 3MH3A teslameter employed as the reference instrument. During the calibration, it was important to minimize angular errors and this was achieved by carefully paralleling the MFS-3A and 3MH3A probe inside of the Helmholtz coil. After the calibration, the maximal

relative measurement error recorded in the entire measurement range was less than ±0.5% compared to the corresponding measurements taken by the Senis 3MH3A teslameter.

Temperature stability of the proposed dosimeter was evaluated in the temperature range between 25°C and 100°C. Temperature stability of offset voltage is better than 0.06 mV/°C and temperature stability of sensitivity is better than 0.01 %/°C. Based on these parameters, it can be concluded that the proposed teslameter has excellent temperature stability.

Due to its simplicity and small sizes, the proposed teslameter can be easily upgraded to be a magnetic field dosimeter that can be easily worn by professional workers in power plant facilities to evaluate dangerous

impact of increased magnetic field.

Thanks to its low price, good accuracy and excellent temperature stability, the proposed teslameter represents good alternative to commercially available teslameters with similar properties.

REFERENCES

[1] Z-Y. Tong, Z-Y. Dong, M-M. Tong: "Analysis of magnetic field generated by overhead cables", Measurement, Vol. 89, 2016, pp. 169-170.

[2] R.S. Popović: *"Hall Effect Devices"*, Taylor & Francis, 2003, New York.

[3] Crozier et al. "Magnetic field dosimeter", US Patent US7936168B2, 2011.

[4] D. N. Kossyvakis, S. G.Vassiliadis, C. G. Vossou, E. E. Mangiorou, K. I. Prekas, S. M. Potirakis: "A wearable magnetic sensing device for identifying the presence of static magnetic fields", Measurement, Vol. 109, 2017, pp. 44-50.

[5] U. Jovanović, I. Jovanović, M. Blagojević, D. Krstić, D. Mančić: "Low-cost teslameter based on hall effect sensor MLX90242", Serbian journal of electrical engineering. Vol. 15(2), 2018, pp. 225-232.

[6] Ametes: 'Magnetic Field Sensor - 3 Axis, MFS-3A", 2011, Zurich, Switzerland.

[7] Sentron: "CSA-1V datasheet", 2004, Zug, Switzerland.

[8] R.S. Popović, Z. Ranđelović, D.Manić: "Integrated hall-effect magnetic sensors," Sensors and Actuators A: Physical, Vol. 91, 2001, pp. 46 -50.

[9] R.S. Popović, P.M. Drljača, P. Kejik: "CMOS magnetic sensors with integrated ferromagnetic parts. Sensors and Actuators A: Physical", Vol. 129, 2006, pp. 94-99.

[10] M. Blagojević, U. Jovanović, I. Jovanović, D. Mančić, R.S. Popović: "Realization and optimization of bus bar current transducers based on hall effect sensors", Measurement Science and Technology, Vol. 27(6), 2016, no. 065102.

[11] M. Blagojević, U. Jovanović, I. Jovanović, D. Mančić, R.S. Popović: "Coreless open-loop current transducers based on hall effect sensor CSA-1V", Facta Universitatis, Series: Electronics and Energetics, Vol. 29(4), 2016, pp. 489-507.

[12] M. Blagojević, U. Jovanović, I. Jovanović, D. Mančić: "Folded bus bar current transducer based on hall effect sensor", Electrical Engineering, Vol. 100, 2018, pp. 1243-1251.

[13] Senis AG: "3MH3A Magnetic Field Digital Teslameter", 2013, Baar, Switzerland.

ACKNOWLEDGEMENTS

BIOGRAPHY of the first author

Uglješa Jovanović received the MSc and Ph.D. degrees in electronics from the University of Niš, Faculty of Electronic Engineering in Niš. His research areas are embedded systems, electric current and magnetic field measurement, radiation dosimeters and photovoltaic systems.

He is currently working as a Teaching Assistant at the Faculty of Occupational Safety in Niš, University of Niš.

TESLAMETAR ZA MERENJE MAGNETNOG POLJA U VISOKO NAPONSKIM OBJEKTIMA

Uglješa Jovanović, Dejan Krstić

Rezime: *U radu je predstavljen ekonomičan troosni teslametar namenjen za merenje intenziteta magnetnog polja u industrijskom okruženju i visokonaponskim objektima. Realizovani teslametar je zasnovan na MFS-3A troosnom senzoru magnetnog polja i može meriti gustinu magnetnog fluksa do ±5 mT u sve tri ose, sa tačnošću boljom od ±0.5% i odličnom temperaturnom stabilnošću. Predloženi teslametar je kalibrisan pomoću vrhunskog referentnog instrumenta, Helmholcovog kalema i temperaturne komore. Rad sadrži opis realizacije i kalibracije predloženog dozimetra. Prikazani su i dobijeni rezultati.*

Ključne reči: magnetno polje, teslametar, MFS-3A ,visokonaponska postrojenja, kalibracija.

STANIMIR ŽIVANOVIĆ[1]
DARKO ZIGAR[2]
JANKO ČIPEV[3]

[1]Sector for Emergency Management, Belgrade
[2]University of Niš, Faculty of Occupational Safety
[3]Mobeco, Leskovec pri Krškem, Slovenia

[1]zivannn@open.telekom
[2]darko.zigar@znrfak.ni.ac.rs
[3] cipevj@putinzenjering.com

FOREST ROADS AS THE KEY TO FOREST PROTECTION AGAINST FIRE

Abstract: *Planning, construction and maintenance of forest roads is extremely important for successful firefighting in a certain area. This study focuses on the current technical infrastructure in the state forests of Serbia. The average openness of forests in Serbia at the end of 2019 was 20.14 m/ha, while 21.89 m/ha was occupied by public roads. In the period from 2011 to 2019, the average openness of state forests with public roads in Serbia decreased by 3.12 m/ha, or by 1.67 m/ha. The openness of forests by forest roads is the largest and optimal in the Vojvodina region (131.5 m/ha) and significantly lower and insufficient in Belgrade regions (0.35 m/ha), Sumadija and Western Serbia (2.8 m/ha), and Southern and Eastern Serbia (1.8 m/ha). Compared to 2011, the openness of forests in 2019 increased in the Vojvodina region and decreased in other regions in Serbia. Forest roads that have asphalt, concrete or cobblestone lanes are the least represented, about 0.27%. The largest representation of forest roads with a base (stone or gravel hard bottom layer) is about 82.7%.*

Key words: forest openness, forest roads, forest fire, Serbia

INTRODUCTION

The total forest area in Serbia is 2,252,400 hectares, of which 1,194,000 hectares or 53.0% are state-owned and 1,058,400 hectares or 47.0% are privately owned [2]. The total area of protected natural assets is 5,471.76 km^2, which is about 6.19% of the total territory of the Republic of Serbia [22].

Forest fires have a major impact on ecosystem stability. Onur and his colleagues [12] state that forest fires are one of the most important factors of environmental risk. Sekulić et.al [15] point out that forest fires in Serbia can pose a serious threat to certain ecosystems and some species, as well as to human safety. Forest fires occur in Serbia almost every year and are a limiting factor in the sustainable development of forestry [27].

Many studies [4, 19, 20, 26, 28, 29, 30, 31] have indicated that there is a correlation between the occurrence of forest fires in Serbia and climate conditions. The distribution of the fire-affected areas and the dynamics of fire outbreaks can be correlated with the climatic characteristics of certain areas [25]. The origin and development of forest fires are conditioned by several constantly changing factors, which define the assessment of forest fire risk. A certain impact on the threat of forests fire also depends on the implementation of measures of forest management, [21] such as the construction and maintenance of averages and the forest roads as well. The total amount of forest roads and locations in the area are important for the services in charge of fire protection. Stefanović [16] points out the importance of planning network roads in forest areas to provide the most efficient fire protection in terms of the most

favorable position in space, which achieves efficient preventive and timely repressive protection against forest fires. The aim of this research was to review the construction of technical infrastructure in the forests of Serbia, in order to work on the prevention and control of forest fires.

MATERIALS AND METHODS

The data of the Republic Statistical Office (2021) from 2011 to 2019 were used in this paper. The openness of forest complexes is conditioned by the presence of roads and their interconnection. The openness of forests in the territory of the Republic of Serbia is expressed in m/ha.

The openness of the forest to the road network (OS) is calculated as follows:

$$O_{š} = L / A \tag{1}$$

where $O_{š}$ is the openness of the forest to the road network (m/ha), L is the calculated length of the forest roads (m) and A is the area of the forest complex (ha).

The internal openness of the forest complex is the connection of the interior of the forest areas with the roads. External openness or public communications is the construction of roads that pass through the forest or directly lean on it. Forest roads are facilities (roads and trains) primarily built for the purpose of forest management and especially for the protection of forest fires (for the passage of fire vehicles and equipment), [23]. Forest roads include only permanent forest roads. Public roads are roads that pass through the forest or directly lean on it. Modern roads are roads that have a road made of asphalt, concrete or stone cubes. An

example of roads with a hard lower layer (stone or gravel) is hard forest roads with a base. The examples of unpaved roads (soft forest roads - dirt roads) and roads without a hard lower layer are shown. The territory of Serbia is divided into 5 statistical regions: Belgrade (Belgrade), Vojvodina (Voj), Sumadija and Western Serbia (SSS), Southern and Eastern Serbia (JIS), and Kosovo and Metohija (KM), [24]. Since Serbia does not have the data for the statistical region of Kosovo and Metohija, they are not included in the coverage of data for the Republic of Serbia (total). Statistical data are considered only for the state forests, since the SBS does not have the data for forests roads of other forms of ownership. The data from the National Forest Inventory (2009) on the area of state-owned forests in Serbia were used for the purposes of this paper.

RESULTS AND DISCUSSION

Forest roads in Serbia and the openness of forest complexes to roads

Data from the National Forest Inventory, which was conducted in the 2004-2006 period and published in 2009, indicate that the degree of forest cover in Serbia is 29.1%, while the optimal forest cover should be 41.4%.

The statistical region of Vojvodina with forests areas has the lowest degree of forest cover in Serbia, Table 1.

Table 1. *Forest regions in Serbia*

Region	Land area km²	Forest area km²	Forestry %
Region of Southern and Eastern Serbia	26.255	10.456	40,3
Sumadija region and Western Serbia	26.483	10.020	37,4
Belgrade region	3.227	508	15,7
Vojvodina	21.506	1.540	7,1

Forest infrastructure is one of the basic conditions for the successful leading of the forest ecosystem.

Table 2 shows the roads of state forests in Serbia for the period from 2011 to 2019. There is a significant decrease in the total length of traffic infrastructure at the end of 2019 compared to the period from 2011 to 2013.

Table 2 shows a significant increase in the length of public roads from 2016-2019 compared to the period 2011-2015.

Table 2 *Roads within the state forests in Serbia, 2011-2019.*

Year	Forest roads (km)				Public roads (km)				Total km
	total	contemporary	soft	solid	total	contemporary	soft	solid	
2011	27783	81	5227	22475	357	297	15	45	28140
2012	27989	86	5311	22592	358	297	15	46	28347
2013	28144	86	5569	22489	358	297	15	46	28502
2014	25903	386	4327	21190	498	342	46	110	26401
2015	25512	156	4674	20682	397	235	52	110	25909
2016	24071	65	4628	19378	1946	118	39	1789	26017
2017	24582	272	5121	19189	1865	139	1717	9	26447
2018	24931	70	4838	20023	2027	61	1733	233	26958
2019	24049	66	4092	19891	2087	198	1684	205	26136

Observing the traffic infrastructure in regions in Serbia, it can be seen that the largest representation of forests is Vojvodina region, Table 3.

Table 3 shows a significant increase in the length of public roads in Vojvodina region compared to other regions in Serbia. It is noticed that the length of public roads was much longer in 2019 compared to 2011 in Vojvodina region and Southern and Eastern Serbia and smaller in the Sumadija region and Western Serbia, Table 3.

Based on the data of forest area and built road network, the openness of state-owned forests is shown in Figure 1.

The average openness of forests in Serbia at the end of 2019 is 20.14 m/ha, or 21.89 m/ha including the public roads.

For example, the openness of forests in Republika Srpska is 9.28 m/ha and 11.21 m/ha including the public roads, [6]; in Slovenia, it is 24.8 m/ha, [10]; in Bulgaria, it reaches 7.90 m/ha, [18]; in Romania 13.73 m/ha, [3]; in Slovakia, it is 20.1 m/ha, [1]; and, in Austria, it is 45 m/ha, [8].

Table 3 *The length of roads in the statistical regions in Serbia, 2011-2019.*

Region	Year	Forest Roads (km)				Public roads (km)			
		total	cont.	soft	solid	total	cont.	soft	solid
Beo		51	6	28	17	-	-	-	-
Voj		20253	25	1403	18825	140	123	15	2
SZS	2011	4759	50	1921	2788	212	174	-	38
JIS		2720	-	1875	845	5	-	-	5
Beo		51	6	17	28	-	-	-	-
Voj		20269	25	1416	18828	140	123	15	2
SZS	2012	4848	50	1934	2864	212	174	-	38
JIS		2821	5	944	872	6	-	-	6
Beo		53	6	17	30	-	-	-	-
Voj		20283	25	1416	18842	140	123	15	2
SZS	2013	684	50	1938	2696	212	174	0	38
JIS		3124	5	2198	921	6	-	-	6
Beo		56	6	20	30	-	-	-	-
Voj		20329	25	1403	18901	158	140	16	2
SZS	2014	2577	16	970	1591	150	112	-	38
JIS		2941	339	934	668	190	90	30	70
Beo		59	6	23	30	-	-	-	-
Voj		20425	29	1494	18902	163	145	16	2
SZS	2015	2709	25	1641	1043	38	-	-	38
JIS		2319	96	1516	707	196	90	36	70
Beo		59	6	23	30	-	-	-	-
Voj		20425	29	1494	18902	163	145	16	2
SZS	2016	2709	25	1641	1043	38	-	-	38
JIS		2319	96	1516	707	196	90	36	70
Beo		59	6	30	23	-	-	-	-
Voj	2017	9355	21	2243	17091	1715	27	1679	9
SZS		3219	54	2022	1143	150	112	38	0
JIS		1949	191	826	932	-	-	-	-
Beo		59	6	23	30	-	-	-	-
Voj		19943	21	2823	17099	1911	28	1682	201
SZS	2018	3406	-	1367	2039	116	33	51	32
JIS		1523	43	625	855	-	-	-	-
Beo		18	6	6	6	-	-	-	-
Voj		19371	22	2243	17106	1919	30	1684	205
SZS	2019	2801	-	858	1943	33	33	-	-
JIS		1859	38	985	836	135	135	-	-
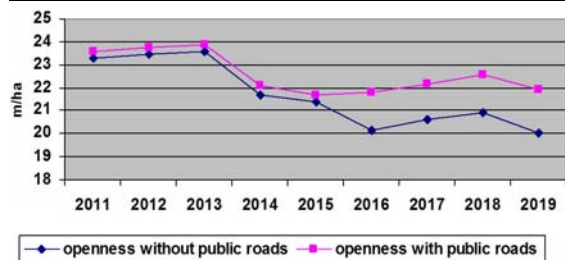
Figure 1. *Average openness of state forests in Serbia, 2011-2019.*

It is worth noting in Table 4 that on the territory of Serbia there is an expressed unevenness of openness of forest areas and that there are many insufficiently open forest areas, so it is necessary to consider the density of forest roads of smaller spatial units.

Forest openness (excluding public roads) is highest in Vojvodina region and significantly lower and insufficient in other regions (see Table 4). It has been shown in Table 4 that the openness of forests in three regions in Serbia is significantly lower than the

recommended density of 7 to 10 m/ha of forest roads in the low relief plains, [7].

Table 4 *Internal openness of state forests in statistical regions of Serbia (m/ha)*

		Region		
Year	Belgrade	Vojvodina	Sumadija and W. Serbia	South. and E. Serbia
2011	1,0	125,8	4,7	2,6
2019	0,35	131,5	2,8	1,8

Danilović and Stojnić [5] state that calculating the density of the road network only on the basis of the ratio of the length of roads passing through the department and the area of the department does not yield precise data, so the spatial distribution of roads is much more important. Pichman and Pentek [13] state that absolute (classical) openness gives a rough picture of the quantitative state of forest roads in an area without information about their spatial distribution.

Importance of forest roads to fire protection

Through careful planning, design and maintenance of the road network, forest opening is of primary importance to forest use and crucial for sustainable management [9]. Krč and Beguš [10] point out that the construction of a network of forest roads is considered a key element for successful forest management. Stefanović et al. [17] state that one segment of the process of planning the forest road network is achieving effective prevention and fire suppression. Good communication in forest areas is extremely important in risk management during forest fire protection. Forest roads play a key role in firefighting activities [11]. Built infrastructure, if it is denser and of good quality, enables access to all forest areas, a shorter arrival and the beginning of firefighting intervention, and rapid delivery and use of firefighting equipment, as well as the possibility to determine the location of a fire barrier. The disadvantage is the passage of the road through the forest area due to the possibility of triggering fires by passengers and vehicles [21]. An overview of the impact of the openness of the forest complex on fire risk, expressed by points, is shown in Table 5.

Table 5 *Impact forest complex openness on forest fire risk*

Openness of the forest complex	Points
The forest complex is open (most areas are accessible by a built road network, fire lines are regularly maintained)	5
The forest complex is partially open (larger parts of the forest complex are poorly accessible, or are accessible by forest roads unsuitable for fire trucks, fire lines are poorly maintained)	20
The forest complex is not open, there are no fire trucks	40

The efficiency of extinguishing forest fires largely depends on the time that elapses from the occurrence of the fire until the arrival of the team at the place of intervention. The period from the moment of fire detection to the notification of the competent services, their arrival and the beginning of fire extinguishing can be quite long. As a consequence, fire can develop without control and significant areas can be caught by fire. If the period from fire occurrence to brigade arrival was shorter, the efficiency of fire extinguishment would increase and the required extinguishing time would be reduced, and thus the area affected by the fire. Table 6 shows the interdependences between the efficiency of extinguishing forest fires and the time of fire occurrence until the arrival of the team at the place of intervention.

Table 6 *Fire extinguishing efficiency depending on the time of occurrence to the beginning of extinguishing*

Time from the beginning of fire to arrival at the scene (min)	Forest fire extinguishing efficiency
≤15	Extremely good
>15≤30	Very good
>30≤60	Good
> 60≤ 90	Depending on several factors
> 90	Unpredictable

Roads, as a natural barrier in the vicinity of a fire, can be used to determine the location of obstacles to the spread of fire, Figure 2.
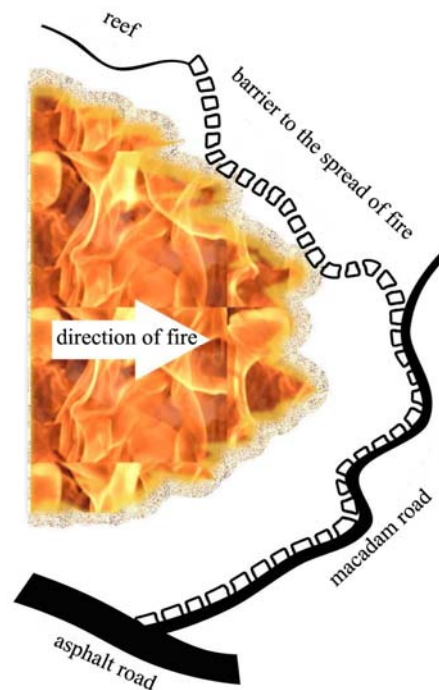

Figure 2. *Location of fire barrier depending on natural barriers*

CONCLUSION

Forest fires are a very significant threat to the stability of forest ecosystems and the environment as a whole. The construction and maintenance of roads in forest areas are of exceptional importance to risk management in forest fire protection. The construction of new roads increases the external and internal openness of the forest areas, and thus provides better communication, which is a prerequisite for the efficiency and effectiveness of the organization of firefighting. On the territory of Serbia, the uneven distribution of the road network is evident, as well as the openness of forest areas. It is a worrying fact that the forest areas which are in Sumadija, Western Serbia, Belgrade, Southern and Eastern Serbia have minimal openness, which means it is difficult to access the places on fire. The fact that the road network did not increase in the 2011-2019 period indicates that this aspect was not taken into account.

For this reason, it is necessary to:

- compile a detailed register of the existing forest road infrastructure of the state and private forests,

- define the criteria to determine the density of the existing forest road infrastructure,

- undertake activities for the construction of new roads in order to achieve optimal openness of the region's forests: Belgrade, Southern and Eastern Serbia, and Sumadija and Western Serbia.

ACKNOWLEDGEMENTS

REFERENCES

[1] L. Ambrušová, D. Halaj, J. Ilavský, J. Marttila (2013): Atlas of the forest sector in Slovakia. Working Papers of the Finnish Forest Research Institute 257, p. 38.

[2] S. Banković, M. Medarević, D. Pantić, N. Petrović (2009): Nacionalna inventura šuma Republike Srbije - šumski fond Republike Srbije. Beograd: Ministarstvo poljoprivrede šumarstva i vodoprivrede Republike Srbje - Uprava za šume, Beograd.

[3] R. Bereziuc, V. Alexandru, V. Ciobanu, E.C. Musat, A-E. Dumitrascu, C. Antoniade, J. Visan (2015): The Density Index of Forest-Road Network Managed by the National Forest Administration (R.N.P.). Proceedings of the Biennial International Symposium - Forest and Sustainable Development. Transilvania University Press, Brasov, pp: 196-203.

[4] M. Ćurić, S. Živanović (2013): Dependence between Deficit and Surplus of Precipitation and Forest Fires. Disaster Advances, 6(6), pp: 64 - 69.

[5] M. Danilović, D. Stojnić (2014): Assessment of the state of a forest road network as a basis for making a program of forest management unit opening. Bulletin of the Faculty of Forestry, 110, pp: 59-72.

[6] S. Dražić, M. Danilović, D. Stojnić, V. Blagojević, R. Lučić (2018): Otvorenost šuma i šumskog zemljišta u Bosni i Hercegovini, entitetu Republici Srpskoj, Šumarski list, 142(3-4).

[7] FAO- Food and Agriculture Organization of the United Nations, (1998): A Manual for the Planning, Design and Construction of Forest Roads in Steep Terrain, FAO, 130 p.

[8] M.R. Ghaffarian, K., Stampfer (2007): Optimum road spacing of forwarding operations: A case study in Southern Austria. In Proceedings of Austro2007/FORMEC 07: Meeting the Needs of Tomorrows Forests – New Developments in Forest Engineering, October 7 – 11, Vienna and Heiligenkreuz – Austria.

[9] S. Grigolato, E. Marchi, A. Laschi, R. Cavalli (2019): Considerations on forest road networks and related works to support the implementation of the operative guidelines of the consolidated law on forests and forest chains, Forest, 16, pp: 49-55.

[10] J. Krč, J. Beguš (2013): Planning Forest Opening with Forest Roads. Croatian Journal of Forest Engineering 34(2), pp: 217-228.

[11] A. Laschi, C. Foderi, F. Fabiano, F. Neri, M. Cambi, B. Mariotti, E. Marchi (2019): Forest Road Planning, Construction and Maintenance to Improve Forest Fire Fighting, Croatian Journal of Forest Engineering 40(1), pp: 207-219.

[12] S. Onur, B. Suha, D. Cenk (2015): Mapping regional forest fire probability using artificial neural network model in a Mediterranean forest ecosystem, Geomatics, Hatural Hazards and Risk.

[13] D. Pičman, T. Pentek (1998): Relativna otvorenost šumskoga područja i njena primjena pri izgradnji šumskih proupožarnih prometnica, Šumarski list 1-2 (19-30).

[14] RZS (2021): http://webrzs.stat.gov.rs, Republički zavod za statistiku, Beograd.

[15] G. Sekulić, D., Dimović, K. K. Jović, Z., N. Todorović (2012): Vulnerability evaluation of climate change-Serbia (in Serbian), WWF (World Wide Fund for Nature) and Center for Environmental Improvement. Belgrade. p.66.

[16] B. Stefanović (2007): Model putne infrasrukture Deliblatske peščare sa aspekta zaštite šuma od požara, Šumarstvo (1-2), pp: 81-91.

[17] B. Stefanović, D. Stojnić, M. Danilović (2015): Multi-criteria forest road network planning in fire-prone environment: a case study in Serbia, Journal of Environmental Planning and Management 59(5).

[18] S. Stoilov, T. Krumov, N. Uchikov (2014): Study of forest road net-work in Central Rhodoppes mountains (in Bulgarian with English abstract). Mechanics, Transport, Communications - Academic journal, Vol. 12(3/3), pp: VIII-1 - VIII-8.

[19] I. Tošić, D. Mladjan, B.M. Gavrilov, S. Živanović, G.M. Radaković, S. Putniković, P. Petrović, I. Krstić Mistridželović, B.S. Marković (2019): Potential influence of meteorological variables on forest fire risk in Serbia during the period 2000-2017. Open Geosci. 11, pp: 414–425.

[20] I. Tošić, S. Živanović, M. Tošić (2020): Influence of extreme climate conditions on the forest fire risk in Timočka Krajina region (Northeastern Serbia), Idojaras 124 (3), pp: 331–347.

[21] M. Vasić (1984): Zaštita šuma od požara, Nolit Beograd.

[22] Zakon o prostornom planu Republike Srbije od 2010. do 2020. godine ("Sl. glasnik RS", br. 88/2010) (2010a).

[23] Zakon o šumama ("Sl. glasnik RS", br. 30/2010, 93/2012, 89/2015 i 95/2018 - dr. zakon) (2010b).

[24] Zakon o regionalnom razvoju (2009) - ("Sl. glasnik RS", br. 51/2009, 30/2010 i 89/2015 - dr. zakon)

[25] S. Živanović (2012): Analiza promene klimatskih elemenata u cilju predikcije šumskih požara. Topola/Poplar, (189/190), pp: 163-170.

[26] S. Živanović (2017): Impact of drought in Serbia on fire vulnerability of forests, Int.J.Bioautomation 21(2), pp: 217-226.

[27] S. Živanović, J.M. Gocić, M. Vukin, V. Babić (2018): Značaj poznavanja uslova vlažnosti na učestalost i intenzitet šumskih požara, Šumarstvo, Beograd, (3-4), pp: 117-126.

[28] S. Živanović, R. Ivanović, M. Nikolić, M. Đokić, I. Tošić (2020a): Influence of air temperature and precipitation on the risk of forest fires in Serbia. Meteorology and Atmospheric Physics, 132(6), pp: 869-883.

[29] S. Živanović, I. Tošić (2020): Influence of climatic conditions on fire risk in Djerdap National park (Serbia) - A Case Study of September 2011, Thermal science, 24(5A), pp: 2845-2855.

[30] S. Živanović (2020): Influence of deficit and surplus of precipitation on the forest fire risk in area of Timocka Krajina, Disaster Advances, 13 (6), pp: 37-41.

[31] S. Živanović, D. Zigar, D. Krstić (2013), The Role of Early Detection of Forest Fire in Environmental Protection, Safety Engineering. 3 (2), pp: 93-97.

BIOGRAPHY of the first author

Stanimir Živanović was born in 1960. He obtained B.Sc., M.Sc. and Ph.D. from the Faculty of Occupational Safety in Niš. He worked in the Ministry of Internal Affairs – Emergency Management, Department in Bor as a fire safety specialist, from 1983 to 2013. He is the author and co-author of three monographs, over twenty scientific papers published in international journals and scientific conferences. His research interests involve fire protection and environmental protection.

ŠUMSKE SAOBRAĆAJNICE U FUNKCIJI ZAŠTITE ŠUMA OD POŽARA

Stanimir Živanović, Darko Zigar, Janko Čipev

Rezime: *Planiranje, izgradnja i održavanje šumskih puteva je od izuzetnog značaja za uspešno gašenje požara na odredjenom prostoru. Ova studija se fokusira na sagledavanje postojeće tehničke infrastrukture u državnim šumama Srbije. Prosečna otvorenost šuma u Srbiji na kraju 2019. godine iznosi 20,14 m/ha i 21,89 m/ha sa javnim putevima. U periodu od 2011. do 2019. godine prosečna otvorenost državnih šuma u Srbiji je smanjena za 3,12 m/ha, odnosno za 1,67 m/ha otvorenosti sa javnim putevima. Otvorenost šuma šumskim putevima je najveća i optimalna na području regiona Vojvodina (131,5 m/ha) a znatno manja i nedovoljna u regionima: Beogradski (0,35 m/ha), Šumadija i Zapadna Srbija (2,8 m/ha), i Južna i Istočna Srbija (1,8 m/ha). U poređenju sa 2011. godinom otvorenost šuma 2019. godine je uvećana u regionu Vojvodine a smanjena u drugim regionima u Srbiji. Šumski putevi koji imaju kolovoz od asfalta, betona ili kamene kocke su najmanje zastupljeni, oko 0,27%. Najveća je zastupljenost šumskih puteva sa podlogom (kameni ili šljunčani tvrdi donji sloj) oko 82,7%.*

Ključne reči: otvorenost šuma, šumski putevi, šumski požar, Srbija

VESNA MILTOJEVIĆ [1]
IVANA ILIĆ KRSTIĆ [2]
ANĐELIJA ORLIĆ [3]

[1]University of Niš,
Faculty of Occupational Safety
[2]University of Niš,
Faculty of Occupational Safety
[3]M.Eng. in Occupational Safety

[1]vesna.miltojevic@znrfak.ni.ac.rs
[2]ivana.ilic@znrfak.ni.ac.rs
[3]snezanaorlic@gmail.com

BURNOUT IN MASTER'S STUDENTS – A CASE STUDY

Abstract: *Burnout is associated with long-term exposure to workplace stress and it comprises exhaustion, cynicism, and the feeling of inadequacy as its dimensions. University students are exposed to a variety of stress-inducing factors during their studies regardless of the fact that they are not employees. The aim of this study is to examine the relations between specific sociodemographic variables and burnout dimensions among students of master academic studies. School Burnout Inventory (SBI-U 9) is used as the research instrument. The obtained results indicate that there is a connection between students' gender and tuition fee status and burnout. Gender is associated with exhaustion and the feeling of inadequacy, while tuition fee status affects all three dimensions.*

Key words: burnout, gender, tuition fee status, preventive measures

INTRODUCTION

Occupational burnout was first investigated in the second half of the 20th century, at first in the so-called helping professions. Soon after, it was discovered that prolonged exposure to stress is not typical for these professions only, so burnout studies were expanded to schoolchildren and university students.

Previous studies have shown that academic burnout occurs as a result of stress caused by both personal and organizational factors. Organizational factors refer to the structure of study programmes: number of courses, organization of classes, duration and time of exam periods, exam schedules in the exam periods, the extent of pre-exam duties, extent of library holdings, internet access, quality of classroom and laboratory equipment, lack of information regarding study programme requirements, and so forth. The list should be appended with interpersonal relationships between the teaching and non-teaching staff and the students as well as between the students themselves, lack of financial support in the form of scholarships, and students' expectations of themselves and their families, friends, and professors [1, 2].

Academic burnout is investigated via three dimensions – exhaustion, cynicism, and the feeling of inadequacy. Exhaustion is related to exertion when performing one's academic duties. Academic cynicism implies an indifference towards one's duties and a sense of detachment from them. Inadequacy refers to the feeling of inefficiency regarding duty fulfillment and the loss of confidence in one's ambitions [3]. The three dimensions are usually investigated using two scales: the Maslach Burnout Inventory – Student Survey (MBI-SS) and the School Burnout Inventory (SBI-U 9).

Literature review suggests that burnout among university students has not been a topic of broader concern for Serbian researchers, especially with regard to students of technical and technological sciences. This motivated the present authors to investigate burnout among students at a faculty of the University of Niš. The aim is to establish the degree of student burnout and the influence of specific sociodemographic characteristics (students' gender and tuition fee status) on exhaustion, cynicism, and the feeling of inadequacy – the three dimensions of academic burnout.

RESEARCH METHODOLOGY

Research instrument

The School Burnout Inventory (SBI-U 9) was used as the research instrument and it contains nine items that examine the three burnout dimensions – exhaustion, cynicism, and the feeling of inadequacy – within three subscales. Exhaustion is examined via four items: (1) *I feel overburdened by my schoolwork*; (2) *I often sleep badly because of matters related to my schoolwork*; (3) *I brood over matters related to my schoolwork a lot during my free time*; and (4) *The pressure of my schoolwork causes me problems in my close relationships with others*; cynicism via three items: (1) *I feel a lack of motivation in my schoolwork and often think of giving up*; (2) *I feel that I am losing interest in my schoolwork*; and (3) *I am continuously wondering whether my schoolwork has any meaning*; and the feeling of inadequacy via two items: (1) *I often have feelings of inadequacy in my schoolwork*; and (2) *I used to have higher expectations of my schoolwork than I do now*. The degree of agreement/disagreement was evaluated on a 6-point Likert scale ranging from 1 (*I completely disagree*) to 6 (*I completely agree*). According to its authors, the scale has a good internal consistency with Cronbach's alpha (α) of 0.88, as do the subscales: exhaustion α=0.80, cynicism α=0.80, and the feeling of inadequacy α=0.67 [4]. The present research yielded α=0.86, which indicates good scale reliability and internal consistency. Reliability was also good for the exhaustion subscale, α=0.73, and cynicism, α=0.88, while a somewhat lower value was obtained for the feeling of inadequacy – α=0.55. Since the scale, as well as the subscales, is small, mean values of correlation between the items were also calculated. In the burnout scale, the mean value of correlations between the items is 0.42, while the

correlation of item pairs ranges from 0.14 to 0.80. In the exhaustion subscale, the mean value of correlations between the items is 0.40, while the correlation of item pairs ranges from 0.24 to 0.50. In the cynicism subscale, the mean value of correlations between the items is 0.71, while the correlation of item pairs ranges from 0.64 to 0.80. In the inadequacy subscale, the mean value of correlations between the items is 0.37, which is the same as the correlation of item pairs. All of the above results confirm the scale's validity on the research sample.

Research sample

The sample comprises 50 students of master academic studies out of the total of 135 enrolled at the Faculty of Occupational Safety, the University of Niš for the 2020/21 academic year. The research encompassed 21 male students (M), 42%, and 29 female students (F), 58%. The majority of the respondents, 37 (74%), have their tuition fee paid from the state budget, i.e. are budget-financed (B), while 13 (26%) pay for their own tuition, i.e. are self-financed (S).

The data were collected via a survey conducted using a Google questionnaire in November 2020.

The results were processed using descriptive statistical methods (frequency, percentages, mean value, standard deviation). The Chi-square test was used to identify the differences according to gender and tuition fee status, whereas eta squared was used to determine the influence between the groups. Data were processed through SPSS 20.0.

RESULTS AND DISCUSSION

Moderate burnout was found in 58.2% of the respondents, severe burnout in 32%, and mild burnout in only 9.2%. Moderate burnout was prevalent regardless of the students' gender and tuition fee status (Table 1).

Table 1. *Burnout degree in relation to gender and tuition fee status*

Gender		Mild	Moderate	Severe	Σ
M	N	6	9	6	21
	%	28.5	42.9	28.6	100
F	N	2	17	10	29
	%	6.9	58.6	34.5	100
Tuition fee status					
B	N	8	19	10	37
	%	21.6	51.4	27	100
S	N	0	7	6	13
	%	0	53.8	46.2	100

Even though the values of Pearson Chi-Square 4.291, df=2, Asymp. Sig. 0.117 and Pearson Chi-Square 3.992, df=2, Asymp. Sig. 0.141 do not indicate a statistically significant relationship, the data shown in Table 1 suggest that a higher percentage of female students and self-financed students exhibit moderate and severe burnout.

The values obtained for all three subscales indicate that a considerably higher percentage of female students

exhibit moderate exhaustion, cynicism, and feeling of inadequacy compared to the male students.

Table 2. *Gender and burnout dimensions*

Exhaustion		Mild	Moderate	Severe	Σ
M	N	6	9	6	21
	%	28.5	42.9	28.6	100
F	N	2	17	10	29
	%	6.9	58.6	34.5	100
Pearson Chi-Square=6.633, df=2, Asymp. Sig. 0.036					
Cynicism					
M	N	11	3	7	21
	%	52.4	14.3	33.3	100
F	N	11	16	2	29
	%	37.9	55.2	6.9	100
Pearson Chi-Square=10.666, df=2, Asymp. Sig. 0.005					
Inadequacy					
M	N	8	8	5	21
	%	38.1	38.1	23.8	100
F	N	2	20	7	29
	%	6.9	69	24.1	100
Pearson Chi-Square=8.001, df=2, Asymp. Sig. 0.018					

Eta squared of 0.045 indicates a moderate influence of gender on exhaustion. A somewhat higher percentage of male students (71.4%) partly agree, agree, or completely agree that they feel overburdened by their schoolwork compared to the female students (68.9%), but more female students in comparison partly agree, agree, or completely agree that they often sleep badly because of matters related to their schoolwork (F: 37.9%, M: 28.6%) and that they brood over matters related to their schoolwork a lot during their free time (F: 86.2%, M: 76.2%); an almost equal number of female and male students believe that the pressure of their schoolwork causes them problems in their close relationships with others (F: 37.9%, M: 38%). Eta squared values indicate that gender does not influence the first item, moderately influences the second item (0.061), and only weakly influences the third and the fourth item (0.011 and 0.020, respectively).

Although eta squared of 0.001 indicates that there is no influence of gender on academic cynicism, this dimension is slightly more pronounced among the male students. Higher percentages of male students partly agree, agree, or completely agree that they feel a lack of motivation in their schoolwork and often think of giving up (M: 23.9%, F: 20.6%), that they feel that they are losing interest in their schoolwork (M: 38.1%, F: 31%), and that they continuously wonder whether their schoolwork has any meaning (M: 47.6%, F: 37.8%). Eta squared values for all three items do not indicate an influence of gender on academic cynicism (0.008, 0.001, and 0.007, respectively).

Eta squared of 0.055 indicates a moderate influence of gender on the feeling of inadequacy, which is more pronounced among the female students, more of whom partly agree, agree or completely agree that they often have feelings of inadequacy in their schoolwork and that they used to have higher expectations of their schoolwork than they do now (37.9% and 65.5%,

respectively) than the male students (28.6% and 57.1%, respectively). Eta squared values indicate a moderate influence for the first item (0.061) and a weak influence for the second (0.030).

Results from previous studies on the relation between gender and academic burnout vary. The results obtained in the present study do not correlate with the results of a study involving university students where it was determined that exhaustion, as a burnout dimension, was more pronounced among male students [4, 5], but they partially correlate with results from other studies [1]. The high percentage of female students who exhibit moderate and severe burnout (Fig. 1) might be explained by the traditional understanding of the place and role of women in Serbian society. Namely, in addition to their professional, or in this case school, duties, they are usually responsible for doing housework and taking care of younger or older members of their households.
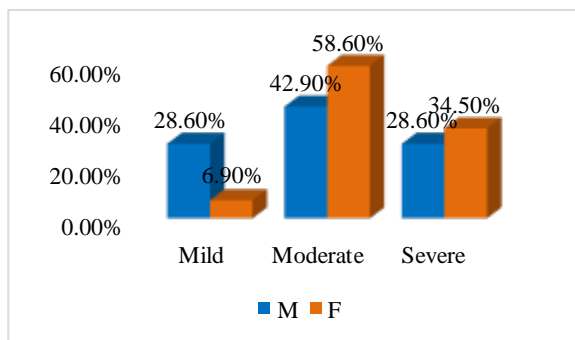

Figure 1. *Students' gender and burnout*

The data shown in table 3 indicate that a higher percentage of self-financed students exhibit moderate exhaustion and cynicism compared to budget-financed ones, but also that more budget-financed students feel inadequate than the self-financed ones. Although no statistical significance was found between the tuition fee status and burnout dimensions, the obtained mean values and eta squared values indicate that there is some influence of the tuition fee status on burnout dimensions, albeit a weak (B: M=2.1081, SD=0.61390; S: M=2.3077, SD=0.75107; eta squared 0.018) and moderate one on cynicism (B: M=1.6486, SD=0.71555; S: M=2.000, SD=0.81650; eta squared 0.043) and the feeling of inadequacy (B: M=1.9459, SD=0.66441; S: M=2.3077, SD=0.63043; eta squared 0.057).

Cumulative percentages indicate that a higher percentage of self-financed students partly agree, agree, or completely agree that they feel overburdened by their schoolwork (77%) compared to the budget-financed students (67.5%), that they often sleep badly because of matters related to their schoolwork (S: 46.2%, B: 29.4%), that they brood over matters related to their schoolwork a lot during their free time (S: 84.7%, B: 81.1%), and that the pressure of their schoolwork causes them problems in their close relationships with others (S: 38.5%, B: 37.8%).

Table 3. *Tuition fee status and burnout dimensions*

Exhaustion		Mild	Moderate	Severe	Σ
B	N	5	23	9	37
	%	13.5	62.2	24.3	100
S	N	2	5	6	13
	%	15.4	38.5	46.2	100
Pearson Chi-Square=2.517, df=2, Asymp. Sig. 0.254					
Cynicism					
B	N	18	14	5	37
	%	48.6	37.8	13.5	100
S	N	4	5	4	13
	%	30.8	38.5	30.8	100
Pearson Chi-Square=2.291, df=2, Asymp. Sig. 0.318					
Inadequacy					
B	N	9	21	7	37
	%	24.3	56.8	18.9	100
S	N	1	7	5	13
	%	7.7	53.8	38.5	100
Pearson Chi-Square=2.876, df=2, Asymp. Sig. 0.237					

Eta squared values indicate that the first item is not influenced by the tuition fee status, the second item is moderately influenced (0.075), while the third and fourth items are only weakly influenced (0.019 and 0.013, respectively).

A higher percentage of self-financed students partly agree, agree, or completely agree that they feel a lack of motivation in their schoolwork and often think of giving up (30.8%), that they feel they are losing interest in their schoolwork (46.2%), and that they continuously wonder whether their schoolwork has any meaning (46.2%) compared to the budget-financed students (18.9%, 29.7%, and 40.5%, respectively). Eta squared indicates that there is no influence of the tuition fee status on cynicism for the first item but that there is a moderate influence for the other two items (0.043 and 0.040, respectively).

The feeling of inadequacy is more pronounced among the self-financed students. Cumulative percentages indicate that more students in this category partly agree, agree, or completely agree that they often have feelings of inadequacy in their schoolwork and that they used to have higher expectations of their schoolwork than they do now (46.2% and 76.9%, respectively) compared to the budget-financed students (29.7% and 56.7%, respectively). Eta squared for both items indicates a moderate influence (0.075 and 0.093, respectively) of the tuition fee status on the feeling of inadequacy.

Such high percentages of students exhibiting moderate and severe burnout (Fig. 2) might be explained by personal factors as well as organizational and social circumstances surrounding the students. Since all self-financed students exhibit moderate or severe burnout, further research into this problem is warranted, as are prompt organizational preventive measures. Special attention should be given to the analysis of how well study programmes are harmonized with the actual needs of the economy and the society, how students find the means to finance their own studies, and how
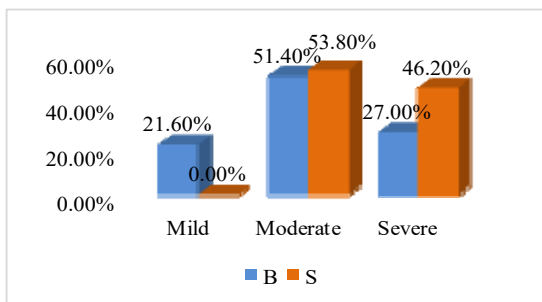
the teaching process is organized.

Figure 2. *Students' tuition fee status and burnout*

Research limitations and significance

The main limitation of this research is the sample size and the examination of the influence of a small number of sociodemographic variables on student burnout. Future studies should focus on aspects such as students' age, financial status (how they provide for themselves during their studies), duration of studies, living situation, health status, and so forth.

The greatest significance of this research is that it brings into focus the fact that there are master's students studying technical and technological sciences who exhibit burnout. Accordingly, the research should serve as a motivation to conduct further research and initiate specific activities by the faculties or universities.

CONCLUSION

The highest percentage of the surveyed students were found to exhibit moderate burnout. Gender differences were also observed for specific burnout dimensions, specifically, exhaustion and the feeling of inadequacy were more pronounced among the female students, while cynicism was prevalent among the male students. In terms of the tuition fee status, moderate and severe burnout were the most pronounced in self-financed students, for all three dimensions.

Burnout can affect the quality of life, which is why research on this issue is necessary in order to avoid long-term negative psychosocial effects on students as well as potential issues that higher education institutions could face if students were to drop out because of burnout.

Regardless of the aforementioned limitations, and because of the high percentage of students exhibiting

moderate and severe burnout, students need to be acquainted with some of the personal burnout prevention strategies and institutions need to devise institutional prevention strategies. This, however, requires additional efforts from every faculty employee and the creation of a special team that would analyze the incidence of burnout and propose organizational preventive strategies.

REFERENCES

[1] G. M. Osorio, R. C. Prado, S. Parrello & R. G. E. Bazan: "Caracteristicas Psicometricas y Estructura Factorial del School Burnout Inventory Student (SBI-U-9) en Estudiantes Universitarios Mexicanos", Revista Iberoamericana de Diagnosticoy Evaluacion — e Avaliagao Psicologica, Vol. 2(55), 2020, pp. 141-150.

[2] M. E. Barradas Alarcón, P. G. Trujillo Castro, A. V. Sanchez Barradas & J. López González: "Burnout estudiantil en universitarios veracruzanos", RIDE, Vol. 7(14), 2017, pp. 15-33.

[3] D. Kutsal & F. Bilge: "Adaptation of Maslach Burnout Inventory-student survey: Validity and reliability study", World Applied Sciences Journal, Vol. 19(9), 2012, pp. 1360-1366.

[4] I. M. Martinez Martinez & A. M. Pinto: "Burnout en estudiantes universitarios de España y Portugal y su relación con variables académicas", Aletheia, Vol. 21, 2005, pp. 21-30.

[5] K. Salmela-Aro, N. Kiuru, E. Leskinen & J. Nurmi: "School Burnout Inventory (SBI). Reliability and Validity", European Journal of Psychological Assessment, Vol. 25(1), 2009, pp. 48-57.

ACKNOWLEDGEMENTS

BIOGRAPHY of the first author

Vesna Miltojević is a full professor at the Faculty of Occupational Safety in Niš. Holding a PhD in sociological sciences, she teaches the following courses: Sociology, Sociology of Occupational Safety, and Social Ecology. A particular area of her interest involves the social aspects of occupational safety and environmental protection, such as motivation for work and safe work, and sustainable development.

Sagorevanje studenata master studija – studija slučaja

Vesna Miltojević, Ivana Ilić Krstić, Andjelija Orlić

Rezime: *Brnaut sindrom vezuje se za dugotrajnu izloženost stresu na radnom mestu, a kao dimenzije se navode iscrpljenost, cinizam i neadekvatnost. Studenti su izloženi raznim stresogenim faktorima tokom studija bez obzira što nisu formalno u radnom odnosu. Cilj istraživanja bio je ispitivanje odnosa nekih sociodemografskih varijabli i dimenzija sagorevanja studenata master akademskih studija. Primenjen je School Burnout Inventory (SBI-U 9). Dobijeni rezultati pokazuju da postoji veza između pola i statusa studenata i sagorevanja. Pol je povezan sa isrpljenošću i neadekvatnošću, a status stunetnata sa sve tri dimenzije.*

Ključne reči: sagorevanje, pol, status studenata, preventivne mere.

BOJANA ZLATKOVIĆ [1]
BILJANA SAMARDZIĆ [2]

[1]University of Niš,
Faculty of Occupational Safety,
[2] University of Niš,
The Faculty of Science and
Mathematics

[1] *bojana.zlatkovic@znrfak.ni.ac.rs*
[2]*biljana@pmf.ni.ac.rs*

PETRI NETS MODELLING OF SYSTEMS WITH REDUNDANCY

Abstract: *Petri nets are very appropriate for modelling and analysis of different systems. In this paper, examples of repairable and irreparable systems modelled using Petri nets have been given. Systems with cold and hot redundancy have been analyzed, also. The redundancy is illustrated using the example of the electric power system.*

Key words: redundancy, Petri nets, reliability.

INTRODUCTION

Petri Nets are a graphical and mathematical modeling tool applicable to many systems [1-6]. They are used for describing and studying information processing systems that are characterized as being concurrent, asynchronous, distributed, parallel, nondeterministic, and/or stochastic. As a graphical tool, Petri Nets can be used for visual - communication similar to block diagrams, networks. In these nets, markers are used to simulate the system dynamics. As a mathematical tool, it is possible to set up the state equations, algebraic equations and other mathematical models which describe the behaviour of a dynamical system.

Petri nets are very appropriate for reliability modelling and analysis of different systems. Petri nets can be applied in the field of systems safety, logistic, industry, computer science, etc. They are simple, easy to expand and analysed using simulation. Petri nets are the only class of graphs allowing complete analysis of reliability [7-11]. If some of the system state coordinates are random variables, Stochastic Petri nets can be used for the analysis of such systems.

Reliability is one of the most important criteria which must be taken into consideration during all phases of system: planning, designing and exploitation. During the exploitation, the system is under influence of different factors, exterior and interior, i.e., wear, corrosion, aging, etc. These factors can change the system's characteristics and have a strong influence on its work. Also, they can change the values of system parameters and their reliability and in limited cases can bring the system to instability or failure, [12, 13].

System reliability can be increased by using redundancy. Examples of repairable and irreparable systems modelled using Petri nets have been given.

The work of the system with cold and hot redundancy was analyzed on specific examples.

SYSTEM RELIABILITY AND REDUNDANCY

The scientific and technical progress of systems results in the appearance and development of reliability theory. Complex systems should have high reliability considering the consequences of their failures

influencing further work and people security.

Increasing the reliability of the system can be achieved in two ways: 1)increasing the reliability of system components, 2) using redundancy.

For the component to better perform its function, when choosing the system components, working conditions must be taken into account: ambient temperature, humidity, pressure, mechanical loads, allowable energy losses, the required stability of parameters, etc., as well as the causes of component failure under system working conditions. The component should be used in conditions that best suit its properties and characteristics. The use of components in normal regimes reduces the intensity of aging, i.e., prolongs the period of normal operation, and also reduces the intensity of the development of potential defects that can lead to component or system failure.

Redundancy means the introduction of an additional number of elements to fulfill the given functions in the given conditions. These additional elements are called spare elements, while the basic and spare elements form a redundant group. If the elements of the system have relatively low reliability, the spare elements are connected in parallel to them and are in the same working conditions. If the elements of the system are sufficiently reliable, the spare elements take over their function upon their failure.

If during the system work, the system is not repaired and its elements are not replaced, it is considered irreparable in which the time of failure-free work refers exclusively to the period from the start of work to the first failure. Otherwise, it is repairable. With these systems, it can be assumed that there is a time of failure-free work until the first failure, from the first to the second failure, from the second to the third, etc. Repairing means replacing defective parts after which the system is restored to a new condition. It is assumed that the recovery time is a random variable with a known probability distribution function. Depending on the work regime of the spare elements, there are three types of system stand by redundancy: cold, hot and warm redundancy. In the case of hot redundancy, the spare elements are in the same operating mode as the basic element and therefore their reliability does not depend on the moment of switching on the place of the basic element, as well as on the failure of other

elements. Such spare element works in parallel with the basic element and is included only when the basic element fails.

In case of cold redundancy, the spare elements are switched off and cannot be canceled in that period, and they start working upon arrival at the place of the basic element. The redundancy is "cold" because the spare element does not work when the basic element is correct. After the repair, the basic element is put into operation again, and the spare is switched off.

If the spare elements are less loaded than in normal operating mode, this is a warm redundancy. The reliability of these elements is higher while they are in reserve than when they are included in the place of the basic element.

The analysis of hot and cold redundancy led to the conclusion that the system reliability indicators, for the same reserve group, are higher for cold redundancy, i.e., a cold redundancy is more reliable than a hot one. On the other hand, redundancy is more reliable if there is a larger reserve group. However, an increase in the reserve group causes an increase in other system parameters: weight, volume, price, etc.

THE BASIC ELEMENTS OF PETRI NETS

Petri net is a special case of a directed graph with an initial state called initial marking, M_0. Also, Petri net represents a bipartite, weighted graph consisting of two kinds of nodes called places and transitions. Nodes are connected by arcs. Arcs are directed either from place to transition or from transition to a place. Places are denoted by circles and transitions by bars or boxes. Arcs are labeled with their weights (positive integers), so the k – weighted arc can be interpreted as a set of k parallel arcs. A place is an input place to a transition if there exists a directed arc connecting this place to the transition, and vice versa.

Each place p is marked with nonnegative integer k. It is said that the place is marked with k tokens. Marking is denoted by m – vector M, where m is the total number of places. The pth element of vector M, denoted as $M(p)$, represents the numbers of tokens in place p.

The presence or absence of a token in a place can indicate whether a condition associated with this place is true or false, for instance. At any given time instance, the distribution of tokens on places, called Petri Net marking, defines the current state of the modeled system.

In its simplest form, a Petri Net may be represented by a transition together with its input and output places. This elementary net may be used to represent various aspects of the modelled systems.

Petri Net can be defined as $\mathrm{PN} = (P,T,I,O,M_0)$, where

1. $P = \{p_1, p_2, \ldots, p_m\}$ is a finite set of places,

2. $T = \{t_1, t_2, \ldots, t_n\}$ is a finite set of transitions, $P \cup T \neq \varnothing$, and $P \cap T = \varnothing$,

3. $I : (P \times T) \mapsto N$ is an input function defining directed arcs from places to transitions, where N is a set of nonnegative integers,

4. $O : (P \times T) \mapsto N$ is an output function defining directed arcs from transitions to places, and

5. $M_0 : P \mapsto N$ is the initial marking.

The following rules are used to govern the flow of tokens.

Enabling Rule: A transition t is said to be enabled if each input place p of t contains at least the number of tokens equal to the weight of the directed arc connecting p to t.

Firing Rule:
(a) An enabled transition t may or may not fire and
(b) a firing of an enabled transition t removes from each input place p the number of tokens equal to the weight of the directed arc connecting p to t. It also adds in each output place p the number of tokens equal to the weight of the directed arc connecting t to p.

Classical Petri nets can be used only for the analysis of qualitative system characteristics because they do not contain the time concept. It is possible to describe the logical structure of the modelled system only.

By introducing the time into Petri nets, the Timed Petri nets are obtained. They can be used for the quantitative analysis of the system too.

In most Time Petri nets, a time delay is given to the transitions. Only in some types of Petri nets, a time delay is given to the places and/or arcs. Tokens of place p become unreachable to all input transitions for a certain time period. Petri nets like this are called *Timed Places Petri nets* (TPPNs). However, it is convenient to give delays to the transitions because they represent activities that are performed on time. When transition becomes enabled it will fire after a certain time. Petri nets like this are called *Timed Transitions Petri nets* (TTPNs). If time is a random variable, we talk about Stochastic Petri nets (SPN).

PETRI NETS MODELLING OF SYSTEMS WITH FAILURES

This section deals with the simple examples of how Petri nets can be used to model systems with failures and how those failures can be removed.

The following figure shows the Petri net of a system consisting of one component that can be repaired after a failure. Note that the presence of a marker in place means that the system is working, while the absence of a marker in place indicates that the system is in a failed state. The presence of a marker in a place indicates the current state of the system and indicates that that place is activated. Also, the presence of markers in the place indicates the occurrence of failure. The transition is activated only after the expiration of the time interval L, which represents the time of proper operation of the system. The system is in the state of failure (marker in

place) until the transition is activated, i.e., after the expiration of time *D*.
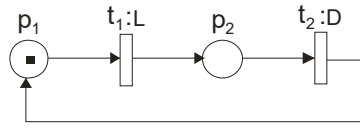
Figure 1. *System with one repairable component*

Figure 2 shows the Petri net of the system, which consists of two components that can be repaired independently in the event of a failure. The entire system fails if both components fail. L_i and R_i $i = 1,2$ indicate the switching times of the appropriate transitions, i.e., the time of correct operation of the component and the time required for repair of the component if a failure occurs, respectively, while *D* in place p_6 indicates that the system is in a state of failure. If, during the repair of one component, another component fails, the repair of the first component is stopped due to the failure of the entire system.
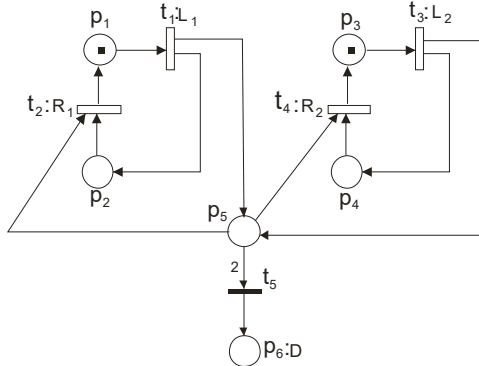
Figure 2. *System with two repairable components*

So far we have analysed the systems that can be repaired after a failure and these are repairable systems. However, some systems cannot be repaired, but components that have failed can be replaced with new ones. Such systems are called irreparable systems. These systems are much easier to model with Petri nets than repairable systems. Figure 3 shows a general scheme of an irreparable system with *n* components. In this system, if one component fails, the entire system goes into failure. The presence of a marker in place means that the system is working properly.

Section 2 discussed the cold redundancy. This is an element that is included in the system in case a component fails. The spare is "cold" because the spare does not work until it replaces the failed component. Figure 4 shows a system in which the component has a working life lasting from L_1 time moments and in case of failure there are three reserves with which it can be replaced with time durations L_2 , L_3 , L_4, respectively. Transition t_5 and place p_6 model system failure status and ensure that the place p_1 is unmarked. The

inhibitory arc prevents more than one marker from being sent from place p_1 to place p_2.
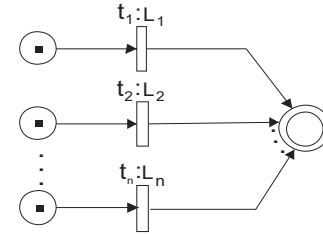
Figure 3. *General scheme of an irreparable system with n components*
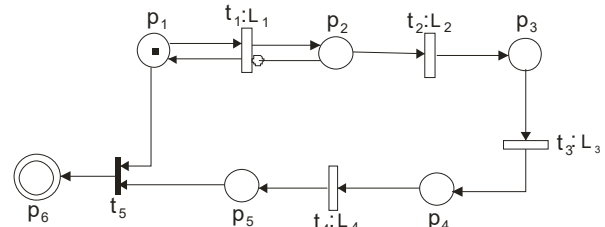
Figure 4. *Scheme of the system with 3 cold redundancies*

The following figure shows a scheme of a system with a hot redundancy.
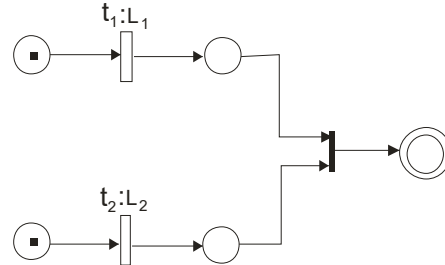
Figure 5. *Scheme of the system with hot redundancy*

The hot redundancy works in parallel with the component, but only turns on when the component fails. Transitions may be immediate (when enabling conditions are fulfilled) or timed with a delay > 0. The delays may be deterministic or stochastic. This means that stochastic Petri nets can be used in this case.

In most cases, a hot redundancy is cheaper than a cold redundancy.

Cold redundancy is best suited to non-critical processes where downtime is not a big concern and human intervention is possible. However, warm redundancy design is suited to processes where time and response are important but a momentary outage is still acceptable.

The redundancy is illustrated using the example of an electric power system, [14]. From power plant *E* through the power lines L_1 and L_2 consumer *C* is powered. Consumer C is connected to the buses *S*. Buses *S* are supplied from the local source *G* which is connected over switch *B*.

The following symbols have been introduced:

- IC - supply interruption of consumer C,
- x - malfunction at the same time of generator G and system for buses supply,
- z - malfunction of generator G and failure of switch B,
- y - malfunction at the same time of both wiring or malfunction of power plant E,
- v - malfunction at the same time of both wiring,
- $\overline{S}$ - malfunction of buses S,
- $\overline{E}$ - malfunction of the power plant,
- $\overline{G}$ - malfunction of the generator,
- $\overline{B}$ - failure of a switch,
- $\overline{L}_1, \overline{L}_2$ - malfunction of both wirings L_1 and L_2.

The appropriate Petri net is given in the next figure. This is an example of hot redundancy.

The presence of tokens in a place denotes that a certain event happened. By using classical Petri net, it can be determined if the failure of consumer C appeared or not. Stochastic Petri nets can be used if we want to determine the probability of failure.
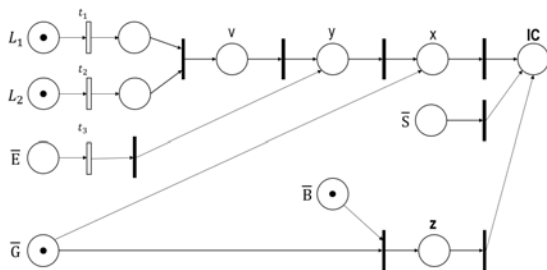
Figure 6. *Petri net of electric power system*

CONCLUSION

The appearance and development of reliability theory is a consequence of the scientific and technical progress of the systems. For the reliability analysis, Petri nets can be used successfully. Petri nets are the only class of graphs allowing complete analysis of reliability. In addition, Petri nets are a graphical and mathematical modeling tool applicable to many systems.

In this paper, examples of repairable and irreparable systems modelled using Petri nets have been given. The systems with cold and hot redundancy have also been analyzed.

REFERENCES

[1]   T. Murata, "Properties, analysis and applications", *Proceedings of IEEE*, 77(4):541-580, April 1989.

[2]   F. Bause, P. S. Kritzinger, "Stochastic Petri nets: An introduction to the theory", 2nd Edition, Vieweg, 2002.

[3]   R. German, C. Kelling, A. Zimmermann, G. Hommel, "TimeNET – A Toolkit for evaluating non – Markovian stochastic Petri nets".

[4]   G. Horton, "Stochastic Petri nets", *Introduction to Simulation* WS02/03 – L08.

[5]   P. J. Haas, "Stochastic Petri nets. Modeling, stability, simulation", Springer, 2002.

[6]   J. A. Borrie, "Stochastic Systems for Engineers", New   York, Prentice Hall, 1996.

[7]   J. M. Nahman, "Metode analize pouzdanosti elektroenergetskih   sistema", Naučna   knjiga, Beograd, 1992.

[8]   W. G. Schneeweiss, "The fault tree method" (From the field of reliability and safety technology), LiLoLe – Verlag GmbH, Hagen, 1999.

[9]   W. G. Schneeweiss, "Petri nets for reliability modeling" (In the fields of engineering safety and dependability), LiLoLe – Verlag GmbH, Hagen, 1999.

[10]   Bojana M. Vidojković, "Primena Petri mreža u analizi   pouzdanosti   upravljačkih   sistema", Magistarski rad, Elektronski fakultet, Niš, 2003.

[11]   B. Danković, B. Vidojković, "A Petri Net-Based Approach to Logic Control and a Case Study", Proceedings of the VI International SAUM Conference on Systems, Automatic Control and Measurements, Niš, September 1998, pp. 253-257.

[12]   M. Tomić, Adamović, "Pouzdanost u funkciji održavanja tehničkih sistema", Tehnička knjiga, Beograd, 1986.

[13]   S.   Jovičić,   "Osnovi   pouzdanosti   mašinskih konstrukcija", Naučna knjiga, Beograd, 1990.

[14]   B. M. Zlatković, B. Samardžić: "A New Approach for the System Time without Failures Determining Using Petri Nets", Safety Engineering, Scientific Journal, Vol. 5, No. 2 (2015), pp. 85–90, Faculty of Occupational Safety, University of Nis, *doi: 10.7562/SE2015.5.02.03*.

BIOGRAPHY of the first author

Bojana M. Zlatković was born in Jagodina, Serbia, in 1976. She received the B.Sc., M.Sc. and Ph.D. degrees from the Faculty of Electronic Engineering, University of Nis. She is currently working as an Associate Professor at the Faculty of Occupational Safety in Nis. Her main areas of research include reliability, probability of stability, chaos theory, etc.

MODELIRANJE SISTEMA SA REZERVOM KORIŠĆENJEM PETRI MREŽA

Bojana Zlatković, Biljana Samardžić

Rezime: *Petri mreže su veoma pogodne za modeliranje i analizu različitih sistema. U ovom radu su dati primeri popravljivih i nepopravljivih sistema modelovanih pomoću Petri mreža. Analizirani su i sistemi sa hladnom i toplom rezervom. Sistem sa rezervom je ilustrovan na primeru elektroenergetskog sistema.*
Ključne reči: rezervisanje, Petri mreže, pouzdanost.

Safety Engineering

**AMINU SUKAIRAJI[1],
USMAN ABUBAKAR
ZARIA[2],
IBRAHIM ALI
MOHAMMED-DABO[3]**

[1,2,3]Department of Chemical
Engineering, Ahmadu Bello
University, Zaria.

[1]augayya@yahoo.com

MODELLING AND EVALUATION OF THE EFFECTS OF HIGH BACK PRESSURE (HBP) ON REFINERY FLARE SYSTEM NETWORK

Safety and reliability of the flare system are often affected by High Back-Pressure (HBP). The primary aim of this study is to simulate a steady-state model of flare system using Aspen Flare System Analyzer and with the aid of real plant data generated from Kaduna Refining and Petrochemical Company (KRPC) Ltd, Nigeria. Three credible scenarios (normal operation/surplus fuel, cooling water failure and power failure) were considered. The results showed that the steady-state model of flare system for normal operation (Surplus Fuel), cooling failure and power failure scenario and the flare system meet performance requirements at a system back pressure of 1.01325 bar, except for cooling water failure scenario which showed the occurrence of high fluid velocity and momentum (rhoV²). Also, flare operation at normal back pressure, for all three scenarios does not exceed design and operational limits. The work recommends that KRPC managers should review options for reducing HBP particularly for cooling failure and power failure scenarios such that the back pressure would not exceed 10% of set pressure for the conventional valves.

Keywords: high back-pressure, safety engineering, flare system, relief valve, performance, Aspen Flare System Analyzer.

INTRODUCTION

Globally, the oil and gas industry is a critical sector of several economies and as such, ensuring the safety of the oil and gas facilities becomes paramount. For this reason, considerable effort has been focused, over the years on the prevention of major incidents. The oil and gas facilities are prone to challenges that can affect the effective operation and threaten process safety. Hence, the oil and gas industry has over the years emphasized process safety and asset integrity so as to prevent unplanned or emergency releases that could result in a major incident and threaten process safety. Process safety is a disciplined framework for managing the integrity of operating systems and processes, handling hazardous substances, and is achieved by applying good design principles, engineering, and operating and maintenance practices [1]. It entails the prevention and control of incidents that have the potential to release hazardous materials and energy such as the flare system in a refinery which can result in toxic exposures, fires, or explosions of facilities and could ultimately result in serious injuries, fatalities, property damage, lost production or environmental damage.

To mitigate the emergency or pressure build-up in the oil and gas facilities such as the refinery, a major safety requirement in oil and gas installations or facilities is a flare system which is usually installed to relieve pressure build-up that may occur during operation, shut down, start-up or due to power or process system failure or hazards associated with process emergencies. Therefore, the importance of flare system installation in several oil and gas facilities and as such, accurate design of the flare system plays a significant role in containing possible process safety hazards in the oil and gas facilities, particularly oil and gas offshore platforms [2,3]. This makes flaring a very important issue in the oil and gas industry.

Flaring is a high-temperature oxidation process used to burn combustible components, mostly hydrocarbons, of waste gases from industrial operations. Gas flaring is the combustion of associated gas produced with crude oil or from gas fields. Primarily gas flaring is employed for safety reasons. Hence, consideration of the release of gas to the atmosphere by flaring and venting becomes an essential practice in oil and gas production. Flaring is the controlled burning of natural gas produced in association with oil in the course of routine oil and gas production operations [1]. Venting is the controlled release of gases into the atmosphere in the course of oil and gas production operations. Solving the problem of this "nuisance" called venting while ensuring safe operation and minimizing undesirable venting, led to the introduction of flaring [4]. As such, one safety concern that frequently occurs in a flare system is the high back pressure, which is the sum of the superimposed and build-up back pressures [1, 5, 6].

However, the pressure that exists at the outlet of a pressure relief device is a result of the pressure in the discharge system [7]. In order to prevent dangerous bursts, explosions, and fires, pressure relief valves are designed and installed to bleed out excess liquid or vapor causing pressure build-up and as such, there are limits to the containable back pressure in the relief valves [8]. Effective and efficient flare system sizing must take into account the number of relief valves discharging into a common flare manifold or header, as the pressure drop

from each relief valve discharge through the flare tip must not exceed the allowable relief valve back pressure for all system flow conditions. For conventional relief valves, the allowable back pressure is typically limited to about 10% of the minimum relief valve upstream set pressure [1, 8, 9]. Several studies have been reported on the impact of back pressure on pressure safety valves in flare systems [1, 2, 3, 5, 6, 9, 10, 11]. However, no studies have been in the relevant current extant literature on the effects of high back pressure (HBP) on the pressure safety valves of the KRPC flare system. It is in view of this that the study evaluates back-pressure,

noise, and flow characteristics due to process upsets within the flare network for normal operation, cooling water failure and power failure scenarios. The objectives of the study are to simulate a steady-state model of flare system using Aspen Flare System Analyzer for three scenarios (normal operation/surplus fuel, cooling water failure and power failure), analyze the effect of back-pressure build-up on the flare system, evaluate the effect of high back-pressure on pressure-relieving devices and to recommend mitigation measures against the effect of HBP on the flare system.
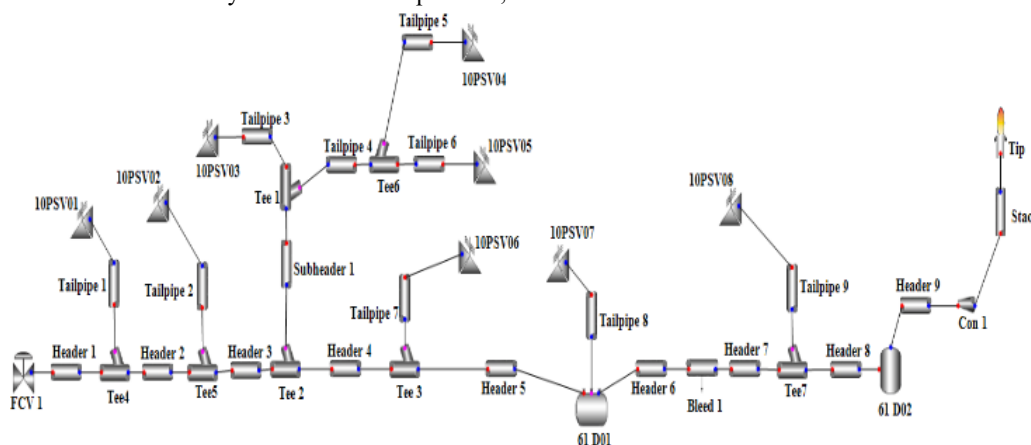
Figure 1: *Simulated model of flare system in Aspen FLARENET*

METHODOLOGY

The following data were collected from KRPC: composition of materials flowing through equipment and pipeline, a flow rate of materials passing through pipelines and equipment/pipeline conditions (phase, temperature, and pressure). This is followed by hazards identification, formulation of credible scenarios and articulation of the consequence modelling steps.

To formulate a structured approach to the identification of hazards, an understanding of contributory factors is essential. These factors include inventory analysis which was used in understanding the relative hazards and shortlisting of release scenarios. Initiating events Table 1: Collected pipe, tailpipe, header, sub-header and stack specification of KRPC flare system.

Assumptions
The following assumptions were made in the course of the modelling and simulation of the flare system using Aspen FLARENET:
1. The process is operating in steady-state condition.
2. Energy losses are assumed negligible.
3. Pressure losses in pipes are negligible

Simulation
Aspen Flare System Analyzer was used for the process simulation of the flare system network. This is because Aspen Flare System Analyzer provides reliable and comprehensive thermodynamic packages, a vast component library and advanced calculation techniques for flare system simulation. The procedure for the simulation mainly involves component selection, model

development by specifying pipes and relief valves sizes, operating conditions (temperature and pressure) as well as the scenario constraint specification for normal operation/surplus fuel scenario, cooling water failure scenario and power failure scenario. Figure 1 presents the simulated model of the flare system.

Table 1: *Design specifications for some elements of the flare system network*

Name	Length (m)	Nominal Diameter	Relief Valves	Mass Flow (kg/hr)
Tailpipe 7	10	2 inch	10PSV03	1500
Header 1	10	32 inch	10PSV05	2000
Header 4	25	32 inch	10PSV07	2000
Header 5	20	32 inch	FCV 1	118680
Header 6	10	32 inch	10PSV01	67440
Header 7	15	54 inch	10PSV02	2000
Header 9	20	54 inch	10PSV04	1130
Stack	60.741	54 inch	10PSV06	1560
Subheader 1	15	6 inch	10PSV08	34580
Tailpipe 3	5	6 inch		
Tailpipe 4	5	6 inch		
Tailpipe 8	10	12 inch		
Tailpipe 1	20	32 inch		
Header 2	25	32 inch		
Tailpipe 2	5	4 inch		
Header 3	20	32 inch		
Tailpipe 6	10	6 inch		
Tailpipe 5	5	2 inch		
Header 8	20	54 inch		
Tailpipe 9	10	28 inch		
Tailpipe 9	10	28 inch		

***Source**: KRPC Flare System Data*

RESULTS AND DISCUSSION
Effect of High Back-Pressure Build-Up on Flare System

The simulated flare system model was successfully done at normal operation, cooling failure and power failure case and used to test and analyse the effect of back pressure on the model flare system in order to ensure the safety and integrity of the whole asset. The effect of higher back pressure on the flare system as it is critical to the integrity of flare system design and operation which can affect either the set pressure or the capacity of a relief valve.

Table 2: *Effect of cooling water failure on back pressure during normal operation scenarios*

Name	1	2.	3.	4.	5.
Header 4	0.0	2.098	0.005	4	1.32080
Header 5	0.0	2.098	0.005	4	1.32079
Header 6	0.0	2.797	0.007	7	1.32073
Header 7	0.0	0.991	0.002	1	1.22072
Header 9	0.0	0.991	0.002	1	1.22070
Stack	0.0	0.991	0.002	1	1.21588
Subheader 1	34.3	52.776	0.119	2360	1.30891
Tailpipe 4	28.9	51.875	0.117	2319	1.35218
Header 2	0.0	0.000	0.000	0	1.32085
Header 3	0.0	0.000	0.000	0	1.32085
Header 8	0.0	0.991	0.002	1	1.22071
Tailpipe 9	0.0	0.000	0.000	0	1.22072
Tailpipe 7	0.0	4.596	0.011	21	1.32079
Tailpipe 3	0.0	0.000	0.000	0	1.32082
Tailpipe 6	0.0	0.000	0.000	0	1.32085
Tailpipe 5	0.0	0.000	0.000	0	1.32085
Tailpipe 2	0.0	0.000	0.000	0	1.32085
Header 1	0.0	0.000	0.000	0	1.35725
Tailpipe 1	0.0	0.000	0.000	0	1.36684
Tailpipe 8	31.7	51.322	0.116	2295	1.36454

Table Legend: 1. Noise (dB), 2. Upstream Velocity (m/s), 3 Upstream Mach No., 4. Upstream Rho V2 (kg/m/s^2), Downstream Static Pressure (bar)

Table 2 presents the effect of normal back pressure at the three scenarios of normal operation, a cooling failure and power failure case considered in this study respectively.

Also, Table 2 shows the effect of normal back pressure on the cooling water failure scenario of the model flare system. The operation of the KRPC's flare system at cooling water failure case shows that design violation occurred at Header 6, Header 7, Header 8 and Header 9 due to a slight increase in the flowing fluid momentum. This could be attributed to internal flow-induced forces across header 6 through to header 9 along with the flare system [2, 6, 12].

In the course of the simulation, it was observed that both upstream and downstream pressures were in the range of 1.31 and 1.38 bar.

From Table 2, it can be seen that the noise generated as a result of the normal back pressure in the PRVs is low. This indicates that in the cooling water failure scenario, the flare system does not generate excessive noise resulting from back pressure in the PRVs with less than 35 dB of noise across the few affected relief valves. However, there was no noise generated at the majority of the relief valve as well as FCV of the model flare system for the cooling water failure scenario. This could be attributed to the low momentum of the flowing fluid resulting from the low fluid velocity at the normal operation case of the model flare system.

Furthermore, the operation of the flare system at the power failure case shows the occurrence of design violation at the Tailpipe. This violation occurred due to back pressures at the relief valve to the tailpipe exceeding the Maximum Allowable Back Pressure (MABP) in the relieving valve which is attributed to a slight increase in pressure at the outlet of 10PSV07 which develops as a result of flow after the PRV opens [11].

It was also found that the noise generated as a result of the normal back pressure in the PRVs is low. This indicates that in the power failure case scenario, the flare system does not generate excessive noise resulting from back pressure in the PRVs with less than 30 dB of noise across all relief valves and FCV of the model flare system. This could be attributed to the low momentum of the flowing fluid resulting from low fluid velocity in the model flare system [6].

Another significant criterion for efficient operation of flare system is the Mach number which is a function of fluid velocity and the maximum velocity for flare headers and subheaders are expected not to exceed 0.6 Mach. As such, this study also examines the effect of back pressure on the flare system.

Table 2 also presents the effect of normal back-pressure on the Mach number at all relief valves of the model flare system for cooling water failure scenario. The maximum Mach number attained for all PSV's of the model flare system for cooling water failure scenario does not exceed 0.122 which is also well below the maximum velocity of 0.6 maximum Mach number for flare headers [1, 13]. This is attributed to the fact that the flare headers are of larger diameter than the other network pipes and the flare network is designed to handle the designed back-pressure [1]. The low Mach number of 0.122 also enhances the avoidance of pipe vibration and noise generation resulting from excess velocity in the flare network.

The maximum Mach number attained for all PSV's of the model flare system for power failure scenario does not exceed 0.092 which is also well below 0.6 maximum Mach number for flare headers design [1, 13]. This is due to the larger diameter of the headers compared to the other network pipes and that the flare network is designed to handle the designed back-pressure [1]. The low Mach number of 0.092 also helps in avoiding pipe

vibration and noise generation resulting from excess velocity in the flare network. Therefore, all case scenarios are well below the maximum design Mach number of 0.6.

Impacts of High Back-Pressure on Pressure Relieving Devices of Flare System

The impact of high back pressure on PSVs of the model flare system was further investigated at high back pressure of 5 bar deviation from normal back pressure of 1.2 bar. The effect of higher back pressure on the flare system is critical to the integrity of flare system design and operation which could affect either the set pressure or the capacity of a relief valve. Table 3 presents the effect of high back pressure at the three scenarios of normal operation, a cooling failure and power failure case considered in this study respectively.

Maximum Allowable Back Pressure was exceeded for 10PSV05, 10PSV07 and FCV 1. It can be seen from the flare system model, that high back pressure in the flare system at normal operation scenario results in high back pressure activities in the Tailpipe 1, Tailpipe 5 and Header 1. This is due to internal pressure development above the maximum allowable back pressure in the flow control valve (FCV) and a few relief valves. This in turn affects the set pressure (the pressure at which the relief valve begins to open) and even the capacity (the maximum flow rate that the relief valve will relieve) of the affected relief valves in the flare system. The set pressure for a conventional relief valve increases directly with back pressure which can be compensated for constant back pressure by lowering the set pressure [8]. The effect of high back pressure experienced in FCV and relief valves result in variation in back pressure (is usually not constant) which is attributed to the affected relief valve or other relief valves relieving into the flare header. Also, it can be seen that the system back pressure exceeded the maximum allowable back pressure of the flare system resulting from 10PSV05, 10PSV07 relief valve and FCV. This indicates that a normal operation scenario, high back pressure would affect the performance of the flare system relief valves and flow through the flare header [2, 12]. Hence, excessive back pressure at a pressure relief valve affects the performance of that valve which could potentially result in instability and a significant reduction in flow capacity across the flare header, jeopardizing the safety of the equipment which the valve is meant to protect. However, it can be seen that at high back pressure and for normal operation scenarios, the flare system does not generate noise resulting from back pressure in the PRVs.

From Table 3, it can be seen from the flare system model, that high back pressure in the flare system at cooling water failure scenario results in design violation at the Subheader, Tailpipe, relief valve and FCV. This resulted in an increase in the system velocity for the Subheader from 13.754 m/s to 13.774 m/s, Tailpipe 4 from 13.738 m/s to 13.745 m/s, Tailpipe 6 from 13.728 m/s to 13.736 m/s and excess fluid velocity of 13.7 m/s for 10PSV05 and 19.3 m/s for 10PSV07 relief valves for cooling water failure scenario. This high velocity in the relief valve 10PSV07 due to high back pressure resulted

in 1456 $kg/m/s^2$ momentum development in the model flare header. However, the momentum generated in 10PSV07 relief valves is well below the design maximum limit of $\rho V2 < 200000$ $kg/m/s^2$ [12], which is acceptable and helps to limit or prevent turbulence or induced vibration that could result in noise, acoustic fatigue, pipe stress, erosion, etc. in the flare network.

Table 3. *Effect of high back pressure on the model flare system for cooling water failure scenario*

Valve	Remark
10PSV05	Velocity Violation at Flange
10PSV07	Maximum Allowable Back Pressure Exceeded
10PSV07	Velocity Violation at Flange
10PSV07	RhoV2 Violation at Flange
FCV 1	Maximum Allowable Back Pressure Exceeded.

PSV: Pressure Safety Valve and FCV: Flow Control Valve

From Table 3, it can be seen that the system back pressure exceeded the MABP of the flare system resulting from the 10PSV07 relief valve (allowable back pressure of 5.12486 bar) and FCV (allowable back pressure of 5.0 bar). This indicates that in the cooling water failure scenario, high back pressure would affect the performance of the flare system relief valves and flow through the flare headers [2, 10, 12]. For this reason, excessive back pressure at a pressure relief valve could potentially lead to instability and a significant reduction in flow capacity across the flare header and could threaten the safety of the equipment which the valve is meant to protect [11]. Therefore, higher back pressure in the model flare system could result in turbulence or induced vibration in the PRVs.

It was also shown that the flare system model at high back pressure for power failure scenario results in design violation across all the relief valves and the control valve except for the 10PSV05. It can be seen that in the power failure scenario, the back pressure of the modelled flare system for all pressure relief valves except 10PSV05 exceeded the allowable back pressure for the power failure scenario. Also, it can be seen that the back pressure at the FCV exceeded allowable back pressure. The high flare system back pressure led to an increase in pressure at the outlet of the affected relief valves which develops as a result of flow after the pressure relief valves open [10]. This would significantly affect performance of the relieving valve by reducing both its set pressure and its capacity leading to chatter (rapid opening and closing), which can damage the valve [1, 11].

Maximum allowable back pressure was exceeded for relief valves 01 to 08, including FCV. Also, it was observed that the impact of high back pressure on the model flare result in design and operation violation across the flare system (Table 3). It was also shown that the impact of high back pressure could affect the relief of hydrocarbon fluid to Tailpipe 1, Tailpipe 5, Tailpipe 3, Tailpipe 7, Tailpipe 8, Tailpipe 9, and Header 1 in the model KRPC's flare system for power failure scenario.

This violation occurred because the back pressures at almost all the relief valve and FCV control valves exceed the maximum allowable back pressure in the relieving valve. This is attributed to an increase in pressure at the outlet of the affected relieving valve which develops as a result of flow after the PRV opens [11, 14, 15], and also because many PSVs are relieving hydrocarbon fluid at the same time for power failure scenario.

Mitigation Measures against High Back Pressure On the Modelled Flare System

High back pressure operation in the flare system is a threat to the safety and efficiency of the flare system and could jeopardize the equipment integrity and safety. The effect of high back pressure on relief valve capacity is much more significant and could reduce the PRV's capacity by approximately 50%.

From the study, it was established that superimposed back pressure has an impact to the opening of the conventional relief valve and as such, the back pressure will result in additional spring force onto the affected relief valve's disk when in a closed position. To mitigate this challenge, the actual spring setting of the affected relief valves could be reduced by an amount equivalent to the amount of superimposed back pressure.

For future maintenance and/or revamping of the flare system, the use of a larger size tailpipe could be considered to reduce back pressure or the use of a balance below type relief valve to overcome high back pressure. The flare unit manager and operator should review options for reducing high back pressure particularly for cooling failure and power failure scenario such that the back pressure would not exceed 10% of set pressure for the conventional valve and balanced or pilot valves may also be considered in the case of replacement of relief valves to mitigate high or excessive back pressure. Other possible remedies include making jump-overs to relieve local back pressure, replacing pipes and pressure safety valves (PSVs), running a parallel flare line, and relieving flare load to a different part of the flare system.

CONCLUSIONS

This study has demonstrated the modelling and evaluation of the effects of high back pressure (HBP) on the pressure safety valves of the KRPC flare system. The KRPC's flare system was modelled and simulated using Aspen Flare System Analyzer for three scenarios of normal operation (surplus fuel, cooling water failure and power failure).

Steady-state model of KRPC's flare system was successfully simulated using Aspen Flare System Analyzer software package for normal operation (Surplus Fuel), a cooling failure and power failure scenario with the aid of plant data generate from KRPC flare system. The simulated KRPC's flare system shows that the flare system meets the operational requirement for normal flare operation and power failure scenario at a system back pressure of 1.01325 bar, except for the cooling water failure scenario which shows the

occurrence of high fluid velocity and momentum (rhoV^2), which means there is a need to avoid the excessive occurrence of cooling water failure scenario in the KRPC's flare system to prolong the life span of the flare system.

The study showed that at normal operation and cooling water failure, the performance of 10PSV05 and 10PSV07 relief valves were affected at a high back pressure of 5 bar; however, in case of power failure scenario, the performances of 10PSV01, 10PSV02, 10PSV03, 10PSV04, 10PSV06, 10PSV07, 10PSV08 relief valves were affected at a high back pressure of 5 bar. This could potentially result in instability and a significant reduction in flow capacity across the flare header and turbulence flow or induced vibration in the PRVs, and jeopardize the safety of the equipment which the valve is meant to protect.

The KRPC's flare unit manager and operator should review options for reducing high back pressure particularly in case of cooling failure and power failure scenario such that the back pressure would not exceed 10% of set pressure for the conventional valve. In addition, balanced or pilot valves may be considered in the case of replacement of relief valves to mitigate high or excessive back pressure. From the study carried out, it is recommended that further study should be made on a predictive model for pollution dispersion of KRPC gas flaring system.

REFERENCES

[1] Muktikanta S. (2013). High Back Pressure on Pressure Safety Valves (PSVs) in a Flare System: Developing the Simulation model, Identifying and analyzing the back-pressure build-up, Master Thesis in Process Technology, Department of Physics and Technology, University of Bergen. October, p. 1 – 80.

[2] Tharakan, J. (2013). Flare header failure: An investigation, Hydrocarbon processing Journal, Suncor Energy Products, Calgary, Alberta, Canada. January

[3] Sotoodeh, K. (2019). Noise and Acoustic Fatigue Analysis in Valves (Case Study of Noise Analysis and Reduction for a $12'' \times 10''$ Pressure Safety Valve). Journal of Failure Analysis and Prevention, Vol. 19, p. 838 – 843. https://doi.org/10.1007/s11668-019-00665-3

[4] Sahoo, M., Thesis, M., & Technology, P. (2013). High Back Pressure on Pressure Safety Valves (PSVs) in a Flare System, (October).

[5] Smith, D., S. and Burgess, L. L. C. (2012). Relief valve and flare action items: What plant engineers should know, Hydrocarbon Processing Journal, Jan 2012 Edition. Houston, Texas.

[6] Shahda, J. (2019). Predicting Control Valve Noise in Gas and Steam Applications: Valve Trim Exit Velocity Head vs. Valve Outlet Mach Number (Dresser Masoneilan, 2010). Available from:

https://www.plantservices.com/assets/Media/1003/WP_Valve.pdf, accessed 10 January.

[7] Marnane, I., Porter, E. & Collins, E. (2010). Air Dispersion Modelling from Industrial Installations Guidance Note. Irish EPA.

[8] American Petroleum Institute (2014), Pressure-relieving and Depressuring Systems, Standard 521, 6th edn, January, p. 1 – 150.

[9] Qassam, A., Management, P., Technology, A., Dyment, J., Technology, A., Mofor, W. Technology, A. (2014). Jump Start: Relief Sizing in Aspen HYSYS.

[10] Prakash, B. T. (2016). Design and Calculation of the Pressure Relief Valves and Rupture Disks System, Research Gate, p. 1 – 50.

[11] Jo, Y., Cho, Y. and Hwang, S. (2020). Dynamic Analysis and Optimization of Flare Network System for Topside Process of Offshore Plant. Process Safety and Environmental Protection, Elsevier.

[12] Frederick, J. M. (2010). Introduction to Unsteady Thermofluid Mechanics, Process Norway (Petroleum), 2 February.

[13 NORSOK Standard (1997). Process Design: Relief Valve. P-001, Rev. 3, November, p. 3 – 27.

[14] Morton, B. R., Taylor, Sir Geoffrey, and Turner, J. S. "Turbulent Gravitational Convection from Maintained and Instantaneous Sources," Proc. Royal Society A, 234, 1–23, 1956.

[15] Chemical and Process Technology (2018). Few Concerns & Recommendations of PSV Discharge Tail pipe, Hydrocarbon Engineering, 18 August.

BIOGRAPHY of the first author

Dr. Usman Abubakar Zaria has obtained a Ph.D. in Process Safety Engineering, Reliability & Risk Management (University of Aberdeen, UK); MSc in Safety Engineering, Reliability & Risk Management (University of Aberdeen, UK) and B.Eng. Chemical Engineering (ABU, Zaria). In addition to his specialist industry experience, he has broad experience in teaching, research and development. He served as a member of various multidisciplinary engineering teams and has played key roles in the delivery of a number of high-profile projects. Currently, Dr. Abubakar Zaria is a Senior Lecturer at the Department of Chemical Engineering, Ahmadu Bello University (ABU), Zaria, Nigeria.

MODELIRANJE I EVALUACIJA EFEKATA VISOKOG POVRATNOG PRITISKA NA SISTEMIMA BAKLJI U RAFINERIJI

Aminu Sukairaji, Usman Abubakar Zaria, Ibrahim Ali Mohammed-Dabo

Rezime: *Visoki povratni pritisak često utiče na bezbednost i pouzdanost sistema baklji. Jedan od glavnih ciljeva ove studije je simulacija stabilnog modela sistema baklji uz upotrebu softvera Aspen Flare System Analyzer koji koristi podatke iz postrojenja kompanije za preradu nafte Kaduna Refining and Petrochemical Company (KRPC) Ltd, u gradu Kaduna u Nigeriji. U obzir su uzeta tri verodostojna scenarija (normalan rad/višak goriva, nestanak rashladne vode i nestanak struje). Rezultati su pokazali da pomenuti model stabilnog stanja sistema baklji za normalan rad (višak goriva), kao i scenario kvara sistema za hlađenje i nestanka struje u sistemu baklji ispunjavaju zahteve performansi ukoliko povratni pritisak iznosi 1,01325 bara, osim u slučaju nestanka rashladne vode kada dolazi do pojave velike brzine i momenta tečnosti (rhoV2). Takođe, rad baklji pri normalnom povratnom pritisku, za sva tri scenarija ne prelazi projektovane i operativne granične vrednosti. U radu su date preporuke na koji način rukovodioci pomenute kompanije (KRPC) mogu preispitati mogućnosti za smanjenje visokog povratnog pritiska, posebno u slučaju nestanka rashladne vode i nestanka struje, tako da povratni pritisak ne prelazi 10% pritiska u konvencionalnim ventilima.*

Ključne reči: visoki povratni pritisak, bezbednosno inženjerstvo, sistem baklji, ventil, performance, Aspen Flare System Analyzer.

BRATIMIR NEŠIĆ[1]
JELENA MALENOVIĆ NIKOLIĆ[2]
SRĐAN JOVKOVIĆ[1]

[1]Academy of Technical and Vocational Studies Niš, Department Niš
[2]University of Niš, Faculty of Occupational Safety in Niš

[1]bratimir@gmail.com
[2]jelena.malenovic@znrfak.ni.ac.rs
[1]srdjan.jovkovic@akademijanis.edu.rs

ESTIMATION OF THE ENERGY POTENTIAL FOR THERMAL TREATMENT OF MUNICIPAL SOLID WASTE ON THE TERRITORY OF THE CITY OF LESKOVAC FOR 2020

Abstract: *In addition to material recycling, municipal solid waste (MSW) can be treated with so-called, energy recycling or thermal treatment. The basic conditions that need to be met for this are that MSW can justifiably not be treated with priority material recycling and should have a certain acceptable energy potential for thermal treatment. The paper presents the morphological composition of MSW, generated amount on the territory of the City of Leskovac for 2020, with emphasis on the calculation of the energy potential of MSW, on the basis of which a decision should be made whether material or energy recycling (thermal treatment) will be applied.*

Key words: *energy potential, municipal solid waste, Leskovac.*

INTRODUCTION

Municipal solid waste is waste generated in the household as well as other waste that due to its nature and composition is similar to household waste such as: non-hazardous waste from industrial, commercial institutions (including hospitals) administrative institutions, craft shops, construction waste, green market waste, garden waste, green waste from parks and cemeteries and waste from street cleaning [1].

The option found in waste management operations between recycling and landfilling - energy recycling or thermal treatment for energy recovery in our country even in academic circles, was mentioned sporadically, more as a theoretical possibility. No serious analyses have been made in terms of the "quality" of MSW and especially its energy potential. Based on the morphology of MSW, it can be concluded that Serbia is dominated by biodegradable waste and that its quality in terms of energy recovery is generally poor because it contains moisture even up to 37% [1]. This means that, without prior treatment, not all potentials of thermal treatment of the MSW, can be used. In addition, controlled combustion in plants is also met with great public resistance due to fears of increased pollution. Although the arguments presented as evidence of pollution are generally not scientifically and practically accurate and valid, they still figure among environmental organizations.

Another aggravating circumstance for wider application is the direct or indirect opposition to classical or material recycling. Thermal treatment or controlled combustion for energy recovery, should not and must not be a competition to material recycling because only MSW that cannot be recycled (impure waste) and with satisfactory thermal power or energy potential is

thermally treated. However, given the already weaker energy quality of MSW, by taking away fractions for recycling such as plastic, paper or textiles, the already low thermal power or energy potential will be additionally reduced. Of course, this paper will also show whether the qualitatively MSW, generated on the territory of the City of Leskovac in 2020, meets the conditions for thermal treatment, i.e. combustion for energy recovery, i.e. whether its thermal power is at least 6 MJ/kg. The paper is dedicated to the analysis of the energy potential of only MSW, which means that sludge and other liquid municipal waste will not be considered.

MATERIAL AND METHOD

The paper presents the morphological composition of municipal solid waste and the generated amount on the territory of the City of Leskovac for 2020. The emphasis is on the calculation of the energy potential of municipal solid waste, on the basis of which a decision should be made whether to apply material or energy recycling, i.e. thermal treatment of municipal solid waste.

Determining the morphological composition of MSW from the territory of the City of Leskovac

In order to obtain data on the quantities of MSW, it is necessary to implement the prescribed methodology for collecting data on the composition and quantities of MSW on the territory of the local self-government unit [2]. First, the tare mass of all trucks for collecting MSW is measured before going out on the field and collecting and then the same trucks are measured when they perform their regular routes in waste collection and when they are at full capacity (gross mass). All measurements are performed on a truck scale at the entrance to the complex of the regional sanitary landfill

"Željkovac" in Leskovac. Measurements are performed during one week, because for that period, all households on the territory of the City of Leskovac are covered by waste collection service.

To determine the morphological composition of MSW it is necessary that samples of MSW, approximately 500 kg, are delivered to the site for analysis from the following sectors or zones [3]:

- City zone, individual housing,
- City zone: collective housing and commercial zone,
- Rural zones within the city territory.

The analysis should be performed on the same day during the week in which the total amount of MSW is determined, so that the weather conditions are similar and the data are more reliable. The sample from each sector should be selected at random, i.e. by selecting different streets from a particular sector and within them randomly selecting bins/containers to be analysed and which will represent the selected sector as representative as possible.

This part of the methodology can be described as follows:

- Samples from all three zones to be analysed need to weigh about 500 kg.
- Samples from three zones in the city, based on the type of housing.
- The streets that best represent a given zone are selected.
- Within the streets, bins/containers whose contents are unloaded into the truck are randomly selected.
- After the collected mass of the MSW sample, trucks from all three zones are brought to the site for sorting and analysis.
- The total amount of MSW collected in one truck is analysed.
- The sample from all three zones, which is manually sorted, should be separated according to the waste catalogue [4].

As a result of the analysis, the amount of MSW by the above categories in kilograms was obtained, as well as the total amount of the sample, then its volume in cubic meters or litres. The obtained data are analysed and evaluated. However, it should be noted that these results cannot be taken as a definitive indicator of the generated quantities of MSW because there are significant and constant seasonal variations. This only further confirms the fact that the measurements of the generated quantities of MSW are very important for the entire waste management system and that they should be performed constantly throughout the year. The morphological composition of the MSW will be the starting point for further analysis, which is the separation of components that have satisfactory thermal power [5].

The characteristics of MSW, which can potentially become an energy resource [6], depend on several factors: type of development, a saturation of the area with non-residential buildings (including business premises), technical equipment of buildings and their heating. The following elements are equally important for the composition of MSW: the wealth of residents, season, composters for green garbage in the yard and selective collection of MSW that can be recycled by residents [6]. The reason for the special analysis is the decrease or increase in the amount of MSW per capita. The reasons may be an increase or decrease in living standards, but also an increase in public awareness of the importance of reducing MSW generation.

Based on the Annual Report on Waste Management for 2020 [7], the total amount of collected MSW for management (disposal or treatment) is 43.798 tons. The morphological composition of the collected MSW from the territory of the City of Leskovac for 2020, is shown in Table 1.

Energy characteristics of MSW fractions

When considering the possibility of thermal treatment or combustion of MSW in plants and their design, as with any fuel, the following characteristics must be known: chemical composition of MSW as fuel, morphological (physical) composition of MSW as fuel and thermal characteristics of MSW as fuel.

Analysis of chemical composition most often refers to the determination of key elements: carbon, hydrogen, oxygen, nitrogen and sulphur. When the chemical composition of MSW is analysed in terms of its energy potential, it can be said that, like other fuels, it consists of a combustible and a non-combustible part. The combustible part consists of carbon (C), hydrogen (H) and sulphur (S), while the non-combustible part consists of impurities such as oxygen (O), nitrogen (N) and ballast [8]. Ballast consists of mineral impurities (A) and water (W). Mineral substances (impurities) in the process of combustion create ash. In practice, the term ash is often used for pre-combustion conditions. This is the wrong terminology because the composition of mineral substances changes before and after combustion. Mineral impurities and moisture are not elements, but they are conditionally taken in elemental analysis and form the so-called external ballast.

Table 1. *Elemental composition of MSW [9, 10]*

PARAMETER	MSW
Water (%)	15 - 40
Ash (%)	20 - 35
Carbon (%)	18 - 40
Hydrogen (%)	1 - 5
Nitrogen (%)	0,2 – 1,5
Oxygen (%)	15 – 22
Sulphur (%)	0,1 – 0,5
Thermal power (MJ/kg)	7 - 15

The most important component is carbon, whose combustion generates most of the heat (34 MJ/kg), so for the process of energy utilization from MSW, the most important is the presence of fractions with the most carbon content (paper, cardboard, rubber, plastic, wood, etc.). It is completely clear that mineral impurities and

moisture are undesirable substances. MSW has an average thermal power, which ranges from 7 to 15 MJ/kg. The heat capacity of MSW in underdeveloped countries is very small and amounts to about 3 MJ/kg while in developed countries it is over 12 MJ/kg. Table 1, shows the elemental composition of MSW [9, 10].

For the thermal treatment of MSW, thermal power is the most important characteristic which is defined as the ratio of the amount of heat released during complete combustion of fuel/MSW and the amount of fuel/MSW from which heat is released [9]:

$$H = \frac{Q}{m} \qquad (1)$$

Wherein:

H (MJ / kg) - thermal power;
Q (MJ) - amount of heat released;
m (kg) - mass of fuel / MSW

Moisture reduces the thermal power because part of the heat created by combustion is used for its evaporation. Accordingly, there is a lower thermal power (H_d) and an upper thermal power (H_g). Lower thermal power is the energy that is released after the complete combustion of fuel/MSW whereby water leaves the process in a state of steam (water vapour). Complete combustion implies complete oxidation of carbon to CO_2, hydrogen to H_2O and sulphur to SO_2, without oxidation of nitrogen. The difference between H_g and H_d is the energy required to convert water from the process from a liquid to a vapour state [9]. In most waste incineration systems, water leaves the plant in a state of steam.

MSW, as a potential fuel, is very heterogeneous in its characteristics and differs significantly from conventional fossil fuels. Calculating the heat capacity of MSW is a complex process for which it is very important to determine representative samples for analysis, with possible variations that may affect the final result. Due to the large differences in MSW composition between waste types and variations over time, it is not easy to arrive at a representative sample in order to obtain a reliable estimate of average heat output. The thermal power of MSW would be most accurately determined by testing in an existing thermal treatment plant, by measuring the thermal power for each fraction of MSW using a calorimeter. The process takes place by burning a known mass of MSW, in the presence of oxygen. The amount of energy released during combustion is determined based on the increase in temperature in the calorimeter [9].

Very often, the upper and lower thermal power of fractions are given in the literature [12, 13], where a large difference between the upper and lower thermal power of some fractions can be noticed. Of course, the lower thermal power is relevant for a realistic calculation. All fractions in MSW do not have sufficient thermal power to be considered as a possible energy source. The fractions suitable for controlled combustion in order to obtain energy are given in Table 2.

Table 2. *MSW Fractions Thermal Power [12, 13]*

MSW FRACTIONS WITH SATISFACTORY THERMAL POWER	LOWER THERMAL POWER (MJ/kg)
Paper and cardboard	11,6 - 18,6
Plastics	28 - 37,2
Textile	15 - 18,6
Rubber	21 - 28
Composite materials (Tetra pack)	25,22
Biodegradables	3,5 - 18,6
Fines	2,6

It should be emphasized that the obtained values of thermal powers refer to MSW from bins and containers. By introducing primary selection to obtain recyclable materials, thermal power would have lower values with respect to separated components rich in energy potential.

Estimation of MSW energy potential from the territory of the City of Leskovac for 2020

The process consists of separating fractions that have satisfactory thermal power and neglecting fractions without energy potential. Since the thermal power is known for fuel fractions, then according to the quantitative composition of these fractions in MSW, the thermal power of the fraction or the entire MSW can be obtained by adding the thermal powers of all its fractions. The following fractions participate in the calculation: paper and cardboard, plastic, textiles, rubber, composite materials (tetra pack), biodegradables and fines. Therefore, the mass fraction of all combustible fractions in the sum is less than 100% because the other mass fraction consists of non-combustible fractions.

The morphological composition of the collected MSW from the territory of the City of Leskovac for 2020, is shown in Table 3.

Table 3. *The morphological composition of the collected MSW from the territory of the City of Leskovac for 2020. [7]*

FRACTION	MASS SHARE (%)
Paper and cardboard	1,69
Glass	0,63
Biodegradable waste	85,00
PET packaging	0,7
Other plastic packaging waste	0,8
Other plastics	0,84
Metal - ferrous packaging	0,5
Metal - aluminum cans	0,01
Composite materials (Tetra pack)	1,05
Rubber	1,03
Textile	1,01
Fine elements	5,50
Other	1,18
TOTAL:	**100,00**

On the other hand, there is an indirect way to calculate the thermal power by applying appropriate formulas, for which it is necessary to know the content of ash, moisture and combustible substances.

For this, it is necessary to determine the following contents in the MSW, under certain conditions [11]:

- A - ash content (typically 10 - 25% after incineration at 550°C);
- W - moisture content (typically 15 - 35% when dried at 105°C);
- B - share of flammable solid fraction (mass fraction of combustible components, i.e. carbon + volatiles).

By knowing parameters: A, B and W, it can be determined whether MSW can be burned without auxiliary fuel. For this purpose, Tanner's diagram shown in Figure 1 is used [11]. If the data are in the COMBUSTION part of the diagram (humidity W < 50%, ash A < 60%, combustible material B > 25%), this indicates that the combustion process does not require auxiliary fuel i.e. it is considered that the MSW is suitable for conversion into energy through heat treatment.
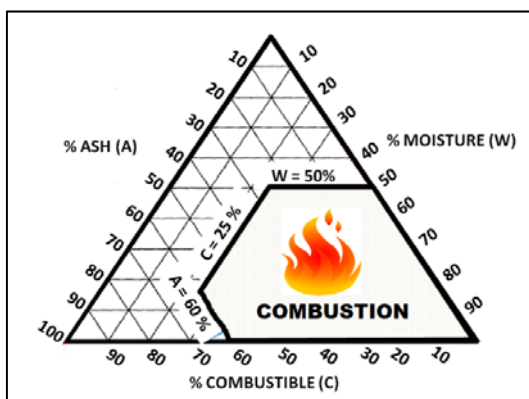

Figure 1. *Tanner's diagram [11]*

Although the values of thermal powers vary considerably from author to author, the average lower thermal powers that appear in the literature for fuel fractions are taken here, so as not to create a false picture of the high energy potential of MSW, especially as the real picture would be reduced for recyclable fractions. The formula for calculating MSW energy potential:

$$E_{Pi} = m_{FPi} \cdot H_{dFi} \qquad (2)$$

Wherein:

E_{Pi} (MJ/kg) – Energy potential of an individual MSW fraction;

m_{Fpi} (-) - Mass share of individual fraction in the total mass of MSW;

H_{dFi} (MJ/kg) - Thermal power of an individual MSW fraction.

Energy potential of MSW collected from the territory of the City of Leskovac for 2020, is shown in Table 4.

Table 4. *Energy potential of* MSW *from the City of Leskovac territory for 2020.*

MSW FUEL FRACTION	Fraction mass share (%)	Fraction mass share (-)	Lower Thermal Power (MJ/kg)	Single Fraction Energy Potential (MJ/kg)
Paper and cardboard	1,69	0,02	16,3	0,33
Plastics	2,34	0,02	32,6	0,65
Textile	1,01	0,01	16,8	0,17
Rubber	1,03	0,01	24,5	0,25
Composite materials (Tetra pack)	1,05	0,01	25,22	0,25
Biodeg-radables	85,00	0,85	11,05	9,39
Fines	5,50	0,06	2,6	0,14
			TOTAL:	**11,21**

By summing the values of energy potentials of all individual fractions, the total energy potential of MSW from the City of Leskovac territory for 2020, was obtained, which amounts to 11,21 MJ/kg. Considering that the limit of energy potential for thermal treatment using the MSW burning technology for energy recovery is 6 MJ/kg, it is obvious that MSW from the City of Leskovac territory for 2020, in terms of energy potential meets this condition.

ANALYSIS OF RESULTS

Although it is completely clear that this is a calculation method, these values of the thermal power of municipal solid waste represent the starting point for further analysis. If there are other data on MSW, for example, the chemical composition of waste fractions, the values of thermal power can be calculated by other calculation methods and compared. When we talk about approximately exact values, possible systematic errors come primarily from the fact that we started from the morphological composition of MSW by seasons and the calculation data were obtained by calculating the arithmetic mean. Since the amounts of MSW by seasons were not the same, the use of the arithmetic means already makes the first mistake in the calculation.

Another error comes from the difference in the values of thermal power of individual fractions of MSW, which can be found in the literature. In this paper, the average values of the lower thermal power of the fractions are taken, which can be found in the literature. Also, these are literary values that refer to certain fractions of certain humidity and quality, which is often not the case in practice because the thermal power is reduced due to excessive humidity, dirt and the like.

It is known that the thermal power of 6 MJ/kg, is the minimum value with which the thermal treatment of MSW for energy recovery can be planned. Although our reality indicates that there will be no construction of such a plant in the near future, further analysis refers to combustion in furnaces within some production activities, primarily in cement plants.

In addition to energy quality, in order to consider the option of thermal treatment of MSW for energy purposes, the condition of quantity must be met, i.e. there must always be sufficient quantities of MSW for combustion. Given that small amounts of generated MSW in all municipalities in Serbia, except large cities (Belgrade, Nis, Novi Sad, Kragujevac and Pristina), it would mean collecting MSW from several municipalities, which can be a logistical problem, both organizationally and financially.

Considering that MSW recyclable fractions, in well-regulated waste management systems, should be recycled, the question arises as to what will remain for combustion after their separation, i.e. what will be the thermal power value? According to some analysis, that it would be around 3 MJ/kg, which is below any level for a serious analysis of a possible thermal treatment for energy recovery. Also, poor quality in terms of humidity and quantities that vary a lot, would deter interested users of this energy source.

CONCLUSION

It is completely clear that the aim is to use all treatment possibilities in the MSW management, except, of course, landfilling. As an option between recycling and landfilling, MSW thermal treatment for energy recovery is somehow shy away. It seems that almost all countries see this option as a "necessary evil", i.e. they apply it when all other options dry up. Even the data on the quantities of MSW that are treated in this way support this and it seems that there will be no significant changes in the coming years.

When we ask ourselves why this option is so neglected and is avoided at all costs, the first argument is the position of public opinion that thermal treatment plants for MSW, pollute the environment. It even seems that public opinion does not see the position and condition of landfills and how they pollute the environment. When it comes to this argument, it should be emphasized that some problems exist, mostly with the solid content that remains after combustion but not to the extent that is shown. A much bigger problem is the cost of building and maintaining an MSW thermal treatment plant to generate energy. Therefore as an option, the possibilities of MSW thermal treatment are sought in some production activities, e.g. cement plants.

When analysing the literature related to this issue in our country, no concrete data can be found on the quality of our MSW, by related, i.e. close municipalities. The proximity of municipalities is important because of the collection of MSW with minimal logistics costs. The general conclusion is that we have low-quality MSW (apart from Leskovac) in terms of energy power and generally small amounts generated for this purpose.

LITERATURE

[1] B. Nešić, ''Generatori otpada i zagađivači južne i jugoistočne Srbije'', Protecta, Niš, Srbija, 2010.

[2] Pravilnik o metodologiji za prikupljanje podataka o sastavu i količinama komunalnog otpada na teritoriji jedinice lokalne samouprave, Službeni glasnik Republike Srbije 61/2010.

[3] G. Vujić, ''Utvrđivanje sastava otpada i procene količine u cilju definisanja strategije upravljanja sekundarnim sirovinama u sklopu održivog razvoja Republike Srbije'', Fakultet tehničkih nauka, Novi Sad, 2009.

[4] Pravilnik o kategorijama, ispitivanju i klasifikaciji otpada, Službeni glasnik Republike Srbije 56/2010, 93/2019, 39/2021.

[5] S. Stanković, ''*Procena energetskog potencijala čvrstog komunalnog otpada u urbanim područjima Republike Srbije*'', završni master rad, Akademija tehničko-vaspitačkih strukovnih studija, Niš, 2020.

[6] K. Midor, K. Jąderko, ''Analysis of the energy potential of municipal solid waste for the thermal treatment technology development in Poland'', E3S Web of Conferences 22, 2017.

[7] Godišnji izveštaj o upravljanju komunalnim otpadom za 2020. godinu privrednog društva RWW Leskovac DOO, Agencija za zaštitu životne sredine Republike Srbije, Beograd, 2021. Available on: *http://www.sepa.gov.rs*

[8] A.T. Akinshilo, J.O. Olofinkua, O. Olamide, ''Energy potential from municipal solid waste (MSW) for a developing metropolis, International Journal of Engineering, Tome XVI, 2018.

[9] M. Radovanović, ''Goriva'', Mašinski fakultet, Beograd, 1994.

[10] B. Nešić, ''Upravljanje komunalnim otpadom i potencijali za reciklažu južne i jugoistočne Srbije'', Protecta, Niš, Srbija, 2010.

[11] B. Cvetanović, ''Energetski potencijal otpada'' (autorizovana predavanja)*,* Akademija tehničko-vaspitačkih strukovnih studija, Niš, 2018. Available on: https://vtsnis.edu.rs/wp-admin/admin.php?page=fajlovi_predmeta

[12] G. Vujić, ''Upravljanje otpadom u zemljama u razvoju'', Fakultet tehničkih nauka, Novi Sad, 2012.

[13] B. Lokahita, M. Aziz, K. Yoshikawa, F. Takahashi, "Energy and Resource Recovery from Tetra Pak Waste using Hydrothermal Treatment", The Open Science Framework, 2017.

ACKNOWLEDGEMENTS

NIKOLA KRSTIĆ[1]
DRAGAN TASIĆ[2]
DARDAN KLIMENTA[3]

[1,2]University of Niš,
Faculty of Electronic
Engineering in Niš
[3]University of Priština in
Kosovska Mitrovica,
Faculty of Technical
Sciences in Kosovska
Mitrovica

[1]nikola.krstic@elfak.ni.ac.rs
[2]dragan.tasic@elfak.ni.ac.rs
[3]dardan.klimenta@pr.ac.rs

THE INFLUENCE OF GROUND WIRES ON THE RESISTANCE AND REACTANCE OF HIGH VOLTAGE OVERHEAD POWER LINES

Abstract: *In this paper, the influence of ground wires on the resistance and reactance (longitudinal impedance) of high voltage overhead power lines (OPLs) is considered and the method for its calculation is described in detail. This is important considering the power flow calculation and the design of the protection system of OPLs, especially those which use distance relays. In addition to symmetric, asymmetric operating conditions of OPLs are also studied, for the analysis of which symmetric components are used. Specifically, this meant the calculation of longitudinal impedances of OPL for positive, negative and zero sequences in each considered case. Special attention is paid to the symmetric system with zero sequences, because the influence of ground wires on the change of longitudinal impedance of OPLs is the greatest in that case. The cases of OPLs with one (110 kV OPL) and two (400 kV OPL) ground wires are considered, using the values of their parameters that can be found in real systems. Values of longitudinal impedances, obtained with and without ground wires influence or the influence of some of their parameters, are compared, based on which appropriate conclusion is made.*

Key words: ground wire, overhead power line (OPL), symmetric components, longitudinal impedance.

INTRODUCTION

Ground wires, instead of electricity transmission, have protective functions in power systems. These protective functions arise from the fact that ground wires are grounded on both sides via a metal structure and groundings of the poles. One of the main functions is the protection of conductors of overhead power lines (OPLs) from atmospheric discharges. Ground wires achieve this by being placed above the phase conductors of OPLs [1-2], which are thus located in the zones protected by them. In this manner, instead of a phase conductor atmospheric discharge hits the ground wires, and the overvoltage wave and current of the atmospheric discharge [3] are taken to the ground so that they least disturb the operating conditions of an OPL. This significantly reduces the number and intensity of high transient voltages in phase conductors, and thus the number of transient faults [4]. Another important protective function of ground wires is the reduction of fault current flowing through the ground. Namely, ground wires provide a parallel path for the currents during the faults with the ground and take the portion of fault current [5]. This reduces the voltage which appears in the grounding system and the surrounding soil during the fault.

In addition to their basic protection function, ground wires to a certain extent affect the values of electrical parameters of OPLs [6-7]. Specifically, this paper considers their influence on the longitudinal impedance, which includes the resistance and reactance of an OPL. Namely, due to the electromagnetic coupling between the phase conductors and the ground wires, as well as the

fact that the ground wires are grounded on both sides, a current is established in them. This current changes the total magnetic flux of phase conductors, and thus their longitudinal impedance. This effect is most pronounced in asymmetric operating conditions of OPLs [8], and especially in those cases where zero sequence currents appear in the phase conductors [9].

In order to find the current flowing through the ground wires, relationships for calculating the voltage of ground wires are used, where, in addition to the currents in the phase conductors and ground wires, their self and mutual impedances [10-11] also appear. By determining the current of ground wires, a reduced matrix of impedances is formed, which represents the connection between the phase voltages and the phase currents, taking into account the influence of ground wires. Asymmetric operating conditions are analyzed using symmetrical components [12] and by decomposing asymmetric into three symmetric systems, first, with positive, second, with negative, and, third, with zero phase sequence. For each of these three systems, the longitudinal impedances are determined as the main diagonal elements of the reduced impedance matrix in the symmetric component domain. Proper and precise determination of these impedances is very important [13-14], because based on them, a mathematical model for the analysis of OPLs under symmetric and asymmetric operating conditions is created. Mainly, this refers to power flow calculations, and the protection system design, where every change in the value of OPL longitudinal impedance that ground wires make, affects the operation and configuration of overcurrent and especially distance protective relays

Paper is presented at the 15th International Conference on Applied Electromagnetics - ПЕС 2021

especially distance protective relays [15] that are often used in protection systems of high voltage transmission networks.

This paper discusses the cases of OPLs with one and two ground wires (110 kV and 400 kV voltage level), compares the obtained values of longitudinal impedances for different cases, and based on that provides appropriate conclusions.

PROCEDURE FOR CALCULATING THE INFLUENCE OF GROUND WIRES

Impedance matrix in the symmetric component domain

Symmetric components represent a popular and frequently used method for analyzing the state of the power system described by the asymmetry of voltages and currents. This method decomposes the asymmetric into three symmetric systems, two three-phase systems with reverse-phase sequences, and one single-phase system with zero phase sequence. In this manner, the calculation is transferred from the phase quantities domain into the domain of the symmetric component and thus simplified. Upon returning from the symmetric components to the phase quantities domain, the transformation matrix $[T]$, is used, i.e.

$$[T] = \begin{bmatrix} 1 & 1 & 1 \\ e^{j\frac{4}{3}\pi} & e^{j\frac{2}{3}\pi} & 1 \\ e^{j\frac{2}{3}\pi} & e^{j\frac{4}{3}\pi} & 1 \end{bmatrix} \quad (1)$$

A matrix relationship that links the phase voltage vector $\vec{V}_{abc}$ with the phase current vector $\vec{I}_{abc}$, is:

$$\vec{V}_{abc} = [Z_{abc}] \times \vec{I}_{abc} \quad (2)$$

where $[Z_{abc}]$ is impedance matrix in the phase domain. By transformation of the phase currents and voltages into the symmetric component domain, and by multiplying the left and right side of the relationship (2) with the inverse transformation matrix $[T]^{-1}$, the following can be obtained:

$$\vec{V}_{dio} = [T]^{-1} \times [Z_{abc}] \times [T] \times \vec{I}_{dio} \quad (3)$$

Based on the relationship (3), the impedance matrix in the symmetric component domain is:

$$[Z_{dio}] = [T]^{-1} \times [Z_{abc}] \times [T] \quad (4)$$

Determination of the longitudinal impedance of an OPL with ground wires

Longitudinal electrical parameters of OPLs with ground wires, which would enable modeling of OPLs not only for symmetric but also for asymmetric operating conditions, include the longitudinal impedance (resistance and reactance) for the positive, negative and zero phase sequences. In order to obtain these parameters, it is necessary to start from the matrix relationship that links voltages and currents in the phase domain, taking the influence of ground wires into

account. For the case of OPL with one ground wire this relationship can be written as:

$$\begin{bmatrix} V_a \\ V_b \\ V_c \\ 0 \end{bmatrix} = \begin{bmatrix} Z_p & Z_{pp} & Z_{pp} & Z_{pg} \\ Z_{pp} & Z_p & Z_{pp} & Z_{pg} \\ Z_{pp} & Z_{pp} & Z_p & Z_{pg} \\ Z_{pg} & Z_{pg} & Z_{pg} & Z_g \end{bmatrix} \times \begin{bmatrix} I_a \\ I_b \\ I_c \\ I_{gw} \end{bmatrix} \quad (5)$$

Where are: Z_p is the self-impedance of a phase conductor with ground return, Z_{pp} is the mutual impedance between two phase conductors, Z_{pg} is the mutual impedance between a phase conductor and the ground wire, and Z_p is the self-impedance of a ground wire with a ground return.

As can be seen from the relationship (5), the voltage of the ground wire is equal to zero because the ground wire is grounded on both sides. Also, the relationship (5) can only be applied in the case of the symmetrical arrangement of phase conductors or in the case when transposition is performed, which is usually done for high voltage OPLs. Accordingly, the same is assumed here. The elements of the impedance matrix are determined by means of the following relationships:

$$Z_p = R_p + R_g + j\omega L_p = R_p + R_g + j\omega \frac{\mu_0}{2\pi} ln \frac{D_{ekv}}{r_{pe}} \quad (6)$$

$$Z_{pp} = R_g + j\omega M_{pp} = R_g + j\omega \frac{\mu_0}{2\pi} ln \frac{D_{ekv}}{D} \quad (7)$$

$$Z_{pg} = R_g + j\omega M_{pg} = R_g + j\omega \frac{\mu_0}{2\pi} ln \frac{D_{ekv}}{D_{pg}} \quad (8)$$

$$Z_g = R_{gw} + R_g + j\omega L_g = R_{gw} + R_g + j\omega \frac{\mu_0}{2\pi} ln \frac{D_{ekv}}{r_{ge}} \quad (9)$$

where R_p is the resistance of one phase conductor, R_g is the resistance of a ground return path, R_{gw} is the resistance of the ground wire, L_p is the self-inductance of phase conductor with ground return, M_{pp} is the mutual inductance between any phase conductors, M_{pg} is the mutual inductance between phase conductors and the ground wires, L_g is the self-inductance of the ground wire with ground return, D_{ek} is the depth of an equivalent ground return path, r_{pe} is the equivalent radius of a phase conductor, D is the geometric mean distance between the phase conductors, D_{pg} is the geometric mean distance between the phase conductors and the ground wires, r_{ge} is the equivalent radius of the ground wire, μ_0 is the magnetic permeability of vacuum, ω is the angular frequency.

It must be pointed out that in all the previous relationships for determining the self and mutual impedances, the resistance of pole grounding is neglected (equal to zero).

In the case where more than one conductor is used per phase, instead of the equivalent radius of a phase conductor, an equivalent radius of a bundled phase conductor

$$r_{be} = \sqrt[n]{n \cdot R^{n-1} \cdot r_{pe}} \quad (10)$$

is used in all the previous relationships, where r_{pe} is the radius of the individual conductors in the bundle, R is the bundle radius of the symmetric set of conductors, and n is the number of conductors per phase.

The depth D_{ekv} and the resistance R_g of the equivalent path through the ground having the resistivity ρ_g at a frequency f are determined by:

$$D_{ekv} = 658.87\sqrt{\frac{\rho_g}{f}} \quad [m] \tag{11}$$

$$R_g = \frac{\omega\mu_0}{8} \quad [\Omega/m] \tag{12}$$

Based on the relationship for the voltage of ground wire (5), the current flowing through a ground wire is:

$$I_{gw} = -\frac{Z_{pg}(I_a+I_b+I_c)}{z_g} \tag{13}$$

Using (13) it is possible to reduce the matrix from (5), and form a matrix relationship that consists only of variables and impedances relating to the phase conductors:

$$\begin{bmatrix} V_a \\ V_b \\ V_c \end{bmatrix} = \begin{bmatrix} Z_p^g & Z_{pp}^g & Z_{pp}^g \\ Z_{pp}^g & Z_p^g & Z_{pp}^g \\ Z_{pp}^g & Z_{pp}^g & Z_p^g \end{bmatrix} \times \begin{bmatrix} I_a \\ I_b \\ I_c \end{bmatrix} \tag{14}$$

where the elements of this reduced matrix are as follows:

$$Z_p^g = Z_p - \frac{z_{pg}^2}{z_g} \tag{15}$$

$$Z_{pp}^g = Z_{pp} - \frac{z_{pg}^2}{z_g} \tag{16}$$

By inserting the matrix relationship (14) into (4), the reduced impedance matrix in symmetric components domain becomes:

$$[\boldsymbol{Z_{dio}}] = \begin{bmatrix} Z_p^g - Z_{pp}^g & 0 & 0 \\ 0 & Z_p^g - Z_{pp}^g & 0 \\ 0 & 0 & Z_f^g + 2Z_{pp}^g \end{bmatrix} \tag{17}$$

The longitudinal impedances for positive Z_d^g, negative Z_i^g and zero phase sequences Z_0^g, are the main diagonal elements of the reduced impedance matrix, obtained as:

$$Z_d^g = Z_i^g = Z_p - Z_{pp} = R_p + j\omega\frac{\mu_0}{2\pi}\ln\frac{D}{r_{pe}} \tag{18}$$

$$Z_0^g = Z_p + 2Z_{pp} - 3\frac{z_{pg}^2}{z_g} \tag{19}$$

by the means of (15), (16) and (17). If the influence of ground wires is not considered, the longitudinal impedances from (18) and (19) are:

$$Z_d = Z_i = Z_p - Z_{pp} = R_p + j\omega\frac{\mu_0}{2\pi}\ln\frac{D}{r_{pe}} \tag{20}$$

$$Z_0 = Z_p + 2Z_{pp} \tag{21}$$

Based on the real and imaginary parts of the complex impedance (21), zero-sequence resistance and zero sequence reactance of an OPL without ground wires are:

$$R_0 = R_p + 3R_g \tag{22}$$

$$X_0 = \omega(L_p + 2M_{pp}) = \omega\frac{\mu_0}{2\pi}\ln\frac{D_{ekv}^3}{r_{pe}D^2} \tag{23}$$

Based on the relationship (19), zero-sequence resistance and zero-sequence reactance of an OPL with one ground wire, taking (22) and (23) into consideration, are expressed as:

$$R_0^g = R_0 - 3\frac{(R_g^2 - \omega^2 M_{pg}^2)(R_{gw}+R_g) + 2R_g\omega^2 L_g M_{pg}}{(\omega L_g)^2 + (R_{gw}+R_g)^2} \tag{24}$$

$$X_0^g = X_0 - 3\frac{2(R_g+R_{gw})R_g\omega M_{pg} - (R_g^2 - \omega^2 M_{pg}^2)\omega L_g}{(\omega L_g)^2 + (R_{gw}+R_g)^2} \tag{25}$$

In the case of OPL with two ground wires, the procedure for obtaining the longitudinal electric parameters is the same, but with insertions of one additional row and one additional column in matrix equation (5), i.e.

$$\begin{bmatrix} V_a \\ V_b \\ V_c \\ 0 \\ 0 \end{bmatrix} = \begin{bmatrix} Z_p & Z_{pp} & Z_{pp} & Z_{pg} & Z_{pg} \\ Z_{pp} & Z_p & Z_{pp} & Z_{pg} & Z_{pg} \\ Z_{pp} & Z_{pp} & Z_p & Z_{pg} & Z_{pg} \\ Z_{pg} & Z_{pg} & Z_{pg} & Z_g & Z_{gg} \\ Z_{pg} & Z_{pg} & Z_{pg} & Z_{gg} & Z_g \end{bmatrix} \times \begin{bmatrix} I_a \\ I_b \\ I_c \\ I_{gw} \\ I_{gw} \end{bmatrix} \tag{26}$$

This relationship, in the same manner as (5), takes into account the symmetrical arrangement of the phase conductors and ground wires. The voltages of ground wires are again equal to zero because of their grounding, while the currents are the same due to the symmetrical arrangement. The elements of the impedance matrix from (26) are the same as those in the impedance matrix from (5), and they can be obtained using (6)-(9), while the newly-introduced element, the so-called mutual impedance between the ground wires Z_{gg}, is determined as:

$$Z_{gg} = R_g + j\omega M_{gg} = R_g + j\omega\frac{\mu_0}{2\pi}\ln\frac{D_{ekv}}{D_{gg}} \tag{27}$$

where M_{gg} is mutual inductance, and D_{gg} is the distance between the ground wires.

In this case, the current flowing through one ground wire is:

$$I_{gw} = -\frac{Z_{pg}(I_a+I_b+I_c)}{Z_g+Z_{gg}} \tag{28}$$

Now, the elements of the reduced impedance matrix in the phase domain can be found as:

$$Z_p^{gg} = Z_p - 2\frac{z_{pg}^2}{Z_g+Z_{gg}} \tag{29}$$

$$Z_{pp}^{gg} = Z_{pp} - 2\frac{z_{pg}^2}{Z_g+Z_{gg}} \tag{30}$$

The reduced impedance matrix in the symmetric component domain, which is obtained in this particular case, has the same form as the matrix in (17). Based on this fact and using the relationships (29) and (30), the longitudinal impedances for the positive, negative, and zero phase sequences of the OPL with two ground wires are:

$$Z_d^{gg} = Z_i^{gg} = Z_p - Z_{pp} = R_p + j\omega \frac{\mu_0}{2\pi} ln \frac{D}{r_{pe}} \quad (31)$$

$$Z_0^{gg} = Z_p + 2Z_{pp} - 6\frac{Z_{pg}^2}{Z_g + Z_{gg}} \quad (32)$$

Based on (32), zero-sequence resistance and zero-sequence reactance of the OPL with two ground wires, taking (22) and (23) into consideration, are:

$$R_0^{gg} = R_0 - 6\frac{(R_g^2 - \omega^2 M_{pg}^2)(R_{gw} + 2R_g) + 2R_g \omega^2 M_{pg}(L_g + M_{gg})}{(\omega L_g + \omega M_{gg})^2 + (2R_g + R_{gw})^2} \quad (33)$$

$$X_0^{gg} = X_0 - 6\frac{2R_g \omega M_{pg}(2R_g + R_{gw}) - (R_g^2 - \omega^2 M_{pg}^2)\omega(L_g + M_{gg})}{(\omega L_g + \omega M_{gg})^2 + (2R_g + R_{gw})^2} \quad (34)$$

RESULTS AND DISCUSSION

This section presents the obtained results together with their discussions. The results are tabulated for the longitudinal positive, negative and zero sequence impedances of the OPLs with one and two ground wires (Tables I and II). The two tables also contain the ground wire currents obtained for the zero sequence currents of 1 per unit (p.u.) flowing through the phase conductors. The tabulated results include and compare four different cases. In Case 1, the influence of ground wires is ignored, in Case 2, all resistances are neglected, in Case 3, only ground wire resistance is neglected, and in Case 4, in the most accurate case, all the parameters are taken into account. The results are generated for the cases of typical pole constructions of the 110 kV and 400 kV OPLs, which exist in Serbia.
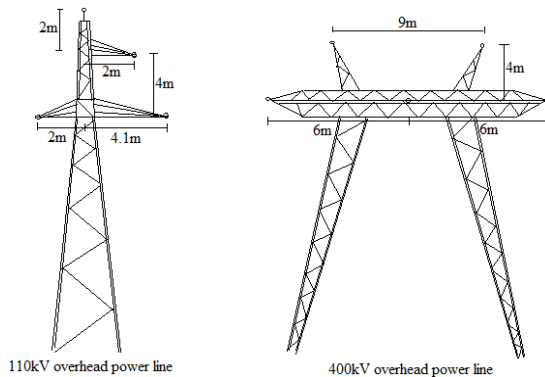

Figure 1. *110* kV *and 400* kV *OPLs*

Fig. 1 shows schematic representations of the 110 kV and 400 kV OPLs, with all the dimensions used in the calculation. As can be seen from Figure 1, the 110 kV OPL is equipped with one ground wire, and the 400 kV OPL is equipped with two ground wires. An *Al-Fe* conductor with a diameter of 16mm and a resistance of 0.2992 Ω/km is used for the ground wires of both OPLs. The phase conductors of the 110 kV OPL are made of *Al-Fe* conductors having a diameter of 19 mm and resistance of 0.1572 Ω/km, while the phase conductor of the 400 kV OPL is made of *Al-Fe* conductors having a diameter of 26.6 mm and resistance of 0.0802 Ω/km. The values of 100 Ωm and 50 Hz are used for the soil

resistivity and the power system frequency, respectively. In addition, the 400 kV OPL has two conductors per phase with an interaxial spacing of 0,4 m. This was the main reason to use the equivalent radius of bundled phase conductors (10) for the calculation in the case of 400 kV OPL. Table 1 outlines the results (longitudinal impedances and ground wire currents) obtained for the 110 kV OPL with one ground wire.

Table 1. *Longitudinal impedances and ground wire currents of the 110* kV *OPL with one ground wire*

Case	$Z_d^g(\Omega/km)$	$Z_i^g(\Omega/km)$	$Z_0^g(\Omega/km)$	$I_{gw}(p.u.)$
1	0.157+j0.405	0.157+j0.405	0.305+j1.376	0
2	0+j0.405	0+j0.405	0+j0.943	-1.323
3	0.157+j0.405	0.157+j0.405	0.203+j0.946	-1.33+j0.11
4	0.157+j0.405	0.157+j0.405	0.361+j0.979	-1.16-j0.35

The results (longitudinal impedances and ground wire currents) obtained for the 400 kV OPL with two ground wires are outlined in Table 2.

Table 2. *Longitudinal impedances and ground wire currents of the 400* kV *OPL with two ground wires*

Case	$Z_d^{gg}(\Omega/km)$	$Z_i^{gg}(\Omega/km)$	$Z_0^{gg}(\Omega/km)$	$I_{gw}(p.u.)$
1	0.08+j0.295	0.08+j0.295	0.228+j1.202	0
2	0+j0.295	0+j0.295	0+j0.642	-0.901
3	0.08+j0.295	0.08+j0.295	0.104+j0.644	-0.91+j0.06
4	0.08+j0.295	0.08+j0.295	0.256+j0.667	-0.83-j0.18

Tables 1 and 2 confirmed that the longitudinal positive and negative sequence impedances of the OPLs are always equal regardless of whether the influence of ground wires are taken into account or not (18), (20) and (31). This can be explained by the fact that OPLs are static components of the power systems, and they have the same impedance for every symmetrical arrangement of the phase conductors and ground wires (as considered in this paper), in which the sum of all phase currents is equal to zero. Independence of longitudinal impedances of the OPLs for positive and negative sequence (sum of all phase currents is equal to zero) from the ground wires is evident considering the expressions for ground wire currents (13) and (28).

Unlike the positive and negative sequences, based on (19), (23) and (32), ground wires have an influence on OPL longitudinal zero sequence impedance. Comparing the results in Tables 1 and 2 for case 1 and case 4, it can be concluded that ground wires slightly increase zero-sequence resistance and in a greater extent reduce zero sequence reactance of the OPL. Also, by comparing the results from case 3 with those in case 4, for both tables, it can be seen that neglection of the ground wires resistance, does not have much effect on zero-sequence reactance, but leads to a big decrease in zero-sequence resistance value, for both OPL. Considering results from cases 2 and 4 it can be concluded that, besides the calculation simplification and the loss of resistance information, neglection of all resistances only slightly reduces the zero-sequence reactance of the OPLs. This change in zero-sequence impedance of OPLs which ground wires create mainly affects the protection system

of OPL, which operation is based on the proper determination of fault loop impedance.

Based on Tables 1 and 2, it can be observed that the ground wire current is approximately in counter-phase with zero-sequence currents in phase conductors which have 1 p.u. value. The ground wire resistance slightly reduces the intensity and increases the phase angle of the ground wire current. Moreover, a higher intensity of the ground wire current is obtained for the 110 kV OPL, due to the smaller interaxial spacings between the phase conductors and the ground wire and the fact that the 110 kV power line has only one ground wire.

CONCLUSION

In this paper, the influence of ground wires on the longitudinal resistance and reactance of OPLs was successfully quantified. It was shown that, regardless of the number of ground wires, in the case of symmetrically arranged conductors of OPLs or the case of achieved transposition, the ground wires do not affect the longitudinal positive and negative sequence impedances. In addition, it was found that the influence only exists for the longitudinal zero sequence impedance of OPLs, so that the corresponding resistance slightly increases, while the corresponding reactance decreases. Moreover, it was shown that ignoring the resistance of the ground wires significantly reduces the zero-sequence resistance of the OPLs. In the end, based on the obtained results, it can be concluded that in asymmetric operating conditions in which zero sequence currents appear, ground wires change the values of resistance and reactance of OPLs, which must be considered especially when designing their protection system.

REFERENCES

[1] M. Djurić, Power system elements (Elementi EES-a), Beopres, Beograd, 2009.

[2] N. Tleis, Power system modelling and fault analysis – theory and practice, Elsevier Ltd., 2008.

[3] M. A. Schroeder, Transient voltages in transmission lines caused by direct lightning strikes, *IEEE Transactions on Power Delivery*, Vol. 20, 2005, pp. 1447-1452.

[4] D. C. Pan, Reduction of the number of faults caused by lightning for transmission line, *International Journal of Electrical and Computer Engineering*, Vol. 9, No. 5, 2019, pp. 3366-3374.

[5] M. Vintan, About a coupling factor influence on the ground fault current distribution on overhead transmission lines, *Advances in Electrical and Computer Engineering*, Vol. 10, No. 2, 2010, pp. 43-47.

[6] J. R. Carson, Wave propagation in overhead wires with ground return, *Bell Systems Tech. J.*, 1926, pp. 539-554.

[7] S. Kurokawa, J. Pissolato Filho, M.C. Tavares, C.M. Partela, A.J. Prado, Behaviour of overhead transmission line parameters on the presence of ground wires, *IEEE Transactions on Power Delivery*, Vol. 20, 2005, pp. 1669-1676.

[8] Ž. Eleschova, M. Ivanič, Impact of asymmetry of overhead power line parameters on short circuit currents, *Transactions on Electrical Engineering*, Vol. 5, 2016, pp. 112-115.

[9] J. Nahman, Zero-sequence representation of nonuniform overhead lines, *Electric Power Systems Research*, Vol. 25, 1992, pp. 65-72.

[10] Y. Wang, S. Liu, A review of methods for calculation of frequency-dependent impedances of overhead power transmission lines, *Proceedings of the National Science Council, Republic of China*, Vol. 25, 2001, pp. 329-338.

[11] D. G. Triantafyllidis, G. K. Papagiannis, D. P. Labridis: Calculation of overhead transmission line impedances a finite element approach, *IEEE Transactions on Power Delivery*, Vol. 14, 1999, pp. 287-293.

[12] C. L. Fortescue, Method of symmetrical co-ordinates applied to the solution of poly-phase networks, *34th Annual Convention of the AIEE (American Institute of Electrical Engineers),* Atlantic City, NJ, USA, Vol. 37, 1918, pp. 1027–1140.

[13] E. Costa, S. Kurokawa, Estimation of transmission line parameters using multiple methods, *IET Generation Transmission and Distribution,* Vol. 9, 2015, pp. 2617-2624.

[14] M. Cenky, J. Bendik, Ž. Eleschova, Advanced methods for computation of electrical parameters for overhead transmission lines, *Journal of Electrical Engineering*, Vol. 68, 2017, pp. 143-147

[15] J. N. Rai, Modeling and simulation of distance relay for transmission line protection, *National Conference on Emerging Trends in Electrical and Electronics Engineering (ETEE)*, 2015, New Delhi, India.

BIOGRAPHY of the first author

Nikola N. Krstić was born in 1995. in Niš, Serbia. He graduated in 2018. and completed his master's academic studies in 2019. at the Faculty of Electronic Engineering, University of Niš.

His main areas of research include power system analysis, optimization and renewable energy sources. He is currently working as a Teaching Assistant at the Faculty of Electronic Engineering, University of Niš.

UTICAJ ZAŠTITNIH UŽADI NA AKTIVNU OTPORNOST I REAKTANSU VISOKONAPONSKIH NADZEMNIH VODOVA

Nikola Krstić, Dragan Tasić, Dardan Klimenta

Rezime: *U ovom radu je razmatran uticaj zaštitnih užadi na aktivnu otpornost i reaktansu (podužnu impedansu) visokonaponskih nadzemnih vodova (OPLs) i detaljno opisana metoda za njegovo izračunavanje. Ovo je važno pri određivanju tokova snaga i projektovanju zaštitnog sistema nadzemnih vodova, posebno onih koji koriste distantne releje. Pored simetričnih razmatrana su i nesimetrična radna stanja nadzemnih vodova, za čiju analizu je korišćen metod simetričnih komponenti. Ovde se konkretno misli na određivanje podužne impedanse nadzemnog voda za direktni, inverzni i nulti redosled, u svakom razmatranom slučaju. Posebna pažnja je posvećena simetričnom sistemu nultog redosleda, jer je uticaj zaštitnih užadi na promenu podužne impedanse nadzemnog voda najveći u tom slučaju. Obrađeni su slučajevi nadzemnih vodova sa jednim (110 kV vod) i dva zaštitna užeta (400 kV vod), koristeći stvarne vrednosti njihovih parametara. Vrednosti podužnih impedansi nadzemnih vodova, dobijene sa i bez uvažavanja zaštitnih užadi ili nekih od njihovih parametara, su međusobno upoređene, na osnovu čega su izvedeni odgovarajući zaključci.*

Ključne reči: zaštitno uže, nadzemni vod, simetrične komponente, podužna impedansa.

ANA MILTOJEVIĆ[1]
TATJANA GOLUBOVIĆ[2]
MARINA STOJANOVIĆ[3]

University of Niš,
Faculty of Occupational Safety in Niš

[1]ana.miltojevic@znrfak.ni.ac.rs
[2]tatjana.golubovic@znrfak.ni.ac.rs
[3]marina.stojanovic@znrfak.ni.ac.rs

NITROSAMINES – CARCINOGENIC CHEMICAL "INTRUDERS" IN OCCUPATIONAL ENVIRONMENTS

Abstract: *Nitrosamines, or more precisely* N-*nitrosamines, along with* N-*nitrosamides, belongs to* N-*nitroso compounds, a class of organic compounds that have a nitroso (-N=O) group attached directly to a nitrogen atom. Only a few of them occur naturally while the majority is formed by nitrosation of secondary amines in a living and working environment, food, tobacco smoke, etc. These compounds have scarce application in the industry, but they can be formed* in situ, *so they can be considered as chemical intruders in working environments. Considering their toxicity, especially carcinogenicity, where there is a risk of exposure to* N-*nitroso compounds, appropriate protection measures should be taken, including process control, work practices, protective clothing, use of respirators, legal regulations.*

Key words: *N*-nitrosamines, *N*-nitroso compounds, occupational exposure, carcinogenicity, monitoring

INTRODUCTION

N-Nitroso compounds (NOCs) are a class of organic compounds that have a nitroso (-N=O) group attached directly to a nitrogen atom. They are divided into two groups: *N*-nitrosamines (NOAs), derived from secondary amines (dialkyl, alkyl-aryl, diaryl, or cyclic), and *N*-nitrosamides, derived from *N*-alkylated/arylated amides, ureas, or carbamates (Figure 1).
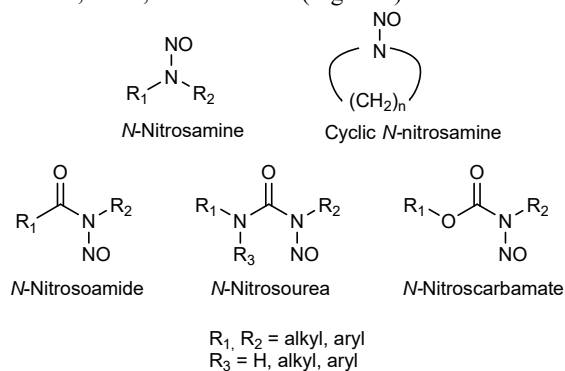

Figure 1. *Structures of* N-*nitroso compounds*

Only a few *N*-nitroso compounds occur naturally, while most of them can be readily synthesized by a reaction of nitrosable substance, secondary amine or *N*-substituted amide, and nitrosating agent, i.e. nitrosonium cation (NO⁺) (Figure 2). The nitrosation can occur either *in vitro*, e.g. in a living and working environment, or *in vivo*, e.g. in the stomach, by simultaneous ingestion of nitrosable substance and nitrosating agent [1]. The sources of nitrosable substances are numerous, while there are two main sources of NO⁺ [2]:

1. nitrogen oxides, N_2O_3 and NO_2, in equilibrium with N_2O_4, that are mostly generated by oxidation of nitrogen-containing organic matter (e.g. during the combustion of fossil fuels),

2. nitrates (NO_3^-) and nitrites (NO_2^-), which are used as industrial and consumer products, as well as food-preservatives, in an acidic medium.
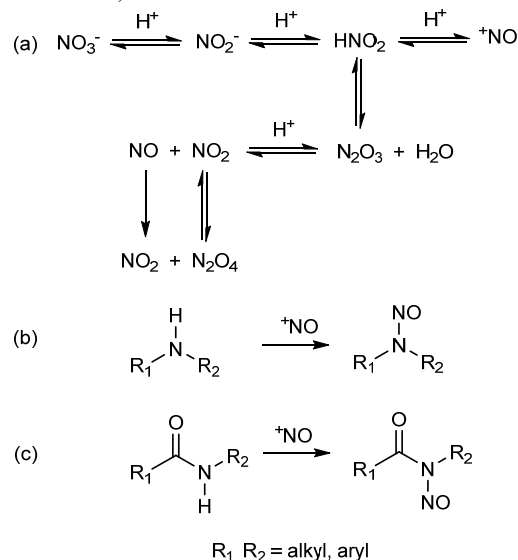
Figure 2. *General mechanism of (a) nitrosonium cation, (b)* N-*nitrosamines and (c)* N-*nitrosoamides formation*

Although the first report on NOAs dates back to the mid-19th century, this class of compounds remained in relative obscurity for almost a century, until their biological properties (especially the knowledge that they are carcinogenic) unveiled them to the scientific community [3]. In particular, over the last few decades, the occurrence of NOAs in the human diet has warranted much concern, since they are either generated from various food constituents containing

amine groups and nitrites, used as food preservatives or are generated during the food preparing processes [1, 4].

The average daily human exposure to NOCs is estimated to be 1 μmol of these compounds (in total). Important sources of exposure, besides the dietary one (72% of the total exposure), are occupational exposure (25%), exposure *via* tobacco smoke (2%), and *via* consumer products (1%), such as cosmetics and personal care products, products that contain rubber, etc. [5]. The primary interest in human exposure to NOAs was centered around their occurrence in food-staffs and *in vivo* formation from precursor chemicals. The emphasis on human exposure to these compounds was shifted towards working environments with the finding of *N*-nitrosodimethylamine (NDMA) in the atmospheres near manufacturing facilities producing and/or using dimethylamine [6].

As occupational exposure comprises ¼ of the total human exposure to these carcinogenic compounds, herein we will discuss the potential sources of nitrosamines formation in working environments, their physical properties, reactivity, and toxicity, as well as potential preventive measures to reduce occupational exposure to this important carcinogens.
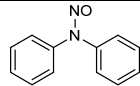
PHYSICAL AND CHEMICAL PROPERTIES OF NITROSAMINES

The physical properties of NOAs depend on the type of substituent (R_1, R_2, Figure 1). For example, NDMA is an oily liquid soluble in water and polar solvents, while *N*-nitrosodiphenylamine (NDPA) is a solid substance insoluble in water and soluble in non-polar organic solvents. Some of the physical properties of NDMA and NDPA, two nitrosamines with the most frequent occurrence in working environments, are given in Table 1.

Considering their chemical reactivity, nitrosamines are fairly labile compounds sensitive to prolonged thermal treatment, photochemical irradiation, as well as to excessive conditions of pH [6]. Moreover, they may undergo "transnitrosation", and this reaction is credited for their biological activity [9].

TOXCICITY OF NITROSAMINES

It has been proven that over 300 NOCs are carcinogenic in one or more animal species and that more than 40 animal species, including higher primates, are susceptible to NOCs-induced carcinogenesis. The International Agency for Research on Cancer (IARC) has classified NOAs as Group 2A or Group 2B carcinogens. Extensive experimental and some epidemiological data suggest that NOAs are carcinogenic for humans and that the intake of these compounds may be regarded as an aetiological risk factor for certain types of cancer, including cancers of the esophagus, stomach, nasopharynx, liver, kidneys, etc. [2].

Table 1. *Physical and chemical properties of NDMA [7] and NDPA [8]*

Physical/chemical property	NDMA	NDPA
Structure		
Molecular weight	74.08	198.23
Physical state	liquid	amorphous solid; plates
Color	yellow	orange-brown; yellow
Odor	no distinct odor	no data
Melting point (ºC)	-50	66.50
Boiling point (ºC)	151-154	no data
Density (g/cm³, at 25 ºC)	1.01	1.23
Vapour pressure (Pa, at 25 ºC)	1080	13.33
Solubility in water (mg/l)	miscible	40
LogK$_{ow}$	-0.57	2.57-3.13
Henry's law constant (Pa m³/mol, at 25 ºC)	3.34	66.87

Generally, nitrosamines, *per se*, are stable under physiological conditions and have to undergo metabolic activation before they express carcinogenic or mutagenic potential [10]. The activation occurs by the action of cytochrome P450-dependent mixed-function oxidase system at the carbon adjacent to the *N*-nitroso group to yield an intermediate radical (**1**, Figure 3). The radical further undergoes either hydroxylation or denitrosation [7]. Hydroxylation yield an α-hydroxynitrosamine (**2**) that breaks down to the corresponding carbonyl compound and monoalkyl/monoarylnitrosamine, in the case of NDMA, formaldehyde (HCHO) and methylnitrosamine. The latter is very unstable and undergoes rearrangement to the strongly methylating methyldiazonium ion (**4**). The diazonium ion (**4**) alkylates a variety of biological macromolecules, such as DNA, RNA, and proteins, releasing molecular nitrogen (N_2). The alkylation of DNA is generally considered to be the critical step in the initiation of cancer [7]. Another metabolic pathway is denitrosation of the formed intermediate radical (**1**) that may lead to the formation of alkyl-/aryl-amine and a corresponding carbonyl compound, in the case of NDMA, methylamine (CH_3NH_2) and formaldehyde (HCHO). The latter is also highly reactive and may react with macromolecules.
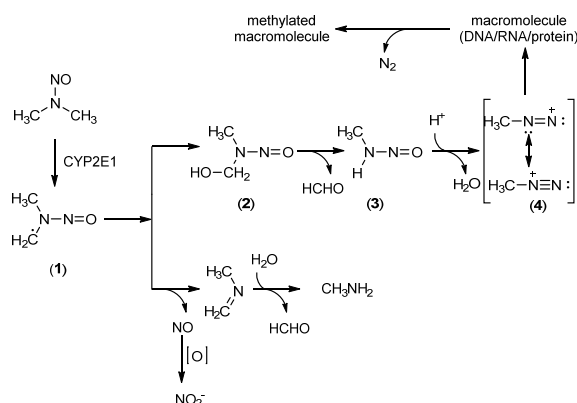
Figure 3. *Metabolism of MDMA*

NITROSAMINES IN WORKING ENVIRONMENTS

The first case on the *N*-nitroso compounds poisoning in the working environment was reported by Freund in 1937 who described the hepatotoxic effects of NDMA on two chemists that had been accidentally poisoned by this compound [6]. A decade later, Hamilton and Hardy reported the toxic effects of NDMA that was used in an automobile factory [11]. In 1954, Barnes and Magee noticed the appearance of cirrhosis of the liver among three men working in the research laboratory of an industrial facility, in which NDMA was used as a solvent [11]. They further evaluated the toxic effects of NDMA on laboratory animals and concluded that this compound was highly hepatotoxic.

NOAs, *per se*, have wide application neither in the industry nor in general. In chemistry, NOAs can be useful synthetic building blocks in organic synthesis [1, 12, 13]. In industry, they were used in the manufacture of dyestuffs, lubricating oils, explosives, insecticides, fungicides, organic accelerators, antioxidants in the production of rubber [9]. Although now used only as a research chemical, NDMA was previously used for many industrial applications [12], as an industrial solvent, nematocide, in the synthesis of the rocket fuel 1,1-dimethylhydrazine, a solvent in the plastics and fiber industry, an additive for lubricants, and to increase the dielectric constant in condensers [9]. More often, workers are exposed to NOAs as a result of their *in situ* formation in working environments, where the precursors of these compounds, amines and nitrosating agents, are either used directly or are formed as side products, as well as a result of intramolecular rearrangements.

US National Institute for Occupational Safety and Health (NIOSH), conducted a study [14] to examine workers exposure to five NOAs (*N*-nitrosodimethylamine (NDMA), *N*-nitrosodiethylamine (NDEA), *N*-nitrosomorpholine (NMOR), *N*-nitrosodiphenylamine (NDPA), and *N*-nitrosopyrrolidine (NPYR)) in different industries, including the dye industry, rubber industry, fish meal factory, leather industry, manufacturing of synthetic

metalworking fluids, foundries, and the soap, detergent, and surfactant industry. These carcinogenic compounds were found in 25 of 40 surveyed plants. Alongside the 5 mentioned NOAs, *N*-nitrosodiisopropylamine (NDiPA) was found in the rubber industry, and *N*-nitrosodiethanolamine (NDE1A) is the industry of manufacturing metalworking fluids [6, 14]. The levels of NOAs in some industries are given in Table 2.

Table 2. *NOAs in some industries [6]*

Industry	NOA	Level range ($\mu g/m^3$)
Rubber	NDMA, NDEA, NMOR, NFPA, NDiPA	0.005 – 16
Leather (tanning)	NDMA, NMOR	0.3 – 10.8
Fish processing	NDMA	0.01 – 0.06
Soap, detergent, and surfactant	NDMA	up to 0.8
Iron and steel casting	NDMA, NDEA	n.r.
Manufacturing and users of synthetic metalworking fluids	NDE1A	n.r.
Dye	n.r.	n.r.

n.r. – not reported

Among surveyed industries, the highest level of NOAs, was detected in the rubber manufacturing facilities, as various amines, nitrosamines, and other nitroso or nitro compounds are used for the production of rubber [6]. Also, a high level of NOAs, in particular NDMA, was found in the leather industry, more precisely in tanneries, that used dimethylamine sulfate in the unhairing process [14]. NDMA in these tanneries is formed in a rection of dimethylamine and airborne nitrogen oxides, in either the gas phase or on surfaces [14]. Moreover, NDMA was found in the air and the total sample in the fish processing industry and it is assumed that this compound is formed from dimethylamine, which is naturally present in fish, and nitrites (which are often added as preservatives) or nitric oxide from the atmosphere [14]. The only *N*-nitroso compound detected in the soap, detergent, and surfactant industries was NDMA that is most likely formed by the reaction of dimethylamine, which is used in the synthesis of cationic surfactants, with ambient levels of nitrogen oxides [14]. In iron and steel casting plants NDMA and NDEA were detected. NDMA is formed from dimethylamine from an unknown source, while NDEA is most probably generated from triethylamine that is reported to be used in these plants, while the source of nitrozating agents in these industries is nitrogen oxides, which is generated by the many combustion sources within the foundry [14]. Furthermore, those who work with metalworking fluids may be exposed to NDE1A, which is a known

contaminant in metalworking fluids formulated with nitrite and ethanolamines [14]. In the paint industry, NOAs can be formed as undesirable by-products since nitrites and amines are often used in the production of paints [14].

Possible ways of occupational exposure to NOAs are explosive manufactures, ore smelters, and amine manufactures, as well as *via* pesticides, where they can occur as impurities or as inadvertent contaminants [15]. Detectable levels of NOAs contaminants were found in the following classes of pesticides: substituted dinitroaniline derivatives, dimethylamine salts of phenoxyalkanoic acid herbicides, di- and triethanolamine salts of several pesticides, some quaternary ammonium compounds, and some morpholine derivatives. One of the most rigorous options of EPA to regulate the safe use of these pesticides was to forbid their use, but manufacturers overcame the problem of NOAs formation in pesticides by changing the chemical process of synthesis (the example of trifluralin), by the elimination of nitrite-salts in the formulation (chlorinated phenoxy- and benzoic acid herbicides), by the changing metallic container, to which nitrites were added as corrosion inhibitors, with the non-metallic ones [15].

ANALYSIS OF NITROSAMINES IN WORKING ENVIRONMENTS

As NOAs are present in working environments in very low amounts (ppm or ppb), the analytical technique used for their analysis has to be: sensitive, selective, free of false results, and capable of dealing with a wide variety of sample types. There are several steps in NOAs analysis in the workplace: sampling, concentration (extraction), chromatographic separation of the extract, and detection. Analytical methods for measuring NOAs concentrations in working environments include not only analysis of NOAs but also the analysis of their precursors (nitrosable substances and nitrosating agents) [6].

The sampling includes a collection of area and process air samples, as well as process water samples. The purpose of the analysis of the process-air samples is to determine if any specific process could be contributing to the airborne NOAs. For air sampling, wet-air traps and dry-solid sorbent traps are used [6]. Wet-air traps are impinger traps containing a sorbent such as KOH, KOH with piperidine, pyrrolidine, and morpholine, potassium biphthalate-hydrochloric acid buffer solution, phosphate-citrate buffer solution. Dry-solid sorbent traps are cartridges containing a dry sorbent and the most frequently used ones are ThermoSorb/N, ThermoSorb/A, and TrhermoSorb/A with morpholine coated onto the sorbent. ThermoSorb/N air sampling cartridge is used to sample air for NOAs, while ThermoSorb/A is an amine trap used to sample NOAs precursors (secondary amines). The role of piperidine, pyrrolidine, or morpholine in the sorbent trap, is to estimate the nitrosating capacity of the sampled air, i.e.

to determine the level of airborne nitrosating agents, such as NO_2. The mentioned compounds can be directly nitrosated by NO_2 and the amount of *N*-nitrosated products is proportional to the square of concentrations of NO_2 [6].

The process-water samples are examined for both *N*-nitroso compounds and amine precursors. The amine precursors are determined by nitrosating a portion of the sample and examining it for NOAs. The step that precedes the analysis of NOAs in water samples is the extraction (concentration) of these compounds from water. The two most frequently used concentration techniques are: 1) liquid-liquid extraction with an organic solvent, such as dichloromethane, and 2) and solid-phase extraction, i.e. adsorption on a sorbent material such as a XAD resin [6].

For separation, gas chromatography (GC) and high-pressure liquid chromatography (HPLC) may be used. Gas and high-pressure liquid chromatographs that are used for NOAs analysis are usually coupled to the detector specifically designed for NOAs detection – thermal energy analyzer (TEA) [16]. The method of detection is based on one of the most significant physical properties of NOAs – the relative ease of the dissociation of the N-NO bond upon heating. NOAs are subjected to catalytical pyrolysis in the GC carrier gas or, in the case of HPLC, a liquid sample is swept through the catalytic pyrolyzer by argon carrier gas where all organic materials are being vaporized and/or pyrolyzed. Pyrolysis of NOAs leads to the homolytic cleavage of the N-NO bond and release of nitrosyl radical ($^\bullet$NO). In the detector, this radical is oxidized by ozone to generate electronically excited NO_2, which on decay to the ground state manifests chemiluminescence (Figure 4). The intensity of chemiluminescence is proportional to the concentration of NOA present in the sample.
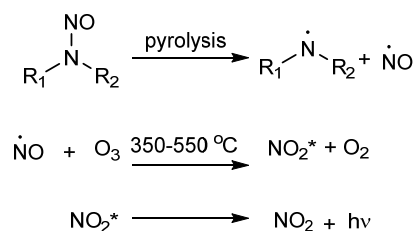
Figure 4. *The processes occurring in the thermal energy analyzer (TEA)*

Besides this, the detection of NOAs, for example, NDMA, has been accomplished by flame ionization detector, nitrogen–phosphorus detectors, the Hall electrolytic conductivity detector operated in the reductive mode, electron ionization low-resolution mass spectrometry, high-resolution mass spectrometry, chemical ionization tandem mass spectrometry on an ion trap mass spectrometer, and laser ionization time-of-flight mass spectrometry. Liquid chromatography has also been used in conjunction with a photolysis reactor and (electrospray ionization) mass spectrometry [17].

Currently, the recommendation of the Occupational Safety and Health Administration (OSHA) is to use Thermosorb/N media or a 15 ml isopropanol bubbler for air sampling, except for *N*-nitrosophenylamine which is unstable in isopropanol, and the samples are further analyzed by TEA or HPLC. Samples must be protected from light during and after sampling and either stored in a freezer or analyzed within six days after collection. The limit of the detection is 0.26 μg/m³ [14].

PROTECTIVE MEASURES IN WORKING ENVIRONMENTS

In the occupational environment, where there is a risk of exposure to hazardous chemicals, it is necessary to perform a risk assessment [18]. Moreover, appropriate protection measures should be taken, which include process control, work practices, protective clothing, use of respirators [19]. The reducing risk from NOAs exposure at the workplace can be accomplished by [20]:

- Technological improvement,
- Use of "safe" amines,
- Avoidance of nitrosating chemicals,
- Reduction in nitrite use,
- Reduction of NO_x pollution,
- Proper ventilation at working places,
- Legal regulations.

Processes in which the formation of *N*-nitroso compounds can occur should be sealed, local and general ventilation should be provided and the reduction of the concentration of these compounds in the air should be accomplished by dilution [14, 21]. Operations and equipment should be isolated. The suggested technological changes, in general, are neither complicated nor unjustifiably expensive and they can be applied in many cases. Moreover, workers must observe special hygiene rules, and certain procedures must be followed for the movement of the material and in case of accidental spills or emergencies.

Currently, there are no OSHA Permissible Exposure Limits (PELs) for NOAs [14]. Mixtures containing more than 1% of NDMA must be maintained in isolated or closed systems The OSHA standard for working with NDMA requires workers to wear respirators that cover half of the face with filters for dust, fog, and smoke (approved by NIOSH / MSHA) in accordance with 29 CFR 1910.134 [14]. Occupational safety and health personnel should select personal protective equipment and other protection measures depending on the results of risk assessments based on expected exposure levels. When choosing personal protective equipment one should bear in mind that NOAs are uncharged, very soluble, and can readily diffuse through many media and "barriers", including rubber gloves [22].

CONCLUSION

N-Nitrosamines are highly toxic, carcinogenic and mutagenic compounds that endanger human health. These compounds do not have wide application in industry, nor in general, but they can be formed *in situ* in those working environments where secondary amines and nitrosating agents (nitrites/nitrates or nitric oxides) occur. The industries where the highest levels of NOAs are found are the rubber and leather industry, dye industry, fish meal factory, manufacturing and users of synthetic metalworking fluids, foundries, and the soap, detergent, and surfactant industry. Considering their toxicity, especially carcinogenicity, where there is a risk of exposure to NOAs, appropriate protection measures should be taken, including process control, work practices, protective clothing, use of respirators, legal regulations, etc. The fact that these compounds can be formed from a wide range of precursors under different conditions, makes the prevention of nitrosamines a multifaceted problem with no single solution.

REFERENCES

[1] A. Miltojević, N. Radulović: "Structural elucidation of thermolysis products of methyl *N*-methyl-*N*-nitrosoanthranilate", RSC Advances, Vol. 5, 2015, pp. 53569-53585.

[2] A. Tricker, R. Preussmann: "Carcinogenic *N*-nitrosamines in the diet: occurrence, formation, mechanisms and carcinogenic potential", Mutation Research, Vol. 259, 1991, pp. 277-289.

[3] W. Lijinsky: "*Chemistry and biology of* N-*nitroso compounds, Cambridge monographs on cancer research*", 1992, Cambridge University Press, Cambridge, UK.

[4] M. Scotter, L. Castle: "Chemical interactions between additives in foodstuffs: a review", Food Additives and Contaminants, Vol. 21, 2004, pp. 93-124.

[5] A. Tricker: "*N*-Nitroso compounds and man: sources of exposure, endogenous formation and occurrence in body fluids", European Journal of Cancer Prevention, Vol. 7, 1998, pp. 244-246.

[6] D. Rounbehler, J. Fajen: "N-*Nitroso compounds in the factory environment*", 1983, US Department of Health and Human Services, Public Health Service, Centers for Disease Control, National Institute for Occupational Safety and Health, Cincinnati, Ohio.

[7] WHO: "*N*-Nitrosodimethylamine in drinking-water, Background document for development of WHO guidelines for drinking-water quality", 2008, WHO Press, Geneva, Switzerland https://www.who.int/water_sanitation_health/dwq/chemicals/ndma_2add_feb2008.pdf (Accessed August 11, 2021).

[8] Agency for Toxic Substances and Disease Registry (ATSDR), US Department of Health and Human Services, Agency for Toxic Substances and Disease Registry: "Toxicological profile for *N*-nitrosodiphenylamine", 2017, https://www.atsdr.cdc.gov/toxprofiles/tp16.pdf (Accessed August 11, 2021).

[9] WHO Task Group on Environmental Health Criteria for Nitrates, Nitrites and *N*-Nitroso Compounds: "Environmental health criteria 5: Nitrates, nitrites, and *N*-nitroso compounds", 1978, WHO, Geneva, Switzerland.

[10] M. Kroeger-Koepke, S. Koepke, G. McClusky, P. Magee, C. Michejda: "α -Hydroxylation pathway in the *in vitro* metabolism of carcinogenic nitrosamines: *N*-nitrosodimethylamine and *N*-nitroso-*N*-methylanilin", Proceedings of the National Academy of Sciences of the United States of America, Vol. 78, 1981, pp. 6489-6493.

[11] J. Barnes, P. Magee: "Some toxic properties of dimethylnitrosamine", British Journal of Industrial Medicine, Vol. 11, 1954, pp. 167–174.

[12] J. Beard, T. Swager: "An Organic chemist's guide to *N*-nitrosamines: their structure, reactivity, and role as contaminants", Journal of Organic Chemistry, Vol. 86, 2021, 2037-2057.

[13] D. Zlatković, D. Dallinger, O. Kappe: "A novel pathway for the thermolysis of *N*-nitrosoanthranilates using flash vacuum pyrolysis leading to 7-aminophthalides", Organic & Biomolecular Chemistry, Vol. 18, 2020, pp. 8371-8375.

[14] OSHA: "OSHA hazard information bulletins *N*-nitroso compounds in industry", Safety and Health Information Bulletins, 1990, https://www.osha.gov/publications/hib19900315 (Accessed August 11, 2021).

[15] G. Zweig, W. Garner: "Policy and regulatory aspects of *N*-nitroso contaminants in pesticide products", In: *N*-Nitroso Compounds, Eds: R. Scanlan, S. Tannenbaum, Washington, 1981, pp. 383-389.

[16] D. Fine, D. Rounbehler, W. Yu, E. Goff: "A new Thermal Energy Analyzer for direct high-performance liquid chromatographic and gas chromatographic analysis of *N*-nitrosamides", IARC Scientific Publications, Vol. 57, 1984, 121-129.

[17] R. Liteplo, M. Meek, W. Windle: "*N*-Nitrosodimethylamine", https://www.who.int/ipcs/publications/cicad/en/cicad38.pdf (Accessed August 11, 2021).

[18] I. Krstić, D. Krstić, A. Kusalo: "Analiza pokazatelja za procenu profesionalnog rizika", Safety Engineering, Vol. 1, 2011, pp. 45-58.

[19] D. Fine: "*N*-Nitroso compounds in the workplace", In: Monitoring Toxic Substances, ACS Symposium Series Vol. 94 (Ed. D. Schuetzle), 1979, pp. 247-254.

[20] R. Preussmann, B. Spiegelhalder, G. Eisenbrand: "Reduction of human exposure to environmental *N*-nitroso compounds", In: *N*-Nitroso Compounds, ACS Symposium Series Vol. 174 (Eds. R. Scanlan, S. Tannenbaum), 1981, pp. 217-228.

[21] A. Miltojević, A. Stojković, M. Stojanović, T. Golubović: "*N*-Nitroso compounds – "uninvited guests" in the working environment", 16th International Conference of Occupational Health and Safety, OSH Priority, 2019, pp. 115 – 122.

[22] W. Mergens, H. Newmark: "Blocking Nitrosation Reactions *In Vivo*", In: *N*-Nitroso Compounds, ACS Symposium Series Vol. 174 (Eds. R. Scanlan, S. Tannenbaum), 1981, pp. 193-205.

ACKNOWLEDGEMENTS

BIOGRAPHY of the first author

Ana Miltojević was born in Niš, Serbia, in 1985.
She received the diploma and the Ph.D. degree in chemistry from the University of Niš, Faculty of Sciences and Mathematics. Her main areas of research include organic and environmental chemistry, occupational toxi-cology, instrumental methods of analysis, etc. She is currently working as an Assistant Professor at the University of Niš, Faculty of Occupational Safety in Niš.

NITROZAMINI – KARCINOGENI HEMIJSKI "ULJEZI" U RADNOJ SREDINI

Ana Miltojević, Tatjana Golubović, Marina Stojanović

Rezime: *Nitrozamini, ili tačnije* N-*nitrozamini, zajedno sa* N-*nitrozamidima, pripadaju* N-*nitrozo jedinjenjima, klasi organskih jedinjenja koja imaju nitrozo (-N=O) grupu vezanu direktno za atom azota. Samo nekoliko njih ima prirodno poreklo, dok se većina formira nitrozvanjem sekundarnih amina u životnoj i radnoj sredini, hrani, duvanskom dimu, itd. Ova jedinjenja nemaju široku primenu u industriji, ali se mogu formirati* in situ*, pa se mogu se smatrati hemijskim uljezima u radnom okruženju. S obzirom na toksičnost, posebno karcinogenost, u radnim sredinama u kojima postoji rizik od izloženosti* N-*nitrozaminima, treba preduzeti odgovarajuće mere zaštite, uključujući kontrolu procesa, radnu praksu, zaštitnu odeću, upotrebu respiratora, zakonske propise.*

Ključne reči: *N*-nitrozamini, *N*-nitrozo jedinjenja, izloženost na radnom mestu, karcinogenost, monitoring.

TEODORA GAVRILOV[1]
NIKOLA DJURIC[1]
DRAGAN KLJAJIC[1]

[1]University of Novi Sad,
Faculty of Technical Sciences

[1]teodora.gavrilov@uns.ac.rs
[2]ndjuric@uns.ac.rs
[3]dkljajic@uns.ac.rs

AN OVERVIEW OF 1998 VERSUS 2020 EDITION OF GUIDELINES FOR LIMITING EXPOSURE TO ELECTROMAGNETIC FIELDS

Abstract: *One of the most important documents defining recommendations for limiting exposure to almost inevitable electromagnetic radiation was released in 1998 by International Commission on Non-Ionizing Radiation Protection (ICNIRP). This document is "Guidelines for Limiting Exposure to Time-varying Electric, Magnetic and Electromagnetic Fields (up to 300 GHz)". However, the growing knowledge about the electromagnetic field (EMF)-tissue interaction and appearance of innovative telecommunication technologies, raised the need for the improvement of these Guidelines. Thus, the ICNIRP published the latest version of its recommendations in 2020. The purpose of this paper is to briefly present some important differences between the ICNIRP 1998 and 2020 Guidelines and to enlighten their reflection on national EMF legislation.*

Key words: electromagnetic fields, EMF exposure, ICNIRP.

INTRODUCTION

The operation of the majority of devices (mobile phones and accompanying telecommunication infrastructure, Bluetooth, Wi-Fi, etc.) is based on the emission of electromagnetic fields (EMFs). Thus, an unavoidable EMF radiation is present in the surrounding environment, raising concerns on potential adverse effects on human health [1]-[5]. For that reason, recommendations for limiting exposure to EMF have been defined in "Guidelines for Limiting Exposure on Time-varying Electric, Magnetic and Electromagnetic Fields (up to 300 GHz)", which was published in 1998, by International Commission on Non-Ionizing Radiation Protection (ICNIRP) [6].

Considerable developments of numerous technologies that use EMF, over a wide spectrum range, have happened since that time. Therefore, the relation between EMFs and potentially adverse health outcomes became more important for the general public. Accordingly, the Guidelines 1998 had to be revised and updated in order to follow the advances in relevant scientific knowledge.

The ICNIRP has updated the radio-frequency part of the 1998 Guidelines, through the "Guidelines for Limiting Exposure to Electromagnetic Fields", issued in 2020 [7]. Here are considered some adequate measures for the protection of human exposure to radiofrequency EMFs in the range from 100 kHz to 300 GHz.

The main objective of research in this paper is to compare those two Guidelines, presenting their main differences and enlightening their deliveries to the national EMF legislation [8].

In-depth analyses of the 1998 and 2020 Guidelines will be performed, while comparison will be made taking into account the overall protection approach, the technical changes to the basic restrictions, as well as to the everyday used reference levels.

THE 1998 GUIDELINES

At the beginning of the 1990s, a powerful development of modern technologies occurred. For that reason, the World Health Organization (WHO) initiated the investigation of the biological effects of radio-frequency EMFs effects. The guidelines for limiting exposure to EMFs with a purpose to protect people and the environment were adopted in 1998, as a consequence of performed research. These Guidelines have been developed by ICNIRP, in partnership with WHO.

The 1998 Guidelines were the basis of EMF legislation in many countries, and around that time, the progressive limitation of EMF exposure was established, providing protection against adverse health effects.

In the 1998 Guidelines, the results of laboratory and epidemiological studies, the basic exposure criteria and reference levels for practical hazard assessment were assembled. Presented Guidelines have been applied to public exposure, as well as occupational exposure. Besides, the results of studies on direct and indirect effects of EMF on people were presented. Direct effects result from direct interaction of fields with the body, while indirect involve interactions with an object at a different electric potential from the body.

THE 2020 GUIDELINES

The production process of Guidelines 2020 lasted for seven years. In March 2020, 22 years after the publication of Guidelines 1998, ICNIRP stated: "The guidelines have been developed after a thorough review of all relevant scientific literature, scientific workshops and an extensive public consultation process. They provide protection against all scientifically substantiated adverse health effects due to EMF exposure in the 100 kHz to 300 GHz range" [7].

In general, Guidelines 1998 were conservative; however, the Guidelines 2020 continued with this

Paper is presented at the 15th International Conference on Applied Electromagnetics - ПЕС 2021

approach preserving the main restrictions same as in Guidelines 1998. Improved scientific accuracy led to an update of limits, which provided the restrictions for exposure circumstances, that have not been considered in the ICNIRP Guidelines 1998.

It should be emphasized that there is an ICNIRP recommendation for countries to update their national regulations in line with the Guidelines 2020.

RESULTS AND DISCUSSION

In general, the scope of both Guidelines is very similar. However, the Guidelines 2020 has some freshly added EMF restrictions, and changes to the old restrictions, while some restrictions have been removed.

The new restrictions are associated with novel technological developments, particularly 5G network technology. Relying on more precise scientific knowledge regarding the relation between spatial averaging of exposure and temperature rise, some restrictions have been changed. Also, in some situations it was proven that some restrictions were not necessary to provide protection from adverse health effects, so they were removed.

An important difference between the two Guidelines is that Guidelines 1998 did not make a distinction between pregnant and non-pregnant women in terms of occupational exposure restrictions. There is no evidence showing that occupational exposure of the fetus would result in adverse health effects. The fetus might be exposed above the more conservative general public restrictions, and, in Guidelines 2020, the fetus and pregnant women were associated with the general public.

Furthermore, the research of the impact of warming from other sources on health was quite advanced compared to the research done 20 years ago, so the ICNIRP filled that part in the new Guidelines.

Also, every step in enacting restrictions can be seen in the Guidelines 2020, due to a large amount of scientific research. The level of transparency is increased and this is one of the important differences.

Finally, the scope of these Guidelines is very similar – whether the adverse effects appear as a consequence of acute or chronic exposure, aside from age or health and of the biophysical mechanism responsible for the effect, the guidelines provide protection against all adverse effects.

Differences in basic restrictions

Basic restrictions are restrictions on exposure to time-varying electric, magnetic and electromagnetic fields that are based directly on established health effects [7]. They are linked with occurrences in the human body.

The physical quantities used to specify basic restrictions in Guidelines 1998 include current density, specific energy absorption rate (SAR), and power density (S).

The quantity SAR is used for the whole-body exposure restriction in both Guidelines, where their differences are presented in Table 1.

Table 1. *Differences between whole-body average SAR in basic restrictions; occupational (O) and general public (GP) exposures*

1998			2020		
f	Whole-body average SAR		f	Whole-body average SAR	
	O	GP		O	GP
100 kHz-10 MHz	0.4	0.08	100 kHz-6 GHz	0.4	0.08
10 MHz-10 GHz	0.4	0.08	6 GHz-300 GHz	0.4	0.08

The restrictions in Guidelines 1998 are for frequencies up to 10 GHz, but novel technologies are using much higher frequencies. Thus, to ensure that exposure to new technologies does not lead to an excessive rise in body temperature, the restrictions in the Guidelines 2020 cover the range up to 300 GHz.

Research has shown that Guidelines 1998 restrictions were even more conservative than it was thought in the beginning, so the SAR values did not change. However, the averaging time for whole-body averaged SAR was changed from 6 to 30 minutes in Guidelines 2020.

Regarding local exposures, the SAR was used up to 10 GHz and power density was used above 10 GHz, in Guidelines 1998. Unfortunately, the superficial exposure at higher frequencies can be underestimated by SAR, while deeper exposures at lower frequencies can be underestimated by power density. Thus, the transition frequency (frequency at which quantity changed) is reduced from 10 GHz to 6 GHz, in Guidelines 2020, as shown in Tables 2 and 3.

Table 2. *Basic restrictions for frequencies between 100 kHz and 300 GHz (local SAR – head and thunk, and limbs; and power density); occupational (O) and general public (GP) exposures; 1998*

f	Local SAR (head and thunk)		Local SAR (limbs)		Power density	
	O	GP	O	GP	O	GP
100 kHz-10 GHz	10	2	20	4	-	-
10 GHz-300 GHz	-	-	-	-	50	10

Protection against excessive local temperature rise, in both directions, uses the same SAR that was averaged over 6 minutes. However, a better approximation is provided by the difference in spatial averaging. While SAR is averaged over a 10-g contiguous tissue region in Guidelines 1998, in Guidelines 2020, it is averaged over a 10-g cubic region.

In both Guidelines, different exposure limits for different body regions are defined. Nevertheless, there are small differences in the way body parts are defined. One of them is that the pinna is treated as superficial

tissue (such as the skin), instead of treating it like tissue, which needs more stringent limitations.

Table 3. *Basic restrictions for frequencies between 100 kHz and 300 GHz (local SAR – head/torso and limb; and local Sab); occupational (O) and general public (GP) exposures; 2020*

f	Local SAR (head and torso)		Local SAR (limbs)		Local S_{ab}	
	O	GP	O	GP	O	GP
100 kHz-6 GHz	10	2	20	4	-	-
6 GHz-300 GHz	-	-	-	-	100	20

Local exposures above 6 GHz also contain some changes. Incident power density is a quantity used for frequencies between 10 GHz and 300 GHz, in Guidelines 1998 (Table 2). Because up to 50% of incident power density is reflected away from the body, this is not a measure of exposure of the body. A new quantity, known as absorbed power density (S_{ab}), is used for frequencies between 6 GHz and 300 GHz, in Guidelines 2020.

Power densities are to be averaged over any 20 cm^2 of the exposed area, but in Guidelines 2020, local S_{ab} is to be averaged over a 4 cm^2 surface area of the body. With the application of this change, an acceptable exposure over 20 cm^2 cannot be concentrated in a small region and rise temperature excessively.

There is an additional constraint for frequencies above 30 GHz: exposure averaged over a square 1 cm^2 surface area of the body is restricted to two times that of the 4 cm^2 restriction. The degree of focus increases with an increase in frequency. The beams below 30 GHz are not focused enough to make damage there, so this restriction was introduced only for frequencies above 30 GHz. Changes in the averaged area and the introduction of an additional limit for highly focused beams above 30 GHz are especially important for ensuring safety with 5G and future technologies.

Equivalent maximum exposures in the body (above and below 6 GHz) are provided by setting the values of basic restriction for EMFs, whose frequency is greater than 6 GHz. For that reason, the larger values are set for S_{ab} in Guidelines 2020, in comparison to values for incident power density in Guidelines 1998. However, the peak exposure in the body for frequencies larger than 6 GHz is now lower than it was in the Guidelines 1998, because the 20 cm^2 averaging area has been replaced with 4 cm^2.

The excessive temperature in local tissue can be raised by brief, intense exposures, although the average power over 6 minutes is smaller than the 6 minutes average restrictions. For that reason, there are additional restrictions in Guidelines 2020, applicable to continuous and discontinuous EMF. They depend on the exposure duration and guarantee that brief intervals of exposure do not cause excessive temperature rises.

These restrictions are applicable only for frequencies above 400 MHz, since an excessive temperature rise could not occur in this way below 400 MHz. The specific energy absorption (SA) is a quantity used for frequencies between 400 MHz and 6 GHz, whereas absorbed energy density (U_{ab}) is used for frequencies above 6 GHz. The functions for SA and U_{ab} are presented in Table 4, where t is time in seconds.

Table 4. *Basic restrictions for frequencies between 400 MHz and 300 GHz (local SA – head/torso and limb; and local U_{ab}); for intervals <6 min; occupational (O) and general public (GP) exposures*

400 MHz-6 GHz	Local Head/Torso SA	O	$3.6[0.05+0.95(t/360)^{0.5}]$
		GP	$0.72[0.05+0.95(t/360)^{0.5}]$
	Local Limb SA	O	$7.2[0.025+0.975(t/360)^{0.5}]$
		GP	$1.44[0.025+0.975(t/360)^{0.5}]$
6 GHz-300 GHz	Local U_{ab}	O	$36[0.05+0.95(t/360)^{0.5}]$
		GP	$7.2[0.05+0.95(t/360)^{0.5}]$

Due to these restrictions, 5G and other future technologies that are in compliance will not cause excessive temperature rise due to brief exposures.

Also, in Guidelines 1998, there is a restriction regarding situations in which sub-millisecond EMF pulses can create audible sound. This restriction is not used in Guidelines 2020, since it has been shown to be a sensory phenomenon and to have no adverse health effect.

Differences in reference levels

The reference levels have been derived by ICNIRP from computational and measurement studies. They have a practical means of demonstrating compliance using quantities that are evaluated more easily than the basic restrictions. Nevertheless, these quantities provide an equivalent level of protection for conditions of maximum exposure scenarios.

Reference levels for continuous whole-body were provided in Guidelines 1998. However, not all types of basic restrictions were covered by Guidelines 1998 reference levels. However, in Guidelines 2020, there is a corresponding reference level for every basic restriction – making it one of the differences between the Guidelines. Unfortunately, situations, where it is not possible to use reference levels, will continue to occur, because of complexities associated with near and far-field differences.

Quantities which define reference levels are measurable. Guidelines 1998 include electric field strength (E), magnetic field strength (H), magnetic flux density (B) and power density (S). In Guidelines 2020, they are known as incident electric field strength (E_{inc}), incident magnetic field strength (H_{inc}) and incident power density (S_{inc}), plane-wave equivalent incident power density (S_{eq}), incident energy density (U_{inc}), and

plane-wave equivalent incident energy density (U_{eq}). All of them are measured outside the body. There is also a current measured inside the body (I).

It was noticed that above approximately 2 GHz, values of E-field and H-field do not always provide adequate evaluation and thus, for whole-body reference levels above 2 GHz, they are not used in Guidelines 2020.

Reference levels for contact currents were also included in Guidelines 1998. However, they are not defined in Guidelines 2020, because it is necessary to take into account various parameters that cannot be specified in advance.

Reference levels for EMFs in the far-field zone are defined in Guidelines 1998. These reference levels, according to Guidelines, can also be used in the near-field zone. However, matching with basic restriction and introducing additional reference levels, leads to the complexity of near-field measurements. Hence, reference levels are differently defined in the far-field zone, radiative near-field zone and reactive near-field zone.

Other factors which are out of the scope of the Guidelines 2020 also affect how well the reference levels correspond to the basic restrictions. Due to this, other essential characteristics of the exposure scenario (e.g. size and shape of the antenna) need to be thought out for precise specification of the far-field, radiative near-field and reactive near-field zones. To ensure consistency between reference levels and basic restrictions, the input from a technical standards body needs to be specified.

The Guidelines from 2020 clearly state that in situations where EMF levels are not sufficiently informative to ensure that reference levels meet basic restrictions, reference levels cannot be used, but basic restrictions must be respected.

As mentioned previously, in Guidelines 2020, there is a range of new reference level categories. Because limited research below 30 MHz was available in 1998 when reference levels were set, reference levels are very conservative. In Guidelines 2020, there are updated reference levels, because of novel information on the relationship between basic restrictions and both the electric and magnetic field reference levels provided by research and scientists (it does not affect the basic restrictions). As higher values of reference levels are needed to achieve the basic restrictions, the reference levels are therefore increased. For that reason, E-field and H-field reference levels are higher in Guidelines 2020 than in Guidelines 1998, for the frequencies between 100 kHz and 30 MHz.

The monotonic increase in the values of the reference levels of E- and H-fields with decreasing frequency, starting from 30 MHz, is present in Guideline 2020. Also, there are no differences in whole-body average reference level values above 30 MHz between the Guidelines. Nevertheless, the same reference level values will result in different magnitudes of exposure to a person, because of different rules for the application of reference levels.

As it is said before, one of the differences is that separate reference level values for exposures in the far- and near-field zones were not specified in Guidelines 1998, and in the near-field zone, the values of the reference level of the far-field zone were used. In Guidelines 2020, reference levels in the near- and far-field are separated. For that reason, there will certainly be no excessive exposure in the near field zone.

Another difference is that in the Guidelines 2020, for frequencies above 2 GHz in the near field zone, a measure of power density is used instead of E-field and H-field (which was used in the Guidelines 1998 for average whole body reference levels over the entire frequency range of 100 kHz to 300 GHz).

Differences in simultaneous exposures to multiple frequency fields

Changes in basic restrictions and reference levels cause the corresponding changes in the equations, which describe simultaneous exposures to multiple frequency fields.

As power density is no longer a quantity used for whole-body exposures, that collection is deleted in the equation for the whole-body average basic restrictions (for frequencies in the range of 10 GHz and 300 GHz).

In the Guidelines 1998, there is no equation for the local SAR and the local absorbed power density, but in new guidelines, there are derived following equations, (1) and (2).

$$\sum_{i=100\,\text{kHz}}^{6\,\text{GHz}} \frac{SAR_i}{SAR_{BR}} + \sum_{i>6\,\text{GHz}}^{30\,\text{GHz}} \frac{S_{ab,4cm,i}}{S_{ab,4cm,BR}}$$
$$+ \sum_{i>30\,\text{GHz}}^{300\,\text{GHz}} MAX\left\{\left(\frac{S_{ab,4cm,i}}{S_{ab,4cm,BR}}\right),\left(\frac{S_{ab,1cm,i}}{S_{ab,1cm,BR}}\right)\right\} \le 1. \tag{1}$$

$$\sum_{i=100\,\text{kHz}}^{400\,\text{MHz}} \int_t \frac{SAR_i(t)}{360 \times SAR_{BR}} dt + \sum_{i>400\,\text{GHz}}^{6\,\text{GHz}} \frac{SA_i(t)}{SA_{BR}(t)}$$
$$+ \sum_{i>6\,\text{GHz}}^{30\,\text{GHz}} \frac{U_{ab,4cm,i}(t)}{U_{ab,4cm,BR}(t)}$$
$$+ \sum_{i>30\,\text{GHz}}^{300\,\text{GHz}} MAX\left\{\left(\frac{U_{ab,4cm,i}(t)}{U_{ab,4cm,BR}(t)}\right),\left(\frac{U_{ab,1cm,i}(t)}{U_{ab,1cm,BR}(t)}\right)\right\} \le 1. \tag{2}$$

Equation (1) is for time intervals larger than 6 minutes, and equation (2) is for time intervals smaller than it. The equations for electric and magnetic fields strength (incident fields) are also updated, in line with changes in the reference levels.

The impact of Guidelines 2020 on national EMF legislation

The Serbian legislation regarding protection to EMF exposure was issued in 2009 and it is based on Guidelines 1998. However, in order to follow scientific advances and new knowledge on EMF, changes should be made in national legislation to follow the latest Guidelines. Basic restrictions and reference levels must be changed (their quantities and limit values), as well

as in the equations which express the simultaneous exposure to fields of different frequencies. Some proposals for changes in Serbian legislation are offered in [8].

CONCLUSION

The modernization of EMF Guidelines was absolutely necessary, since the Guidelines 1998 is not fully in line with the progress of telecommunication technology.

The newest issue of Guidelines for limiting exposure to electromagnetic fields is for the protection of humans exposed to radiofrequency electromagnetic fields in the range from 100 kHz to 300 GHz.

The Guidelines cover many novel applications such as 5G technologies, Wi-Fi, Bluetooth, mobile phones, and base stations. However, it should be expected that recommendations from 2020 will be updated in the next few years, following the forthcoming developments in new-age technologies.

Finally, the Guidelines 2020 should be adopted in our national legislation, in order to reflect modern recommendations for limiting exposure to EMFs.

REFERENCES

[1] Scientific Committee on Emerging and Newly Identified Health Risks – SCENIRH, "Final opinion on potential health effects of exposure to electromagnetic fields (EMF)", http://ec.europa.eu/health/scientific_committe-es/emerging/docs/scenihr_o_041.pdf, 2015.

[2] P. Gajšek, P. Ravazzani, J. Wiart, J. Grellier, T. Samaras and G. Thuróczy, "Electromagnetic field exposure assessment in Europe radiofrequency fields (10 MHz-6 GHz)", *Journal of Exposure Science and Environmental Epidemiology*, volume, 2015, 25, pp. 37-44.

[3] S. Sagar, S. Dongus, A. Schoeni, K. Roser, M. Eeftens, B. Struchen, M. Foerster, N. Meier, S. Adem and M. Röösli, "Radiofrequency electromagnetic field exposure in everyday microenvironments in Europe: A systematic literature review", *Journal of Exposure Science and Environmental Epidemiology*, 2018, 28, pp. 147-160.

[4] C.R. Bhatt, M. Redmayne, B. Billah, M.J. Abramson and G. Benke, "Radiofrequency-electromagnetic field exposures in kindergarten children", *Journal of Exposure Science and Environmental Epidemiology*, 2017, 27, pp. 497-504.

[5] C. Kurnaz, B.K. Engiz and M.C. Bozkurt, "Measurement and evaluation of electric field strength levels in primary and secondary schools in a pilot region", *Radiation Protection Dosimetry*, Volume 179, Issue 3, May 2018, Pages 282-290.

[6] International commission on non-ionizing radiation protection (ICNIRP) – "Guidelines for limiting exposure to time-varying electric, magnetic, and electromagnetic fields (up to 300 GHz)", http://www.icnirp.org/cms/upload/publications/ICNI-RPemfgdl.pdf, 1998 (page visited in May 2021).

[7] International Commission on non-ionizing radiation protection (ICNIRP) – "Guidelines for limiting exposure to time-varying electric, magnetic, and electromagnetic fields (100 kHz to 300 GHz)", https://www.icnirp.org/cms/upload/publications/-ICNIRPrfgdl2020.pdf, 2020.

[8] N. Djuric, T. Gavrilov, D. Kljajic, N. Markovic Golubovic, S. Djuric: "The ICNIRP 2020 Guidelines and Serbian EMF Legislation", *Proceedings of IEEE 29th Telecommunications Forum – TELFOR*, 2021, pp. 1-4.

BIOGRAPHY of the first author

Teodora Gavrilov was born in Novi Sad, Serbia, in 1994.

She received her B.Sc. and M.Sc. degree in Electrical and Computer Engineering, at the Faculty of Technical Sciences, University of Novi Sad, at the Department of Power, Electronics and Telecommunication Engineering.

She works as a Teaching Assistant at the same Department and she is studying for her Ph.D. in Electrical and Computer Engineering.

Her scientific area is theoretical electrotechnics, while her research interests are in the field of theoretical electrical engineering, and theoretical and applied electromagnetics.

Pregled razlika između preporuka iz 1998. i 2020. godine za ograničavanje izloženosti elektromagnetnim poljima

Teodora Gavrilov, Nikola Djuric, Dragan Kljajic

Rezime: *Jedan od najvažnijih dokumenata koji definišu preporuke za ograničavanje izlaganja gotovo neizbežnom elektromagnetnom zračenju objavila je 1998. godine Međunarodna komisija za zaštitu od nejonizujućeg zračenja (eng. International Commission on Non-Ionizing Radiation Protection - ICNIRP). Ovaj dokument je „Smernice za ograničavanje izlaganja vremenski promenljivim električnim, magnetnim i elektromagnetnim poljima (do 300 GHz)“. Međutim, usled značajnog napretka u znanju o interakciji između elektromagnetskih polja i tkiva i pojavi inovativnih telekomunikacionih tehnologija, zasnovanih na elektromagnetnom polju (eng. electromagnetic field - EMF), ove Smernice su morale biti proširene, ažurirane i dalje unapređene. Stoga je ICNIRP objavio najnoviju verziju svojih preporuka 2020. godine. Svrha ovog rada je da ukratko predstavi neke važne razlike između ICNIRP smernica iz 1998. i 2020. godine i da pojasni kako bi se te razlike odrazile na nacionalne pravilnike koji se tiču elektromagnetnih polja.*

Ključne reči: elektromagnetna polja, izlaganje elektromagnetnim poljima, ICNIRP.

BOOK REVIEW / PRIKAZ KNJIGE
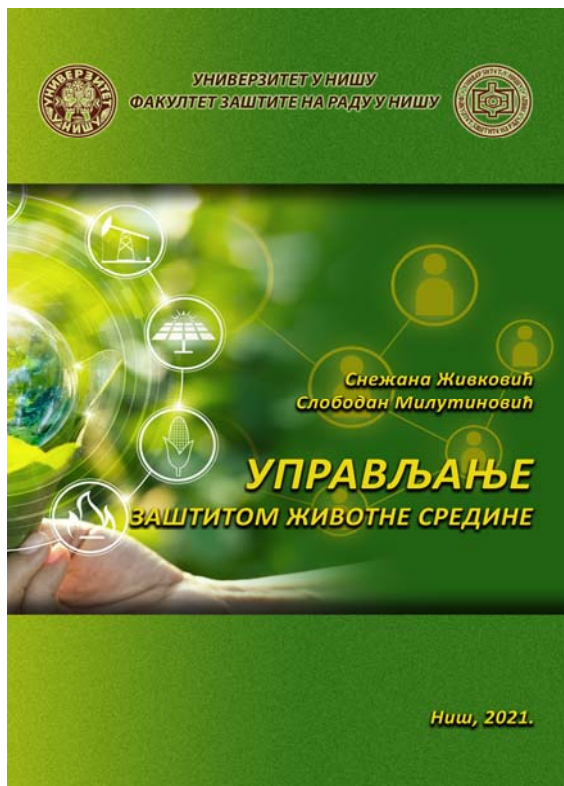
UPRAVLJANJE ZAŠTITOM ŽIVOTNE SREDINE

Snežana Živković, Slobodan Milutinović

Jedan od ključnih problema u savremenim uslovima jeste održivi ekonomski razvoj, odnosno zadovoljenje rastućih ljudskih potreba bez ugrožavanja životne sredine. Nesmotreno i nekontrolisano iskorišćavanje prirodnih resursa poslednjih decenija, rezultiralo je značajnim ekološkim otiskom i dovelo u pitanje dugoročni opstanak čitavog čovečanstva. Eksponencijalni rast stanovništva na planeti stvorio je mnoštvo problema u gotovo svim sferama. Ti problemi su posebno izraženi u domenu nedostatka čiste vode za piće i odgovarajućih sanitarnih uslova, ugrožavanja i istrebljenja biljnih i životinjskih vrsta, povećanja siromaštva u mnogim delovima sveta.

Još od Konferencije UN o životnoj sredini održane u Stokholmu 1972. godine, ulažu se ogromni napori da se zaustavi degradacija životne sredine. Međutim, javna svest o problemima u životnoj sredini je i dalje ograničena. Ekološki izazovi i problemi sa kojima se suočava svako društvo, država i čovečanstvo u celini, nameću potrebu za sistematičnim pristupom u upravljanju zaštitom životne sredine.

Upravljanje zaštitom životne sredine zahteva multidisciplinarnu perspektivu i uključenost svih članova društva. Ovo iz razloga što su zdravlje, životna sredina i socijalni uslovi u stalnoj interakciji, pa poremećaj stanja životne sredine dovodi do ekoloških poremećaja i poremećaja socijalnih odnosa koji su međusobno povezani i uslovljeni. Evoluiranjem samog razumevanja ekoloških problema, glavni fokus trenutnog upravljanja životnom sredinom usredsređena je na integraciju socijalnih i ekoloških sistema. U tom kontekstu, donošenje odluka o životnoj sredini mora se baviti složenošću kako ekoloških sistema, tako i međusobno zavisnih ljudskih, organizacionih i institucionalnih sistema.

Osim toga, upravljanje zaštitom životne sredine uključuje i mnoge prostorne skale, u rasponu od lokalne do globalne, kao i raznovrsne ciljeve, uključujući kontrolu, pravac i tempo razvoja, optimizaciju korišćenja resursa, minimiziranje degradacije životne sredine i sprečavanje nastajanja ekoloških katastrofa. Upravljanjem zaštitom životne sredine mogu se baviti pojedinci i grupe koji imaju različita - pa čak i direktno suprotstavljena mišljenja - kao što je slučaj kada menadžeri zaštite životne sredine zaposleni u velikim multinacionalnim korporacijama dođu u sukob sa menadžerima zaštite životne sredine koji predstavljaju dobrovoljne organizacije.

Tokom višedecenijskog razvoja politike zaštite životne sredine razvijeni su brojni instrumenti, metode i tehnike (procena životne sredine, ekonomska procena, strateška procena uticaja, računovodstvo životne sredine, sistemi upravljanja životnom sredinom, procena životnog ciklusa i ekološki dizajn) čiji je značaj ključan za analizu i upravljanje uticajima na životnu sredinu. Adekvatna analiza upravljanja životnom sredinom, podrazumeva razumevanje načina donošenja odluka u vezi sa životnom sredinom, kao i sagledavanje da li praktične politike i procesi koji su rezultat tih odluka dovode do ekološki i društveno održivih rezultata. Posebno mesto u tom procesu zauzimaju institucije u oblasti zaštite životne sredine.

Imajući sve ovo u vidu, ova knjiga predstavlja još jedan od napora da se podigne svest o neophodnosti zaštite životne sredine i da se o problemima upravljanja životnom sredinom progovori na sistematičan, naučno zasnovan, a ujedno razumljiv način.

U knjizi su posebno obrađene funkcije menadžmenta kao procesa upravljanja, menadžeri, upravljanje zaštitom životne sredine, institucionalni okvir upravljanja zaštitom životne sredine, upravljanje zaštitom životne sredine kao poslovni proces, kao i zaštita životne sredine i kvalitet života.

Svojim sveobuhvatnim i celovitim pristupom, ova knjiga predstavlja nemerljiv doprinos u oblasti zaštite životne sredine i sigurno će naići na adekvatan odjek u naučnoj i stručnoj javnosti.

Tehnical solution / Tehničko rešenje

EKONOMIČAN SISTEM ZA BESKONTAKTNO MERENJE TELESNE TEMPERATURE LJUDI

Uglješa Jovanović, Dejan Krstić, Dragana Krstić, Zoran Jovanović

Merenje telesne temperature ljudi najčešće se vrši kontaktnim temperaturnim senzorima, kod kojih se prenos toplote obavlja usled fizičkog dodira sa telom čija se temperatura meri. Međutim, ovakav proces merenja temperature traje i do nekoliko minuta i podstiče razvoju pandemije zarazne bolesti COVID-19, jer merni instrument postaje potencijalni prenosnik virusa, pa se isti, nakon svake upotrebe, mora sterilisati. Ovaj nedostatak kompenzuje se primenom beskontaktnih merača telesne temperature, zasnovanih na merenju intenziteta infracrvenog (IC) zračenja koje emituje svako telo sa temperaturom iznad apsolutne nule tj. -273.15°C. Dodatnu prednost predstavlja i znatno brže vreme merenja telesne temperature. Pored toga, primenom samostalnih sistema eliminiše se potreba za angažovanjem lica koje vrši merenje telesne temperature primenom ručnih beskontaktnih merača, a koji bi, u tom slučaju, bio potencijalni prenosnik virusa.

Kako bi se postigla odgovarajuća ekonomičnost i modularnost, rad realizovanog sistema zasnovan je na ekonomičnom i široko rasprostranjenom single-board računaru Raspberry Pi 4B. Procesor vrši očitavanje podataka, u realnom vremenu, sa senzora MLX90614 serije DCI koju odlikuje medicinska klasa tačnosti od ±0.2°C, nakon čega vrši njihovu obradu i prikaz na LCD ekranu dijagonale 7". Računar Raspberry Pi 4B montiran je na poleđinu LCD displeja. Komunikacija između senzora MLX90614 i procesora obavlja se putem I²C magistrale, a veza između njih ostvarena je pomoću 2 m dugog 4-žičnog fleksibilnog kabla. Komunikacija između računara Raspberry Pi 4B i LCD displeja obavlja se putem Display Serial Interface magistrale.

Aplikacija za akviziciju, obradu i prikaz rezultata merenja napisana je u Java programskom jeziku i kompajlirana je na ARM64 arhitekturi, što je čini kompatibilnom i sa drugim single-board računarima iste arhitekture. Boot sekvenca operativnog sistema Raspbian, instaliranog na računaru Raspberry Pi 4B, je podešena tako da se realizovana aplikacija automatski startuje prilikom pokretanja operativnog sistema. Proces merenja telesne temperature vrši se tako što procesor računara Raspberry Pi 4B svakih 700 ms očitava vrednost telesne temperature sa senzora MLX90614, koju zatim obrađuje i prikazuje na LCD-u.

Kako bi se dodatno ubrzao protok ljudi i postigla odgovarajuća autonomija u radu sistema, uvedeno je vizuelno alarmiranje izmerene telesne temperature. Naime, ukoliko je izmerena telesna temperatura niža od 36.5°C, njena vrednost biće ispisana zelenom bojom. Ukoliko je izmerena telesna temperatura u granicama od 36.5°C do 37°C, njena vrednost biće ispisana jarkom narandžastom bojom, što ukazuje na potencijalno povišenu telesnu temperaturu. Konačno, ukoliko je izmerena telesna temperatura veća od 37°C, njena vrednost biće ispisana jarkom crvenom bojom, što ukazuje na visoku telesnu temperaturu. Zahvaljujući opisanoj vizuelnoj indikaciji, lice zaduženo za kontrolu telesne temperature može sa bezbedne udaljenosti pratiti izmerene vrednosti i reagovati samo po potrebi. Time se znatno umanjuje izlaganje tog lica posetiocima, odnosno njegova uloga više nije aktivna.

Razlika između uporednih merenja realizovanog sistema i referentnog instrumenta Fluke 574 je veoma mala i iznosi svega ±0.15°C što ukazuje na dobru tačnost merenja realizovanog sistema i potvrđuje mogućnost njegove primene.

Proces merenja telesne temperature realizovanim sistemom je za 60% brži u odnosu na komercijalne toplomere. Naime, realizovanom sistemu treba 4.15 minuta za merenje telesne temperature 50 posetilaca, dok komercijalni toplomer za isto vreme može izmeriti telesnu temperaturu od 32 posetioca, a za merenje telesne temperature 50 posetilaca mu treba 6.7 minuta.

Cena realizacije predloženog rešenja je u granicama između 150$ i 200$ i na ovu cifru najviše utiče cena senzora MLX90614 serije DCI koja fluktuira zbog velike potražnje. Ukoliko bi se za prikaz rezultata koristio LCD displej manje dijagonale, cena realizacije bi mogla biti ispod 100$.

Review of Project / Prikaz projekta

EROZIJA ZEMLJIŠTA I PREVENCIJA OD BUJIČNIH POPLAVA -
razvoj kurikuluma na univerzitetima država Zapadnog Balkana (SETOF)

Slobodan Milutinović, Snežana Živković, Tatjana Golubović, Dejan Vasović

Erozija tla i bujične poplave su destruktivni procesi, sa ozbiljnim posledicama po ekonomiju, društvo i životnu sredinu. Zbog klimatskih promena, koje su takođe izražene u regionu Zapadnog Balkana, intenzitet erozije, kao učestalost i intenzitet bujičnih poplava će se povećati u budućnosti.

Takođe, u regionu su prisutni svi tipovi degradacije zemljišta, kao što su degradacija fizičkih svojstava zemljišta (zbijanje, gubitak strukturne stabilnosti), hemijska (zaslanjivanje, acidifikacija i iscrpljivanje hranljivih materija), biološka degradacija i gubitak plodnog zemljišta (zbog erozije zemljišta i klizišta), što dovodi do trajnog gubitka poljoprivrednog zemljišta.

Imajući u vidu gore navedeno, univerziteti zapadnog Balkana - članovi SETOF konzorcijuma - izrazili su potrebu za poboljšanjem studijskih programa uvođenjem novih ili modernizovanih nastavnih planova i novih kurseva o zaštiti zemljišta od erozije i bujičnih poplava. S obzirom da zemlje EU posvećuju veću pažnju problemu prirodnih katastrofa, uključujući eroziju tla i poplave, kao i obzirom na značajnu ekspertizu članova konzorcijuma iz EU, očekuje se da će projekt povećati svest o važnosti sprečavanja bujičnih poplava, ne samo na nivou visokoškolskih ustanova, već i u praksi na lokalnom, regionalnom i nacionalnom nivou u zemljama Zapadnog Balkana.

Cilj projekta je **razvoj i unapređenje nastavnih planova i programa u visokoškolskim ustanovama i nastavnih planova i programa za obrazovanje profesionalaca na Zapadnom Balkanu (Srbija i Bosna i Hercegovina)** koji će rešavati probleme kontrole erozije tla i zaštite od bujičnih poplava u skladu sa sa direktivama EU.

Projekat SETOF sastoji se iz tri faze. Tokom prve (pripremne) faze, izvršena je identifikacija i analizi postojećih problema kontrole erozije i prevencije poplava u zemljama Zapadnog Balkana i šire u EU, kao i analiza postojećih nastavnih planova i programa na univerzitetima u programskim i partnerskim zemljama. Druga faza obuhvatila je procenu i kritičku evaluaciju postojećih aktivnosti, na osnovu čega su unapređeni studijski programa na osnovnim i master studijama na svim univeryitetima na Zapadnom Balkanu koji učestvuju u projektu i razvijen i akreditovan potpuno novi zajednički studijski program „**Erozija zemljišta i prevencija od bujičnih poplava**". U realizaciji ovog studijskog programa učestvuju nastavnici i saradnici sa tri univerziteta u Srbiji i dva univerziteta iz Bosne i Hercegovine. U trećoj fazi će novi nastavni planovi i programi biti pilotirani kroz aktivnosti prilagođene za glavne zanteresovane grupe, uključujući obuke za profesionalce u lokalnim zajednicama i stručno usavršavanje inženjera.

Prva generacija studenata na novom zajedničkom studijskom program upisana je septembra 2021. godine.

U realizaciji SETOF projekta učestvuju Univerziteti u Novom Sadu, Nišu, Banjaluci i Sarajevu, Univerzitet prirodnih resursa i prirodnih nauka u Beču, Univerzitet „Sveti Ćirilo i Metodije" u Skoplju, Mediteranski univerzitet u Ređo Kalabriji, Institut za šumarstvo Beograd, Institut šumarskih nauka Bugarske akademije nauka, Inženjerska komora Srbije, Šumsko privredno područje „Donjevrbasko" Banjaluka i Kantonalno javno preduzeće "Sarajevo Šume". Koordinator projekta je Šumarski fakultet Univerziteta u Beogradu, dok se aktivnosti na Univerzitetu u Nišu obavljaju na Fakultetu zaštite na radu. Projekat je započet 2018. godine i trajaće do novembra 2022.

INSTRUCTIONS FOR AUTHORS

SAFETY ENGINEERING Journal publishes original scientific contributions and professional papers in the field of occupational safety, environmental safety and fire protection engineering.

Scientific articles:
- research paper (a paper in which unpublished results of authors' research are presented using the scientific method)
- review paper (a paper which contains an original, detailed and critical review of a research problem or a field in which the authors' contributions can be demonstrated by self-citation)
- short communication (short description of important current research findings)
- scientific discussion or criticism (debate on a specific scientific topic based on scientific arguments)

Professional reports:
- professional paper (a paper which describes useful experiences in professional practice, not necessarily based on a scientific method)
- informative contribution (editorial, comment, etc.)
- review of a book, a software, a case study, a scientific event, etc.)

Papers may be written in Serbian and English and published in both hard copy and soft copy on the website of the Faculty of Occupational Safety, University of Niš.

SAFETY ENGINEERING Journal is published twice a year.

Journal subject areas are:
- Occupational Safety Engineering
- Environmental Safety Engineering
- Fire Protection Engineering
- Medical, legal, economic, sociological, psychological, organizational, educational and linguistic aspects of safety engineering.

All papers published in the journal are subjected to peer review by the members of the Editorial Board who determine the time frame for their publication. Comments and suggestions of the editors and reviewers are submitted to the author for final revision.
Manuscripts should be submitted in written and electronic form.
The length of the manuscript is limited to eight A4 two-column pages.
Template for papers can be found on the journal website:

www.znrfak.ni.ac.rs/SE-Journal/index.html
The papers prepared according to the template should be submitted to:

casopis@znrfak.ni.ac.rs

If you have further questions, do not hesitate to contact us at

+381 18 529 711

UPUTSTVO ZA AUTORE

Časopis SAFETY ENGINEERING objavljuje originalne naučne i stručne članke iz oblasti inženjerstva zaštite na radu, inženjerstva zaštite životne sredine i inženjerstva zaštite od požara.

Naučni članci:
- originalan naučni rad (rad u kome se iznose prethodno neobjavljivani rezultati sopstvenih istraživanja naučnim metodom);
- pregledni rad (rad koji sadrži originalan, detaljan i kritički prikaz istraživačkog problema ili područja u kome je autor ostvario određeni doprinos, vidljiv na osnovu autocitata);
- kratko saopštenje (kratak opis najvažnijih tekućih istraživanja);
- naučna kritika (rasprava na određenu naučnu temu zasnovana isključivo na naučnoj argumentaciji).

Stručni članci:
- stručni rad (prilog u kome se nude iskustva korisna za unapređenje profesionalne prakse, ali koja nisu nužno zasnovana na naučnom metodu);
- informativni prilog (uvodnik, komentar i sl.);
- prikaz (knjige, računarskog programa, slučaja, naučnog događaja, i sl.).

Radovi se pišu na srpskom i engleskom jeziku, a objavljuju se u pisanom i elektronskom formatu na sajtu Fakulteta zaštite na radu Univerziteta u Nišu.

Časopis SAFETY ENGINEERING izlazi dva puta godišnje.

Tematske oblasti časopisa su:
- Inženjerstvo zaštite na radu;
- Inženjerstvo zaštite životne sredine;
- Inženjerstvo zaštite od požara;
- Medicinski, pravni, ekonomski, sociološki, psihološki, organizacioni, obrazovni i lingvistički aspekti u inženjerstvu zaštite.

Svi radovi koji se objavljuju u časopis podležu recenziji od strane Uređivačkog odbora koji određuje i redosled njihovog štampanja. Primedbe i sugestije urednika i recenzenata dostavljaju se autoru radi konačnog oblikovanja.
Radovi se predaju u pisanom i elektronskom obliku.
Obim rukopisa je ograničen na osam dvokolonskih stranica formata A4.

Templejt za pisanje radova se nalazi na sajtu časopisa:

www.znrfak.ni.ac.rs/SE-Journal/index.html

Radove pripremljene prema uputstvu za štampanje slati na adresu:
casopis@znrfak.ni.ac.rs

Za sva dodatna pitanja obratiti se na telefon:

018/529-711